SYNTHESIS OF FUNCTIONALISED ALKENES AND THEIR INTERACTION WITH A ZIRCONOCENE-METHYLALUMINOXANE CATALYST SYSTEM

Tuulamari Helaja

University of Helsinki
Faculty of Science
Department of Chemistry
Laboratory of Organic Chemistry
P.O. Box 55, FIN-00014 University of Helsinki, Finland

ACADEMIC DISSERTATION

To be presented with the permission of the Faculty of Science of the University of Helsinki for public criticism in Auditorium A129 of the Department of Chemistry, A. I. Virtasen aukio 1, on January 15th, 2000 at 12 o'clock noon.

Helsinki 1999

ISBN 951-45-8979-3 (PDF version)
Helsinki 1999
Helsingin yliopiston verkkojulkaisut

To Ukki

PREFACE

The experimental work of this thesis was carried out in the Laboratory of Organic Chemistry at the University of Helsinki during the years 1994-1999 under the supervision of Professor Tapio Hase. The copolymerisations and NMR sample preparations were performed in the Laboratory of Polymer Technology at the Helsinki University of Technology (HUT) under the supervision of Docent Barbro Löfgren. This work was financially supported by the Neste Foundation and the Magnus Ehrnrooth Foundation. A grant from the Helsinki University and support from the Academy of Finland for completing the thesis is gratefully acknowledged.

I wish to express sincere thanks to my supervisors Professor Tapio Hase and Docent Barbro Löfgren. I would also like to thank my colleague Tech. Lic. Kimmo Hakala for the polymerisation studies and for the very nice cooperation indeed. Docents Ilkka Kilpeläinen and Jouni Enqvist are acknowledged for their collaboration concerning the NMR measurements.

I thank the official previewers, Professor Markku Leskelä and Doctor Jari Yli-Kauhaluoma, for their evaluation of my dissertation.

I am grateful to Cindy Ruuskanen for her expertise in revising the language of this manuscript.

Finally, I wish to thank my family for the enormous support during these years.

Helsinki, November 1999

Tuulamari Helaja

ABSTRACT

The study entitled ***Synthesis of Functionalised Alkenes and their Reactions with a Zirconocene-Methylaluminoxane Catalyst System*** has been performed in collaboration with the Helsinki University of Technology. In the literature review of the thesis, functionalised copolymers prepared with methylaluminoxane (MAO) activated zirconocene based catalysts are presented. In addition, the review involves a systematic inspection of the MAO structure according to the methods of investigation, which include both spectroscopic and model synthetic approaches. The interaction of MAO with different zirconocenes is similarly treated, emphasising the chemical shift values observed by NMR for the various species formed in the course of the reaction.

Several alkene derivatives having OH, NR^1R^2, OR, COR, CO_2R or $CONR^1R^2$ groups were synthesised for ethene or propene copolymerisations with the MAO activated zirconocene catalyst. During the development of synthetic routes, two novel reactions were discovered. One describes the monoalkylation-reduction of a fully α-disubstituted ester to a *sec* alkenol by *t*-BuLi via a mechanism that does not involve a ketone intermediate. The other presents an α-*C*-alkylation of an *N*,*N*-dialkyl amide by acetaldehyde derived from tetrahydrofuran (THF) ring cleavage. The *C*-alkylation occurs during the aqueous work-up, whereby the amide enolate reacts with the acetaldehyde itself.

The interaction of functionalised alkenes with the MAO-Cp_2ZrCl_2 catalyst was monitored by ^1H and ^{13}C spectroscopy utilising HSQC, HSQC-TOCSY, HMBC, ROESY and NOESY 2D NMR techniques. All of the alkenols studied, including the ones with substantial steric hindrance in the vicinity of the OH group, produced aluminium alkoxides in their reactions. The *prim* and *sec* amines formed RNHAl species in the presence of the catalyst components. Chemical exchange was confirmed for $CH_2=CH(CH_2)_9NHR$ (R=H or *t*-Bu). The $CH_2=CR^1R^2$, $CH_2=C(Me)R$ and (Me)CH=CH(R) fragments were produced from TMS-ethers and MAO/Cp_2ZrCl_2. The unsaturated species $CH_2=CH(CH_2)_5CH_2CH=C(t\text{-Bu})O\text{-Al-X}$ and $Me_2=CH\text{-Al-X}$ (X= MAO) were generated in the reaction of the studied *t*-butylketone derivative or *t*-butyl 10-undecenoate. The ethene or propene copolymerisation experiments indicate that hydroxyl, amino and ether groups are less detrimental to the catalyst system in comparison with the carbonyl functionality.

CONTENTS

LIST OF ORIGINAL PUBLICATIONS

This thesis consists of the following publications (Appendices I-VI), referred to in the text by the Roman numerals given below.

I T. Helaja, B. Löfgren and T. Hase, Synthesis of sterically hindered long-chain alkenols via organolithium compounds, *Acta Chem. Scand*., 1999, **53**, 352.

II T. Helaja, B. Löfgren and T. Hase, *C*- Alkylation of dialkylamides by acetaldehyde generated from *t*-BuLi and tetrahydrofuran, *Tetrahedron Lett*., 1999, **40**, 6125.

III T. Helaja, K. Hakala, J. Helaja and B. Löfgren, Interaction of oxygen functionalized alkenes with a methylaluminoxane-zirconocene catalyst studied by NMR, *J. Organomet. Chem*., 1999, **579**, 164.

IV T. Helaja, K. Hakala, J. Helaja, B. Löfgren and T. Hase, Dynamic NMR study of tri-*t*-butyl carbinol and a carbinol-methylaluminoxane mixture, *Magn. Res. Chem*., (in press).

V K. Hakala, B. Löfgren and T. Helaja, Copolymerizations of oxygen-functionalized olefins with propylene using metallocene/methylaluminoxane catalyst, *Eur. Polym. J*., 1998, **34**, 1093.

VI K. Hakala, T. Helaja and B. Löfgren, Metallocene/methylaluminoxane-catalyzed copolymerizations of oxygen-functionalized long-chain olefins with ethylene, *J. Polym. Sci., Part A: Polym. Chem*., (to be submitted).

REVIEW OF THE LITERATURE

1 INTRODUCTION

Metallocene based catalyst systems utilised for alkene polymerisation generally consist of group 4 (Ti, Zr, Hf) based transition metal compounds activated by organometallic cocatalysts.[1-3] They are frequently referred to as homogeneous catalysts since both the components and their interaction products formed in the course of the polymerisation are soluble in the reaction medium.[1] Alternatively, the presence of solely one type of active centres in the metallocene is defined by the term homogeneous or single-site catalyst.[2]

The early metallocene catalyst systems originated in the late 1950's.[4,5] These were comprised of titanocenes and alkylaluminium halide cocatalysts, typically Cp_2TiCl_2 and $AlEt_2Cl$. However, they exhibited a low polymerisation activity for ethene and none for propene. The activity increased by a factor 20-100 when small amounts of water were introduced into the titanocene/alkylaluminium halide catalyst systems. Exceedingly active metallocene catalysts (a 10^6 fold increase in activity) were discovered in the 1970's by Sinn and Kaminsky.[5] They reported that partially hydrolysed trimethyl aluminium (TMA) activated group 4 metallocenes for polymerisation of both ethene and 1-alkenes. Through separate synthetic experiments, the species accounting for the aforementioned phenomena was identified as methylaluminoxane (MAO).[6]

Despite the enormous scientific effort to characterise MAO, its exact structure has still partly remained an enigma.[3,7] Due to the presence of multiple equilibria in solution, the direct elucidation of the MAO structure has proven difficult. In fact, MAO is described as a mixture of linear and/or cyclic oligomers having the general formula $[Al(Me)O]_n$ ($5<n<20$).[8,9] The association of MAO oligomers affords an estimated molar mass of 900-1500 g/mol.[9,10] In order to achieve high activity, MAO has to be employed in a large excess in comparison to the metallocene component, the ratio commonly being (10^3-10^4):1. However, MAO is the most widely used activator for metallocenes.[5,10]

A unique feature of metallocene catalysts is their ability to produce polymers with desired (so called "tailor-made") properties.[4,11] The polymers' molar mass, molar mass distribution and microstructure (tacticity) can be controlled by a choice of metallocene.[1-3] Moreover, metallocene catalysed copolymerisations of ethene or propene with 1-alkenes afford compositionally uniform products.[1] In

particular, copolymers with functional groups attached to their hydrocarbon backbone are of great interest due to their improved adhesive and permeability properties, affinities for dyes and compatibility with other polar polymers compared with unfunctionalised copolymers.[12-14] Hence, several approaches for the polymer functionalisation have been developed. The approaches involving zirconocene based catalysts activated by MAO are included in the literature review of this thesis. The actual polymerisation mechanisms are beyond the scope of this thesis. Similarly, copolymers are schematically presented with simplified structures *i.e.* solely the functional monomer attached to the copolymer´s hydrocarbon backbone is shown. The different zirconocene catalysts are presented with abbreviated formulas throughout the text. Their structural formulas are included in Appendix VII.

In the second part of this review, the structure elucidation of MAO is examined in terms of characterisation methods. These include nuclear magnetic resonance (NMR), ultraviolet (UV) and infrared (IR) spectroscopies, gel permeation chromatography (GPC) and the synthesis of model compounds. Studies on the interaction of MAO with zirconocene catalysts are similarly presented according to the method of investigation. No attempt was made to determine the type of bonding in the structures depicted for MAO or its reaction products with zirconocenes.

It is noteworthy that the application of MAO in organic synthesis is diminutive at the present even though aluminium compounds in general are widely utilised reagents[15] in the field of organic chemistry. The reactions of MAO with polar compounds are briefly presented in this context. Moreover, some synthetic procedures for aliphatic alcohols and amines are inspected in the last part of the review. The methods affording sterically hindered target molecules are emphasised.

2 SYNTHESIS OF FUNCTIONALISED POLYALKENES UTILISING ZIRCONOCENE BASED CATALYSTS

2.1 Polyborane functionalised copolymers

The synthesis of functionalised polyalkenes employing organoboranes has been studied extensively.[16-19] Alkenylboranes, such as compound **1** in figure 1, have been directly copolymerised with ethene by MAO activated $Et(Ind)_2ZrCl_2$ or Cp_2ZrCl_2.[16,17] The former catalyst produced functionalised polyethene (PE) **2** containing 2.30 mol-% of the borane derivative, whereas in the latter case the comonomer amount of 1.22 mol-% was determined.

The advantages of employing boron-containing copolymers are their stability towards the zirconocene catalyst system and their versatility. In fact, their facile conversions to OH, I, $OSiMe_3$ or NH_2 functional groups have been reported.[16,17] Alternatively, these polar groups have been introduced via hydroboration and subsequent chemical modifications of ethene-1,4-hexadiene copolymers, which were produced with the aforementioned catalysts and MAO.[17,18]

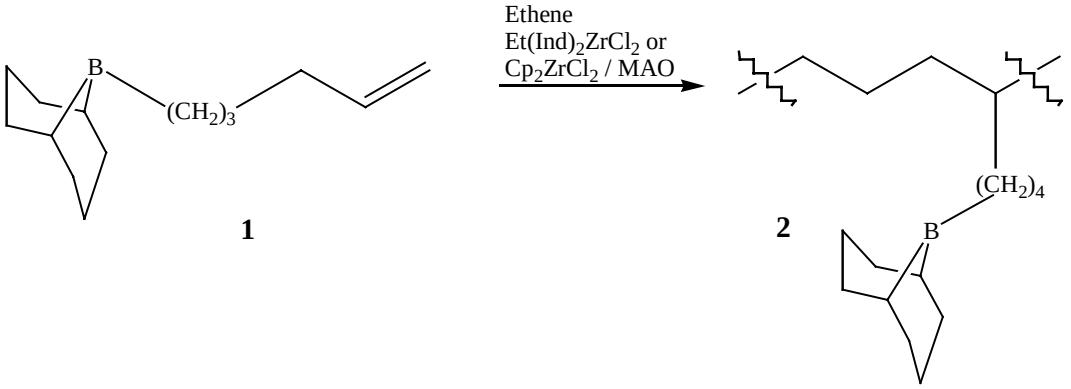

Figure 1. The formation of copolymer **2** from ethene and **1**.[16,17]

The zirconocene-MAO catalyst system, combined with borane chemistry, has also been utilised in the manufacture of copolymers having polypropene (PP) and functional polymer segments.[19] The procedure involves preparation of PP with a terminal C=C bond, its hydroboration and subsequent oxidation in the presence of free radical polymerisable monomers, such as methyl methacrylate, ethyl methacrylate, vinyl acrylate, butyl acrylate and styrene. The copolymers produced by the

aforementioned method were used as additives to improve the interaction of PP with other polymers.

2.2 Oxygen containing copolymers

The copolymerisation of 10-undecen-1-ol with ethene or propene by various MAO activated zirconocenes has been investigated.[20,21] The catalysts (*n*-BuCp)$_2$ZrCl$_2$ and (Ind)$_2$ZrCl$_2$ produced ethene copolymers with alcohol contents of 9.9 and 0.8 wt-%, respectively. Moreover, the evolution of multiple active sites in these catalyst systems was suggested to be due to the bimodal molar mass distributions of the copolymers. In contrast, the catalysts Et(Ind)$_2$ZrCl$_2$, Me$_2$Si(Ind)$_2$ZrCl$_2$, Me$_2$Si(2-MeInd)$_2$ZrCl$_2$ and Me$_2$Si(2-MeBenz[e]Ind)$_2$ZrCl$_2$ produced ethene-10-undecen-1-ol or propene-10-undecen-1-ol copolymers with narrow molar mass distributions.[21] The highest alcohol content in the copolymers was obtained with Me$_2$Si(2-MeBenz[e]Ind)$_2$ZrCl$_2$ for ethene (13.4 wt-%) and with Et(Ind)$_2$ZrCl$_2$ for propene (3.8 wt-%).

Furthermore, the (*n*-BuCp)$_2$ZrCl$_2$-MAO catalyst system produced ethene-10-undecenoic acid and ethene-methyl 9-decenoate copolymers with an acid content of 2.1 wt-% and an ester content of 1.1 wt-%.[22] Ethene copolymerisation with 10-undecen-1-ol or 5-hexen-1-ol afforded products with a higher comonomer content (9.9 or 3.3 wt-%, respectively).[22] The stronger complex formation between the carbonyl functionalised alkenes and (*n*-BuCp)$_2$ZrCl$_2$-MAO in comparison with the alkenols was suggested to account for the lower incorporation of the former into the respective copolymers. The long CH$_2$-chain isolating the OH group from the C=C bond in 10-undecen-1-ol appeared to enhance its incorporation into the copolymer. The finding that 2-methyl-3-buten-2-ol did not copolymerise with ethene supports this conclusion.

Alcohols are known to generate aluminium alkoxides in their reactions with aluminium alkyls.[23,24] Thus, the treatment of alcohol with MAO or TMA prior to copolymerisation could, in principle, diminish the deactivating effect of the free OH group on the catalyst system. However, the pretreatment of 10-undecen-1-ol with MAO appeared to only slightly affect the subsequent ethene copolymerisation by Et(Ind)$_2$ZrCl$_2$.[21] In the case of the bicycloalcohol **3**, the copolymers of the type **5** were produced via an aluminium alkoxide **4** (Fig. 2).[25] The highest comonomer content (6.2 mol-%) was achieved with (Me$_2$SiCp$_2$)ZrCl$_2$ compared with Et(Ind)$_2$ZrCl$_2$ (3.1 mol-%). In a related study, 5-hexen-1-ol, 10-undecen-1-ol or 10-undecenoic acid was treated with TMA *in situ* and

copolymerised with ethene in the presence of $Et(Ind)_2ZrCl_2$ or $(2\text{-MeBenz[e]Ind})_2ZrCl_2$ and MAO.[26] The former catalyst produced copolymers with alcohol or acid content of 5.0-7.4 mol-%. Incorporation of 5-hexen-1-ol and 10-undecen-1-ol by the latter catalyst proceeded less efficiently, affording copolymers with an alcohol content of 1.1 or 4.0 mol-%, respectively. The authors concluded that the pretreatment seemed to only have a minor influence on the comonomer incorporation, the zirconocenes utilised being more crucial to copolymerisation, instead.[25,26]

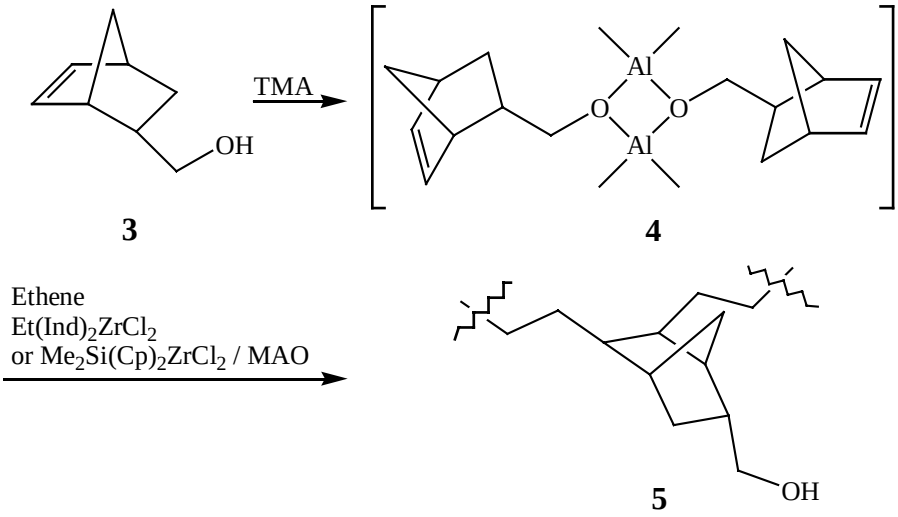

Figure 2. The copolymerisation of **3** with ethene.[25]

An additional example of an oxygen containing comonomer is the phenol derivative **6** depicted in Fig. 3. Copolymers of the type **7**, with narrow molar mass distributions, were obtained from the reaction of **6** and propene catalysed by $Me_2Si(IndH_4)_2ZrCl_2$/MAO.[27] It was presumed that **6** could act as a coordinating anion in the copolymerisation, and hence stabilise the active cationic polymerisation centre. Type **7** copolymers contained 1.3-5.5 wt-% of phenolic units.

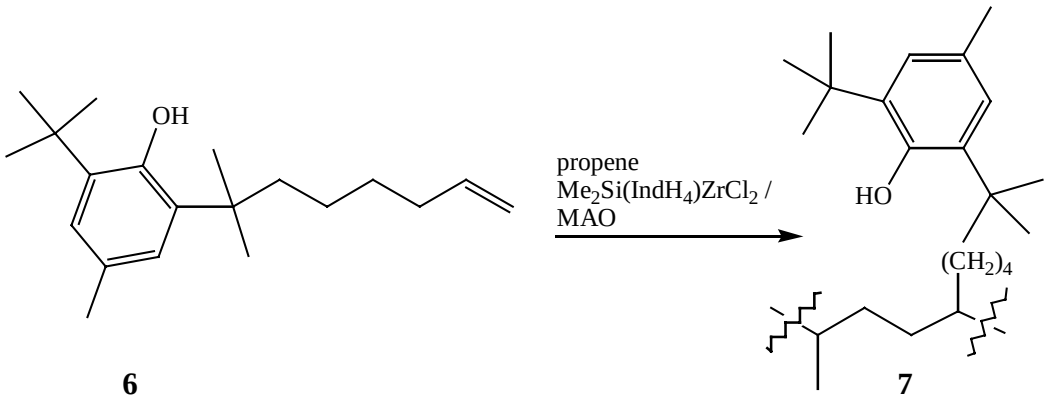

Figure 3. Copolymerisation of **6** with propene.[27]

2.3 Nitrogen, silicon and halogen containing copolymers

Quite a few literature references exist involving a direct copolymerisation of a nitrogen-functionalised alkene with ethene or propene via a zirconocene-MAO catalyst. However, copolymers of the type **9** (Fig. 4a), having amine contents in the range of 6-19 wt-%, were produced in the ethene polymerisation with the silyl protected aminoalkene **8**.[28] The formation of an imide functionality could be accomplished by further treating **9** with styrene-maleic anhydride copolymers.

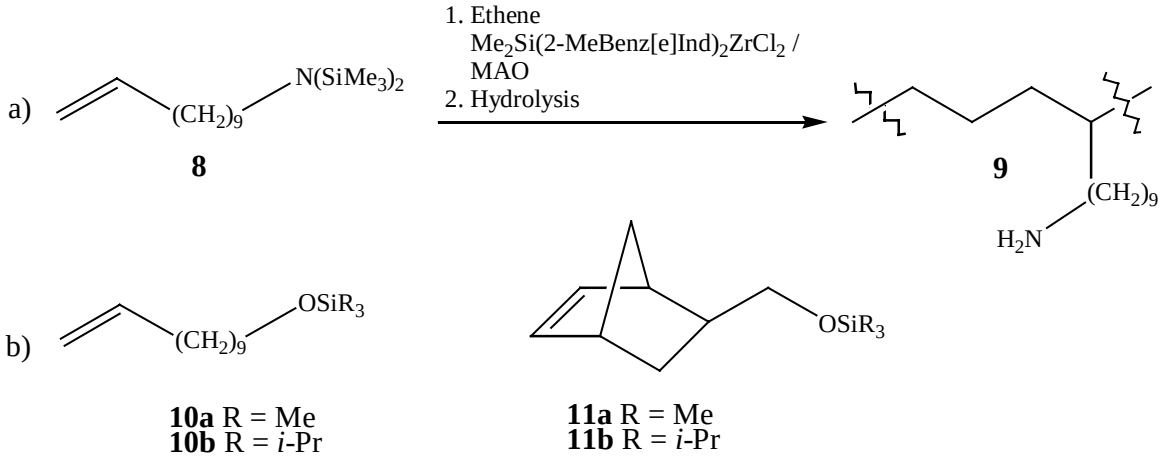

Figure 4. a) Copolymerisation of **8** with ethene[28] and b) the silyl ether derivatives **10a-b**, and **11a-b** used in ethene copolymerisation.[29]

The silyl ether derivatives **10a-10b**, and **11a-b** (Fig. 4b) have been copolymerised with ethene utilising a $Me_2Si(Ind)_2ZrCl_2$ or $Me_2C[(Cp)(Ind)]ZrCl_2$ catalyst and MAO.[29] Comonomer contents of 1.4-20.6 and 13.2-37.7 wt-% were obtained for the ethene-**10b** and ethene-**11b** copolymers, respectively. Compounds **10a** and **11a** deactivated the catalyst system to a substantial degree in comparison with **10b** and **11b**. It was presumed that the catalytically active species reacts with the sterically less hindered $OSiMe_3$ group in preference to the C=C bond and therefore the copolymerisation is impeded. According to a related study,[30] the compound **12** and ethene or propene could be copolymerised by Cp_2ZrCl_2 or $Me_2Si(Ind)_2ZrCl_2$ and MAO. The amount of **12** in the copolymers varied between 17-20 wt-%.

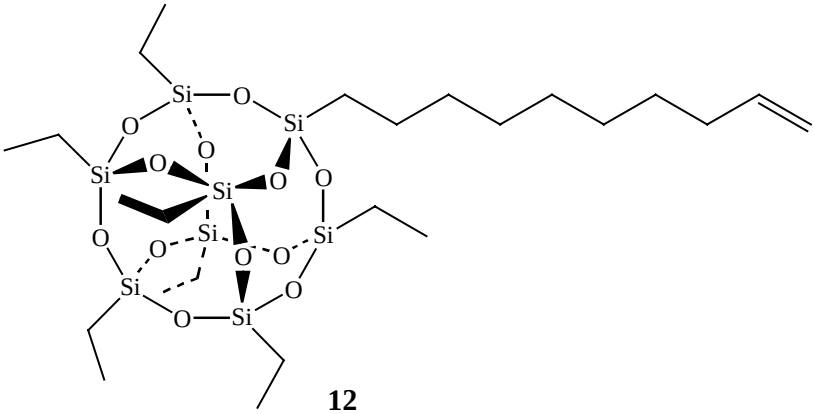

12

The copolymerisation of 11-chloroundec-1-ene and 1-hexene has been accomplished with an $Et(Ind)_2ZrCl_2$/MAO catalyst.[31] Copolymers of the type **13a** or **13b** (Fig. 5) were produced when the reaction medium was toluene or a CH_2Cl_2-heptane solvent mixture, respectively. The authors suggested that **13a** is formed via a Friedel-Crafts type reaction induced by MAO. In contrast to that, the copolymerisation of 5-chloropent-1-ene and 1-hexene did not occur. Apparently it is suppressed due to a complex formation between the chlorine atom and the active catalyst centre.

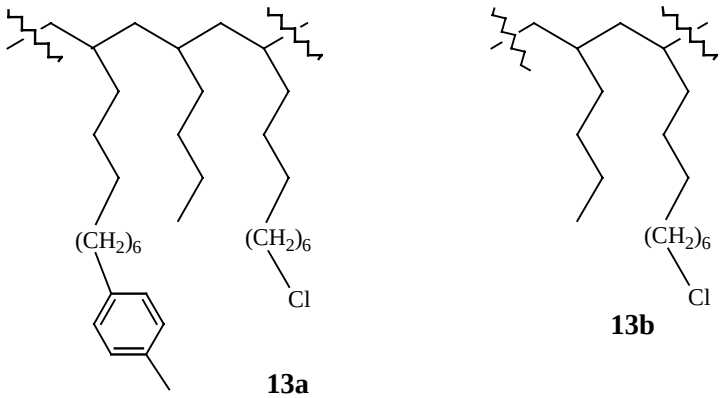

13a **13b**

Figure 5. Copolymers **13a** and **13b** formed in the reaction of 11-chloroundec-1-ene and 1-hexene.[31]

2.4 Copolymerisation of ethene or propene with other alkenes

Even though alkene-alkene copolymers do not contain a polar functionality, they merit a brief presentation of their own due to their wide appearance in the literature.[1,4,5] Applications of these copolymers can be found in package materials, elastic films and fibres, cable coatings and adhesives.[4] In particular, the copolymers containing cycloalkane units can be utilised for optical applications such as compact discs, lenses, films or fibres due to their excellent transparency. In the

following two sections the use of alkenes, aromatics and dienes as comonomers with ethene or propene is reviewed.

2.4.1 Aliphatic and aromatic comonomers

In addition to the numerous ethene-propene copolymerisations performed with MAO activated zirconocenes,[32-42] a variety of ethene or propene copolymerisations with aliphatic acycloalkenes and cycloalkenes exists in the literature. Examples of these are summarised in Table 1.

Table 1. Zirconocene-MAO catalysed copolymerisations of aliphatic alkenes with ethene or propene.

Alkene	Ethene	Propene
	Zirconocene	
1-butene	Cp_2ZrCl_2,[5] $Et(Ind)_2ZrCl_2$,[5] $Me_2Si(Ind)_2ZrCl_2$,[33] $Me_2Si(2\text{-}MeBenz[e]Ind)_2ZrCl_2$,[33] $Me_2Si(IndH_4)_2ZrCl_2$[43]	
4-methyl-1-pentene	$Et(Ind)_2ZrCl_2$,[44] Cp_2ZrCl_2[44]	
1-hexene	Cp_2ZrMe_2,[5] (*n*-BuCp)$_2ZrCl_2$,[42] $(Ind)_2ZrCl_2$,[42,45] $Et(Ind)_2ZrCl_2$,[45,46] Cp_2ZrCl_2,[45] $Me_2Si(Cp)_2ZrCl_2$,[45] $Me_2Si(Ind)_2ZrCl_2$,[5,46] $Me_2Si(IndH_4)_2ZrCl_2$,[46] 1,4-ButanediylSi$(IndH_4)_2ZrCl_2$,[46]	$Me_2C[(Cp)(Flu)]ZrMe_2$,[55] $Et[(Cp)(Flu)]ZrMe_2$,[55] $Et(IndH_4)_2ZrMe_2$,[55] $Et(Ind)_2Zr(NMe_2)_2$,[56] $Et(Ind)_2Zr(NBu_2)_2$,[56] $Me_2Si(2\text{-}Me\text{-}4\text{-}Bu_t\text{-}Cp)_2Zr(NMe_2)_2$,[56]
1-octene	$Me_2Si(Ind)_2ZrCl_2$,[33] $Me_2Si(2\text{-}MeBenz[e]Ind)_2ZrCl_2$,[33] $Me_2Si(Benz[e]Ind)_2ZrCl_2$,[33] $Me_2Si(2\text{-}MeInd)_2ZrCl_2$,[33] $Me_2Si(Cp)_2ZrCl_2$[45] Cp_2ZrCl_2,[33,45]	$Me_2C[(Cp)(Flu)]ZrCl_2$,[33] $Me_2Si(Ind)_2ZrCl_2$,[33,57] $Me_2Si(2\text{-}MeInd)_2ZrCl_2$,[33,57] $Me_2Si(Benz[e]Ind)_2ZrCl_2$,[33,57] $Me_2Si(2\text{-}MeBenz[e]Ind)_2ZrCl_2$,[33,57]
1-hexadecene	(*n*-BuCp)$_2ZrCl_2$,[42] 1,4-ButanediylSi$(IndH_4)_2ZrCl_2$,[46] $Me_2Si(Ind)_2ZrCl_2$,[46] $Et(IndH_4)_2ZrCl_2$[46] $Me_2Si(IndH_4)_2ZrCl_2$[46] $Et(Ind)_2ZrCl_2$,[46]	
cyclopentene	$Et(IndH_4)_2ZrCl_2$,[4] $Et(Ind)_2ZrCl_2$[47]	$Et(Ind)_2ZrCl_2$,[48] $Me_2Si(Ind)_2ZrCl_2$[58]
cycloheptene	$Et(Ind)_2ZrCl_2$[47]	
cyclooctene	$Et(Ind)_2ZrCl_2$[47]	
norbornene	$Me_2C[(3\text{-}Bu_tCp)(Flu)]ZrCl_2$,[4] $Ph_2C[(Cp)(Flu)]ZrCl_2$,[4,9] $Ph_2Si(Ind)_2ZrCl_2$,[9] $Me_2C[(Cp)(Flu)]ZrCl_2$,[9] Cp_2ZrCl_2,[9,48] $Et(IndH_4)_2ZrCl_2$,[9,48] $Et(Ind)_2ZrCl_2$,[9,48-50] $Me_2Si(Ind)_2ZrCl_2$,[4,9,50] $Me_2C[(Cp)(Ind)]ZrCl_2$,[51,52,54] $MeCH(Cp)_2ZrCl_2$,[52-54] $Me_2C[(3\text{-}MeCp)(Ind)]ZrCl_2$,[52-54] $Me_2C[(Cp)(Flu)]ZrCl_2$,[52-54] $Me_2C[(3\text{-}Bu_tCp)(Ind)]ZrCl_2$,[52-54] $Me_2C[(3\text{-}Bu_tCp)(Flu)]ZrCl_2$,[52-54] $Me_2C[(3\text{-}Pr_iCp)(Flu)]ZrCl_2$,[52-54] $Me_2C[(3\text{-}MeCp)(Flu)]ZrCl_2$,[52-54] $Me_2Si[(3\text{-}Bu_tCp)(Flu)]ZrCl_2$,[54]	$Me_2Si(Ind)_2ZrCl_2$[59]
DMON[a]	$Ph_2C[(Cp)(Flu)]ZrCl_2$,[4] $Ph_2C[(Cp)(Ind)]ZrCl_2$[4]	
TMDA[b]	$Ph_2C[(Cp)(Flu)]ZrCl_2$[4]	

a) 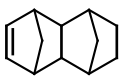 b) 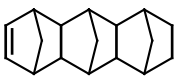

Copolymerisation of cycloalkenes with ethene or propene generally occurs without ring opening,[3,47,58] as presented for norbornene in Fig. 6a.[51-54] However, cyclohexene did not copolymerise with ethene, presumably due to the stability of the six-membered ring.[47] In the case of

compound **14** having an exocyclic C=C bond, the copolymerisation proceeded via a ring cleavage to produce **15** (Fig. 6b).[60]

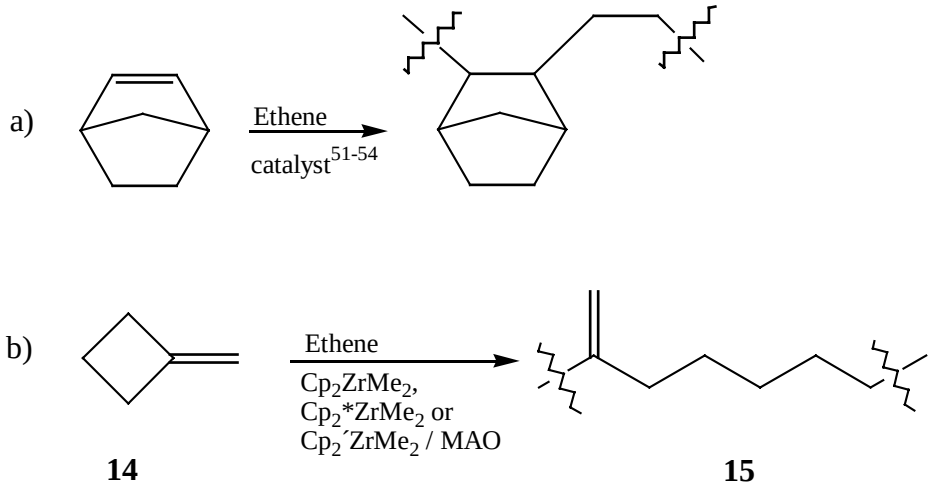

Figure 6. Copolymerisation of ethene with a) norbornene[51-54] (see Table 1 for the catalysts used) and b) compound **14**.[60]

In addition to styrene[61-64] and *p*-methylstyrene,[65] aromatic compounds **16** and **17** have been employed as comonomers in MAO-zirconocene catalysed ethene polymerisations.[66,67]

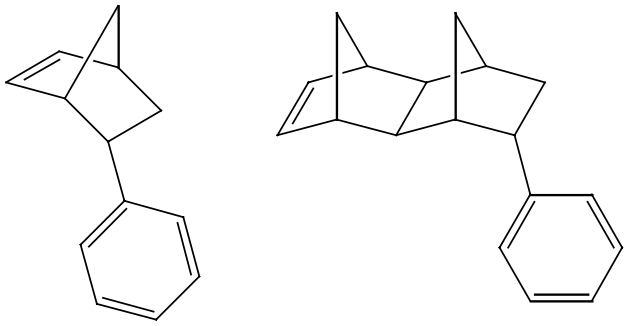

2.4.2 Diene comonomers

Copolymerisations of propene with 1,5-hexadiene and 1,7-octadiene have been performed with MAO activated $Me_2Si(Ind)_2ZrCl_2$ and $Ph_2C[(Cp)(Flu)]ZrCl_2$.[68] Copolymers with diene contents up to 75 mol-% were achieved with the latter catalyst. The appearance of cyclopentane and cycloheptane units in the copolymers, derived from the intramolecular cyclisation of the corresponding dienes, was favoured at a high diene concentration. Propene[69,70] and ethene[69] have

also been copolymerised with 2-methyl-1,3-butadiene, 2-methyl-1,4-pentadiene, 7-methyl-1,6-octadiene, 5,7-dimethyl-1,6-octadiene and 1,7-octadiene in the presence of an $Et(Ind)_2ZrCl_2$-MAO catalyst. The incorporation of branched dienes occurred to a slightly lesser extent than the straight chain 1,7-octadiene.[69]

In the propene-5,7-dimethyl-1,6-octadiene copolymerisation, the sterically more hindered C=C bond of the diene was found to prevent the formation of cyclic units in **18** (Fig. 7a).[70] It could be converted to **19** via epoxidation, however.

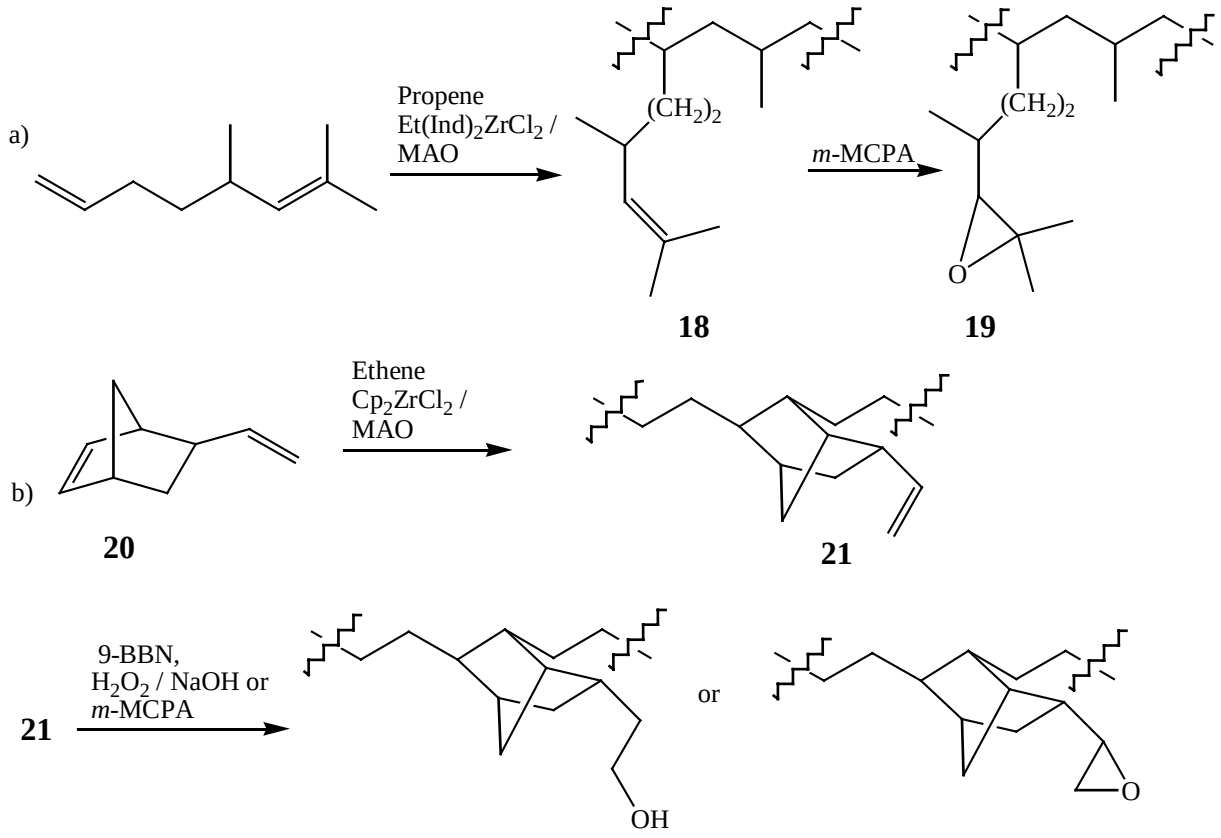

Figure 7. Copolymerisation and further functionalisation of a) propene and 5,7-dimethyl-1,6-octadiene[70] and b) ethene and **20**.[71] (*m*-Chloroperbenzoic acid and 9-borabicyclo[3.3.1]nonane are abbreviated as *m*-MCPA and 9-BBN, respectively.)

An additional example of the copolymer functionalisation is shown for **21**, produced from the diene **20** and ethene (Fig. 7b).[71] A hydroxylated copolymer has also been generated via ethene polymerisation with 4-vinylcyclohexene and the subsequent reaction with 9-BBN and H_2O_2.[72]

3 METHYLALUMINOXANE (MAO)

Aluminoxanes are formed by hydrolysis of aluminium alkyls.[73,74] Generally, an aluminoxane is presented as having a chain of alternating oxygen and alkyl aluminium units with terminal R_2Al groups (structure **22** in Fig. 8).[73]

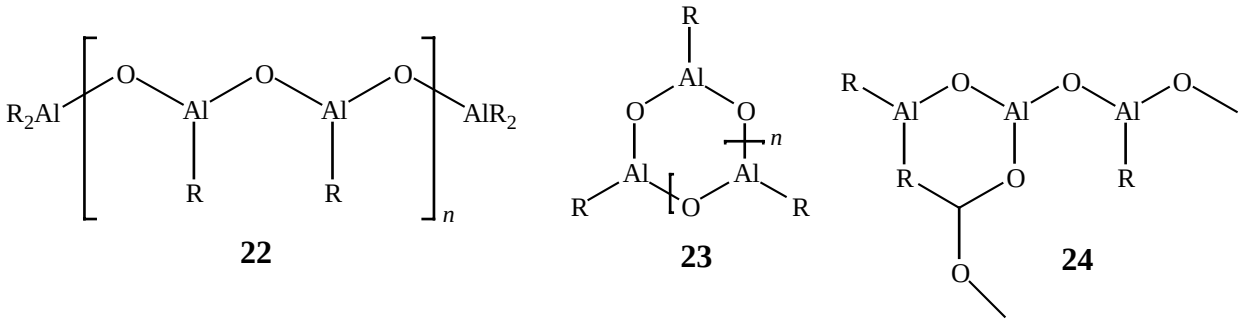

Figure 8. Some structures of alkylaluminoxanes: for MAO R= Me.[73]

The picture is far more intricate owing to the fact that in alkyl aluminoxanes interchain complexation, cyclisation and cross-linking can occur due to the Lewis acidic Al centres and Lewis basic O sites (Fig. 8, structures **23** and **24**).[73,74] The smaller size and superior bridging capability of the methyl group compared with other alkyl groups cause MAO to be particularly prone to the aforementioned conversions. These structural features of MAO are inspected in the following section.

3.1 Structural characterisation by ^{1}H and ^{13}C NMR spectroscopy

The broad ^{1}H resonance centred at δ ca. –0.40 ppm (Fig. 9[75]) is generally attributed to MAO species having different linear or cyclic structures.[76] Alternatively, the polymeric nature of MAO and its tendency to associate could account for the broad appearance of the signals observed.[76]

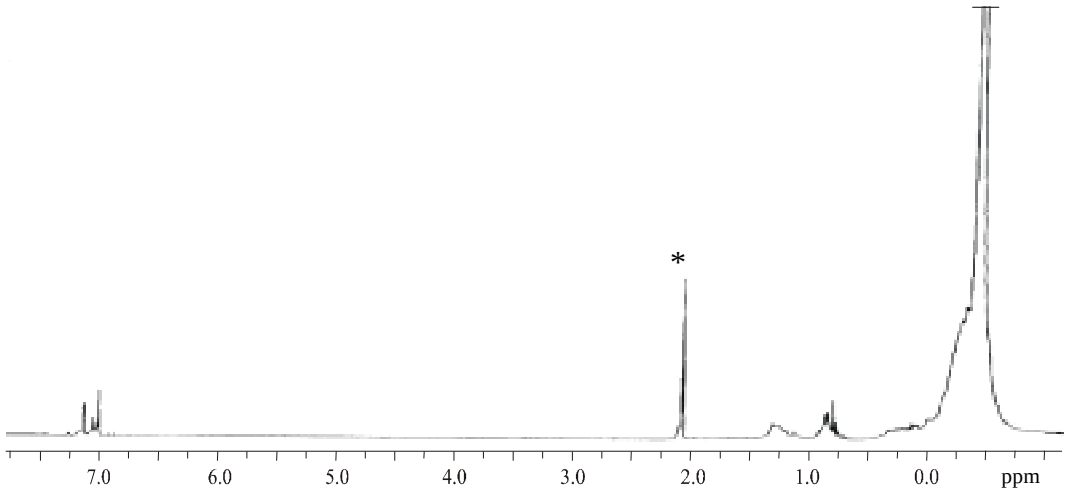

Figure 9. The ^{1}H NMR spectrum of MAO referenced* to the residual C*H*D$_2$ in toluene-d_8 (600 MHz).[75]

The presence of some residual TMA in MAO solutions is commonly acknowledged.[3,8] Several NMR studies on method development for estimating TMA content in MAO,[77-79] and on the impact of TMA to the structural features of MAO,[79-84] have been published. Free TMA appearing as a dimer $(TMA)_2$ and TMA attached to MAO has been suggested to prevail in a toluene solution of MAO.[80] According to the related ^{1}H and ^{13}C NMR studies,[79,81,82] it was deduced that TMA was predominantly bound to MAO. It was further proposed that TMA might participate in the disproportionation reaction of a MAO chain such as **22** in figure 8. This could occur via the $(TMA)_2$-MAO coordination complex **25** (Fig. 10). Hence, the observed ^{1}H and ^{13}C resonances were assigned to the OAlMe$_2$ chain-end groups of the attached $(TMA)_2$ as well as to the bridging and unbridging methyl groups of the free $(TMA)_2$ residue. However, an argument stating that the ^{1}H signals of TMA attached to MAO are disposed under the broad resonance of MAO itself, and hence are not separately observable, has also been presented.[83]

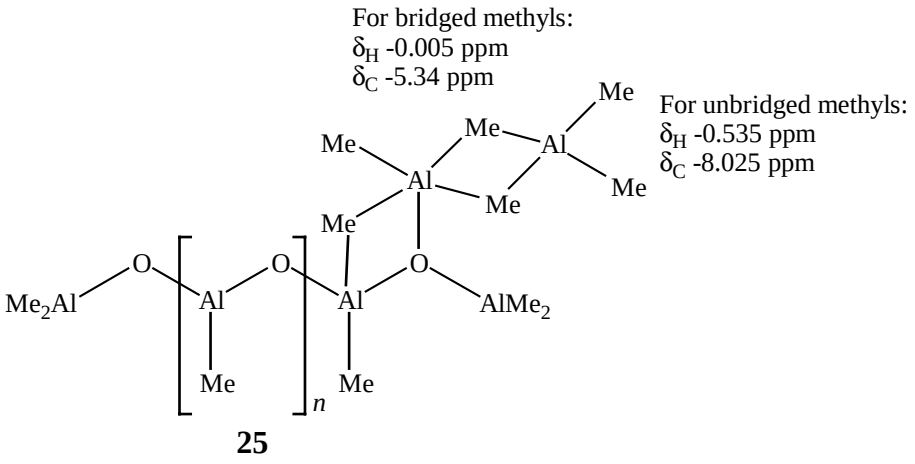

25

Figure 10. $(TMA)_2$-MAO complex **25** ($\delta_{H,C}$ were measured at –78 °C in toluene-d_8).[82]

This is in agreement with the ^1H NMR analysis implying that TMA mediated disproportionation of MAO does not occur even though TMA might be weakly bonded to MAO in solution.[84] Structure **26**, formed by coordination of Al and O atoms from adjacent oligomeric chains, was alternatively proposed.[84]

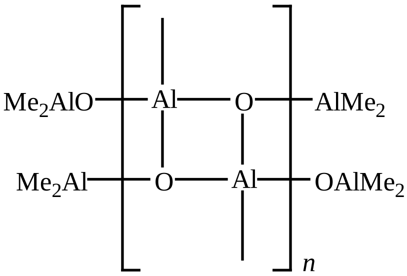

26

3.2 Structural characterisation by ^{27}Al and ^{17}O NMR spectroscopy

The ^{27}Al spectrum of a MAO solution displaying solely one resonance (δ 154 ppm) has been measured at room temperature.[85-88] The resonance was assigned to aluminium atoms with a coordination number of four. The authors suggested that an aluminium atom that is complexed either inter or intramolecularly to an additional oxygen atom, or involved in Al-CH_3-Al bridge bonding, could produce the observed signal.[86-88] A plausible structure **27** accounting for the assignment was proposed.[85]

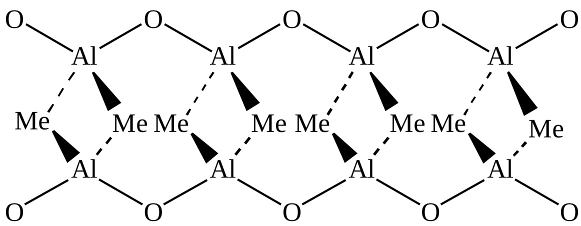

27

An additional ^{27}Al resonance appeared at δ 100 ppm, when the temperature was raised from 25 °C to 90 °C.[83-88] It was assigned to a three-coordinated aluminium present in the MAO structure.[85-87] The assignment was deduced on the basis of the model compound MeAl(2,6-di-*t*-butyl-4-methyl-phenoxy)$_2$ which has been previously shown[89] to have a three-coordinated aluminium (δ_{Al} 100 ppm) bonded to two oxygen atoms and a methyl group.

According to a related study, TMA inherent in MAO and MAO itself displayed their ^{27}Al resonances at δ 149-153 and 60 ppm measured at 25 °C.[83] However, the ^{27}Al signal of MAO reemerged at δ 110 ppm, when the temperature was increased to 40-90 °C (*vide supra*). The corresponding ^{17}O resonance was positioned at δ 67 ppm at 50 °C.[83] The observed ^{17}O and ^{27}Al chemical shifts at the elevated temperature range were similar to the δ-values reported for the synthesised *t*-butyl aluminoxanes such as compound **30**[90] (section 3.4, Fig. 11). Thus, the presence of $(MeAlO)_n$ (*n*= 9-14) oligomers comparable in size with the synthesised cage compounds was suggested to be favoured at increased temperatures, while still larger $(MeAlO)_n$ (*n*= 20-30) clusters with a $MeAlO_3$ environment would predominate at room temperature.[83]

3.3 Structural characterisation by IR and UV spectroscopy

The IR spectrum of MAO exhibited absorption bands at 700-800, 830 and 1272 cm^{-1}.[76,91] These were interpreted as -Al-O-, -O-$AlMe_2$ and -O-Al(Me)-O- structural units of MAO. The latter could form a bridge via its Me group to TMA.[91] The bands at 810 and 619 cm^{-1} were interpreted as evidence for AlO_3 sites in the aluminoxane framework (structures **29** and **31** in Fig. 11).[91] Bridging oxygen atoms of the type Al-O-Al have further been inferred on the basis of the UV absorption band observed at 286 nm.[76]

3.4 Other methods of characterisation

The crystallographic characterisation of the $[Al_7O_6Me_{16}]^-$ anion **28**[92] (Fig. 11) has provided further evidence for the preference of aluminium to the coordination number four rather than three.[74,93] The anion **28** was shown to consist of an Al_6O_6 ring capped by a seventh Al atom. This is, in turn, bonded to three alternate oxygen atoms in the ring. Based on the similarity of **28** to dimeric and trimeric dialkylaluminium alkoxide compounds, fused four- or six-membered rings or both have been proposed as models for MAO (**29**, Fig. 11).[74] The peripheral Al atoms remain three-coordinated in **29**, however. Four-coordinated Al atoms could be achieved if additional methyl bridges originating from TMA were present in **29**.[74,92] Moreover, the synthesis of $[(Bu_t)Al(\mu_3\text{-}O)]_n$ aluminoxanes (*n*= 6, 8 or 9) has further elucidated the structural features of MAO.[90,94] The characterisation of **30** (*n*= 6, Fig. 11) by spectroscopic and crystallographic methods led to a cage

model **31** for MAO (Fig. 11).[90] It contains a trifurcated oxygen acting as a bridge between four-coordinated aluminium atoms.

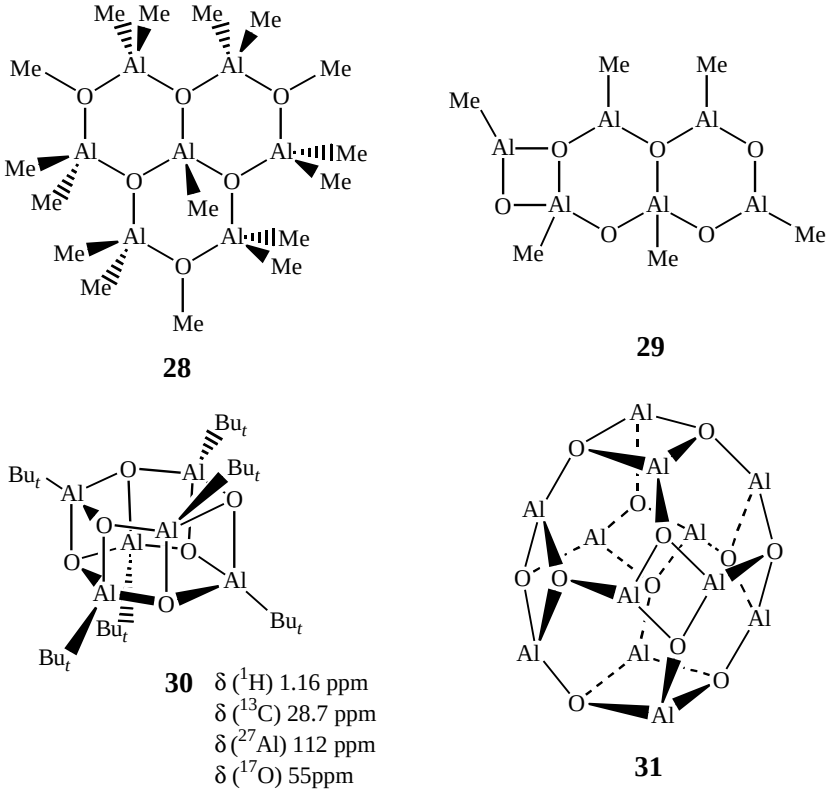

Figure 11. Aluminoxanes **28** and **30** are structurally characterised by X-ray, whereas **29** and **31** represent MAO models deduced on the basis of the two former compounds (methyl groups omitted in **30** for clarity).[74,90,92]

In addition to the model synthetic approach, the structural features of MAO have been investigated by phase separation experiments with diethyl ether[95-97] and molar mass determinations in benzene, 1,4-dioxane, tetrahydrofuran (THF) or TMA.[96] MAO was suggested to resemble the *t*-butyl cage aluminoxanes,[90,94] having a ball-like structure abbreviated as $[Al_4O_3Me_6]_4$.[95-97] Its formation was proposed to occur via a reaction series starting from Me_2Al-O-$AlMe_2$ solvated by TMA.[96] These reactions could proceed further to form longer chains such as Me_2Al-O-$[Al(Me)O]_2$-$AlMe_2$ or six-membered rings via an intramolecular coordination of the O to Al atoms in the chain. It was presumed that these cyclic aluminoxanes produce the fused $Al_8O_6Me_{12}$ **32** of which $[Al_4O_3Me_6]_4$ is derived.[95,96]

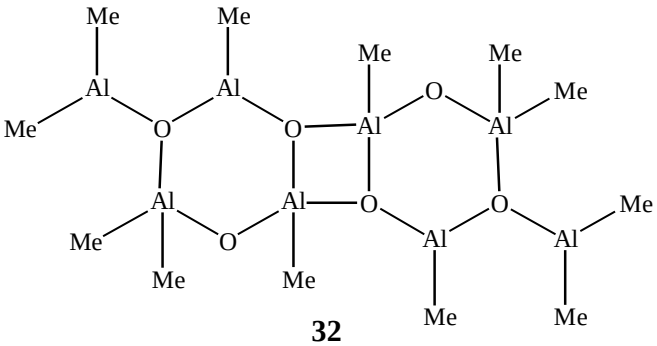

32

MAO synthesised from TMA and $Al_2(SO_4)_3 \bullet 18H_2O$ has also been characterised by GPC.[98] Besides TMA, different $Me_2AlO[Al(Me)O]_nAlMe_2$ fragments having molar masses in the range of 250-1500 g/mol were found (*n*= 2, 7, 11, 17, 23).

3.5 Interaction with zirconocene based catalysts

For the conversion of zirconocenes into active alkene polymerisation catalysts, the generation of zirconocene cations by some strongly Lewis acidic reagent appears to be essential.[2-4,8-10] The active centre is most commonly produced by MAO[10] through complexation and alkylation reactions of the zirconocene catalysts.[3,99-101] The active site has been described as a crown-aluminoxane complex analogous to a crown ether complex of cations.[102] Moreover, the abstracted Cl^- and/or Me^- anions from a zirconocene presumably form $[AlMe_3Cl]^-$ or $[AlMe_4]^-$ species with the TMA present in MAO, and hence displace the negative charge over the MAO.[96] The location of the charge is, however, vague at the present.[1] The formation and detection of the zirconocene cation stabilised by the MAO counter anion is reviewed in the following four literature sections.

3.5.1 ^{1}H NMR studies

The reactions of MAO with Cp_2ZrCl_2, $Cp_2Zr(Me)Cl$, Cp_2ZrMe_2 and $(Cp_2ZrCl)_2O$ have been monitored by ^{1}H NMR.[99,103,104] The reaction pathways suggested in figure 12 involve complex formations between MAO and zirconocenes, followed by alkylation(s), to produce **33**. In the case of $(Cp_2ZrCl)_2O$, a cleavage of the Zr-O bond occurs producing **34** and $Cp_2Zr(Me)Cl$. The species **33** and **34** react further with MAO to form **35**. Methane elimination from **35** affords **36** having a -Zr-CH_2-Al- structural unit. Similarly, a species **37** containing a -Zr-CH_2-Zr- bond could be formed via hydrogen transfer reactions involving the methyl groups of two zirconocene molecules. Species of the types **36** and **37** were concluded to be inactive for polymerisation since the methane evolution

was noticed to increase with simultaneous decrease in the polymerisation rate. However, a methyl exchange with MAO was suggested to reactivate **36** and **37**, forming **35**, a plausible model for the active site.[103] The formation of zirconocene-MAO complexes or ionic species from substituted (R-Cp)$_2$ZrCl$_2$ has also been established (R= *n*-Bu, Me$_3$Si or *t*-Bu).[105,106]

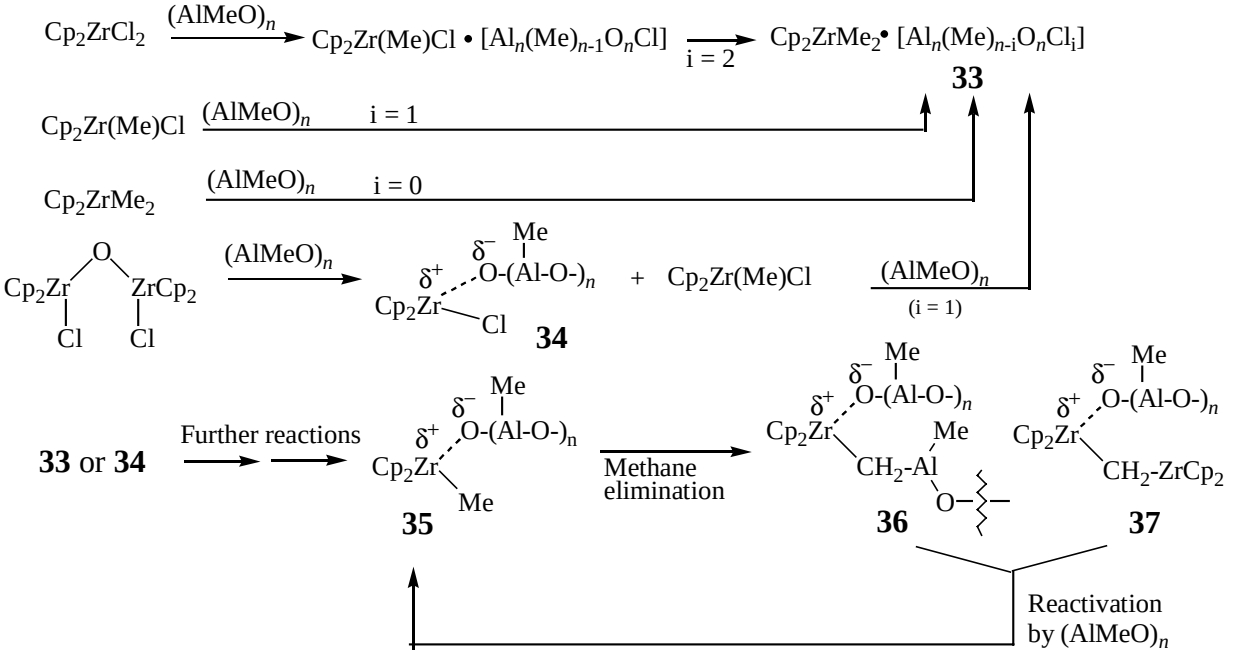

Figure 12. The reactions of MAO depicted as (AlMeO)$_n$ with different zirconocenes (n= 7–12). The partial charges in **34**-**37** reflect the ionic nature of the species (i= the number of Cl atoms).[103]

In addition to MAO, TMA present in the MAO solution has been proposed to account for the alkylation of Cp$_2$ZrCl$_2$.[107] The authors stated that the original C*H*$_3$ resonance of (TMA)$_2$ at δ –0.36 ppm disappeared while monitoring the progress of the Cp$_2$ZrCl$_2$-MAO reaction. The formation of Cp$_2$ZrMeCl (^{1}H δ_{Cp} 5.74 and δ_{Me} 0.36 ppm) besides some unreacted Cp$_2$ZrCl$_2$ (^{1}H δ_{Cp} 5.87 ppm) was observed. According to a related study, the reaction of MAO with Me$_2$Si(Ind)$_2$Zr(NMe$_2$)$_2$ produced the methyl derivatives **38** and **39**, the cationic species **40** and the aluminium compounds **41** and **42** (Fig. 13).[108] The mono and dimethylation of the catalyst was presumed to be accomplished mainly by TMA inherent in MAO.

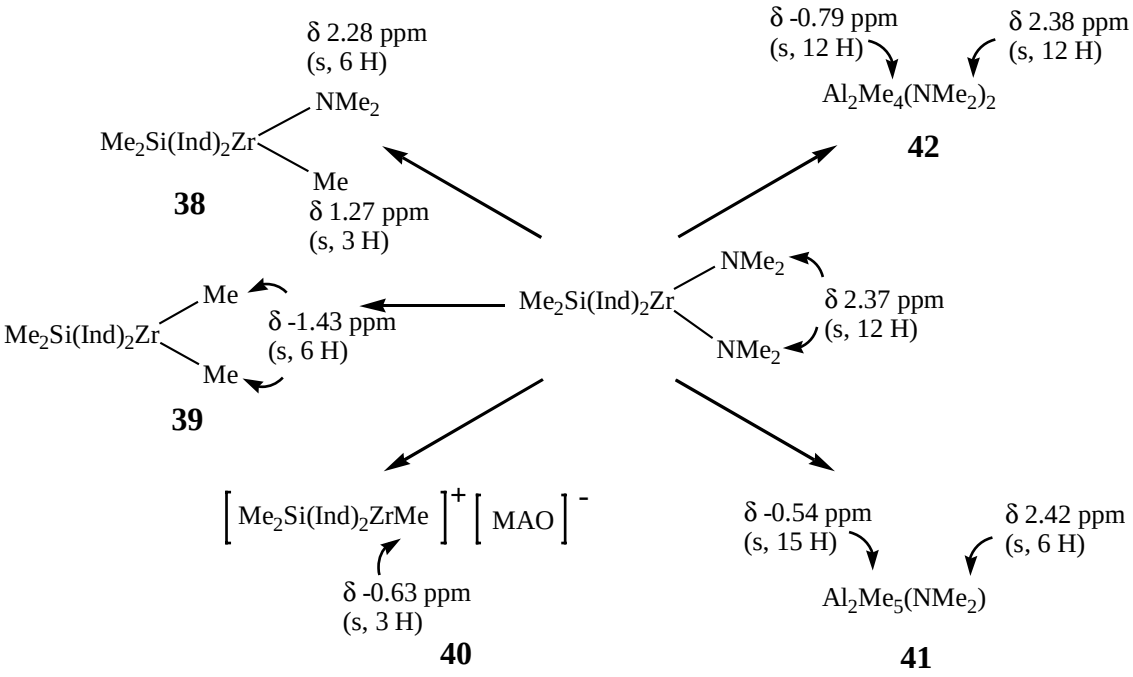

Figure 13. The species **38**-**42** formed in the reaction of MAO and $Me_2Si(Ind)_2Zr(NMe_2)_2$ (in **41** and **42** the NMe_2 and/or Me groups act as bridging ligands).[108] The announced ^1H chemical shift values (δ in ppm) were measured in CD_2Cl_2.

3.5.2 ^{13}C and ^{91}Zr NMR studies

The reaction of Cp_2ZrMe_2 with MAO has been investigated by ^{13}C and ^{91}Zr NMR.[86-88] Formally, an ionic methyl transfer from the zirconocene to Al sites of MAO producing $[Cp_2ZrMe]^+$ solvated by $[Me\text{-}MAO]^-$ (**43** in Fig. 14) was suggested. The availability of a three-coordinated Al atom appeared to be a prerequisite for the methyl exchange to occur, since it was not observed with compounds containing a four-coordinated aluminium such as $(Et_2AlOEt)_2$. The finding that degenerate methyl exchange[109] prevailed between MAO and $Cp_2Zr(^{13}CH_3)_2$, $(Ind)_2Zr(^{13}CH_3)_2$ $Me_2Si(Cp)_2Zr(^{13}CH_3)_2$ and $(Cp^*)_2Zr(^{13}CH_3)_2$ supported the view of a reversible methyl transfer reaction.[86-88]

In addition to the ion pair **43**, the appearance of **44** and **45** and their interconversion in the MAO-Cp_2ZrMe_2 catalyst system (Fig. 14) has been presented.[110] The ion pairs formed exhibited Zr-*C*H_3 resonances at a lower field compared with Cp_2ZrMe_2 due to the electron deficient zirconium. In agreement with the former statement,[110] a cationic zirconocene species (^{13}C δ_{Cp} 114.4 and δ_{Me} 41.3 ppm) was observed from a MAO-Cp_2ZrMe_2 mixture by solid state NMR spectroscopy.[111] The activity of ionic species of the types **44** and **45** in the polymerisation is still under debate.[110,112-114]

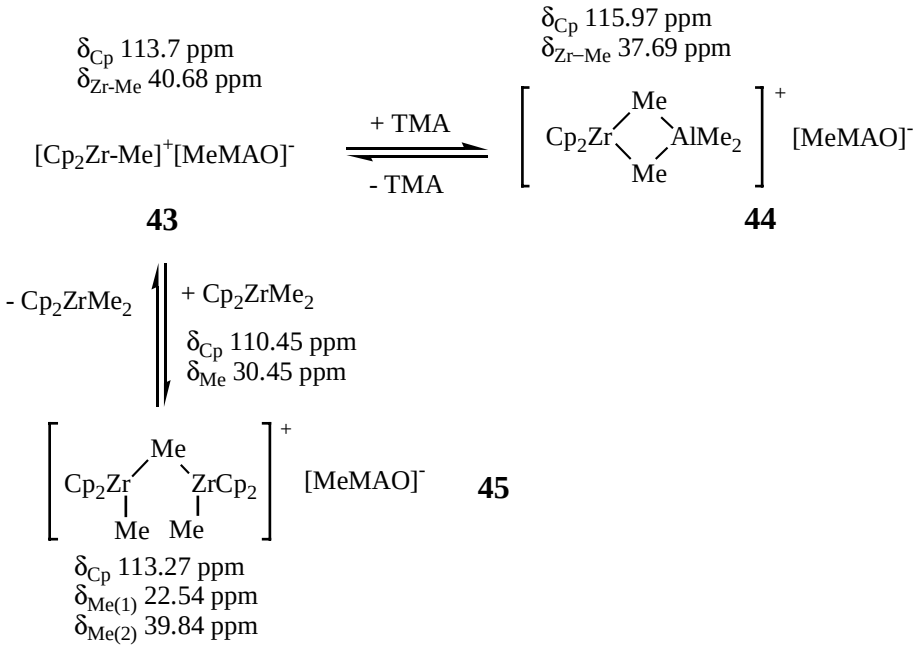

Figure 14. The proposed interconversion of **43**-**45** and the ^{13}C chemical shift values (δ in ppm) assigned for the different species measured in toluene-d_8 at –20 °C (the Me(1) and Me(2) refer to the bridgeheaded and unbridgeheaded methyls, respectively).[110]

Moreover, the ^{91}Zr resonances measured from the Cp_2ZrMe_2-MAO mixture appeared at δ 100 and –100 ppm.[86,88] The former was attributed to the $[Cp_2ZrMe]^+$ cation and the latter to a $Cp_2Zr(Me)$-OAl- species of which Zr-*C*H_3 existed at δ_C 18 ppm. This is in agreement with the chemical shifts obtained for the model compound $Cp_2Zr(Me)(OMe)$.[109] Its ^{91}Zr and $^{13}C_{Me}$ resonances were displayed at δ –127 and 19 ppm, respectively. The presence of residual Cp_2ZrMe_2 in the catalyst mixture could be excluded since its ^{91}Zr resonance (δ_{Zr} 385 ppm) was not detected in the spectrum.[86,88]

3.5.3 UV-Visible (UV/Vis) spectroscopic studies

A detailed description of the plausible ionic species formed in the MAO-$Et(Ind)_2ZrCl_2$ system has been provided by UV/Vis spectroscopic studies.[115,116] $Et(Ind)_2Zr(Me)Cl$ (λ_{max} 390 nm) was observed at a low MAO concentration (the Al/Zr mole ratio <30). Its formation was suggested to occur by TMA mediated methylation of the catalyst. In fact, the UV/Vis spectrum measured from the TMA-$Et(Ind)_2ZrCl_2$ mixture produced an absorption band with the same λ_{max} value.

The appearance of a MAO stabilised zirconocene cation (λ_{max} 440 nm) bearing resemblance to **43** and **44** (Fig. 14) or alternatively, to **46** and **47** (Fig. 15), was observed when the Al/Zr mole ratio remained in the range of 30-140.[115,116] By still increasing the concentration of MAO, another cationic zirconocene species (λ_{max} 470 nm) was generated. It was presumed to be due to the dissociation of the preceeding ion pair at λ_{max} 440 nm. The catalyst activity measured in the hexene polymerisation was in accordance with the concentration variations of the catalyst components, and hence with the λ_{max} changes. An increase in activity was observed for Al/Zr mole ratios exceeding 50.

46 **47**

L = Et(Ind)

Figure 15. Postulated species **46** and **47** with an Uv/Vis absorption band centred at 440 nm.[115,116]

3.5.4 Synthetic studies

In addition to the spectroscopic studies (*vide supra*), a synthetic approach for characterising the catalytically active species has been widely applied. The method comprises synthesis of $[L_2Zr(R)]^+[X]^-$ complexes having counter anions, $[X]^-$, other than MAO. Generally, boron based counter anions such as $[MeB(C_6F_5)_3]^-$,[117-122] $[B(C_6F_5)_4]^-$,[122-125] $[B(C_6F_4TBS)_4]^-$,[122] $[B(C_6F_4TIPS)_4]^-$ [122] and $[BPh_4]^-$[126,127] have been employed (TBS= *t*-butyl dimethylsilyl, TIPS= tri-*i*-propylsilyl). The $[L_2Zr(R)]^+[X]^-$ complexes have been proven to polymerise ethene in the absence of aluminium based cocatalysts, and hence provided evidence for $[L_2Zr(R)]^+$ cations being the active species in zirconocene/MAO catalyst systems. Additional support for this conclusion was obtained when the treatment of the $[L_2ZrMe]^+[B(C_6F_5)_4]^-$ ion pair with TMA produced **44** (Fig. 14) having a $[B(C_6F_5)_4]^-$ counter anion (L= Cp, $Et(Ind)_2$ or $Me_2Si(Ind)_2$).[124] Since residual TMA is known to be present in the MAO solution, species of the type **44** were regarded as the primary products formed in MAO-zirconocene catalyst systems.

A related approach to characterise plausible active species or their precursors involves the synthesis and reactions of cage aluminoxanes $[(Bu_t)Al(\mu_3\text{-}O)]_n$ (*n*= 6, 7 or 9) with zirconocenes.[128] In the

presence of Cp_2ZrMe_2, these compounds have been demonstrated to polymerise ethene. It was presumed that the catalytic activity observed arose from their latent Lewis acidity. Thus, a Lewis acidic site could be generated via ring cleavage as depicted for **48** (Fig. 16) originating from **30** (see Fig. 11 for the structure).

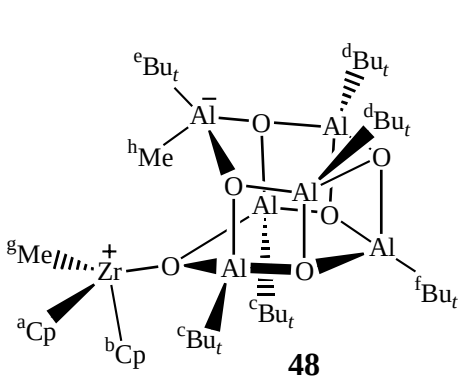

48

δ_H in ppm

[a]Cp 5.92
[b]Cp 5.87
[c]Bu_t 1.36 & 1.37
[d]Bu_t 1.34 & 1.35
[e]Bu_t 1.28
[f]Bu_t 1.15
[g]Me 0.71
[h]Me -0.50

Figure 16. The ^{1}H chemical shifts assigned for **48** formed in the reaction of **30** and Cp_2ZrMe_2. The spectrum was measured in toluene-d_8 at 11 °C. The exact location of + and – charges is not known.[128]

Moreover, the presence of four-coordinated aluminium atoms in cage compounds was suggested to be crucial for their catalytic activity since the aluminoxane **49** having both three and four-coordinated Al atoms did not activate Cp_2ZrMe_2 in ethene polymerisation.[128]

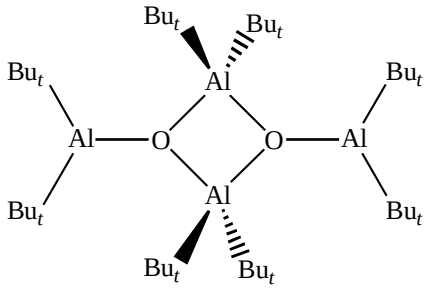

49

3.6 Interaction with polar compounds

Relatively few studies involving the reactions of MAO and polar compounds can be found in the literature.[129-131] The interaction of 10-undecen-1-ol and MAO has been monitored by ^{1}H, ^{13}C and ^{27}Al NMR spectroscopy.[129] TMA present in MAO was suggested to account for the formation of **50** and **51** (Eq. 1 and 2, R= 10-undecenyl).

$2\ AlMe_3 + 2\ ROH \longrightarrow [Me_2AlOR]_2 + 2\ CH_4$ Eq. (1)

50

50 $+ 2\ ROH \longrightarrow [MeAl(OR)_2]_2 + 2\ CH_4$ Eq. (2)

51

In addition, the occurrence of an aluminium species with a six-coordinated central Al atom, $Al_4Me_6(OR)_6$, was observed. According to a related solid state ^{13}C and ^{27}Al NMR study, Al-O-$(CH_2)_n$-O-Al- fragments were formed in the reaction of MAO and 1,6-hexanediol (n= 6) or 1,10-decanediol (n= 10).[130]

In organic synthesis, MAO has been utilised as a Lewis acid reagent in the Diels-Alder reactions of cyclopentadiene and various dienophiles including aldehydes, ketones and esters (Fig. 17a).[131] Moreover, MAO effected the amidation of methyl benzoate (Fig. 17b).

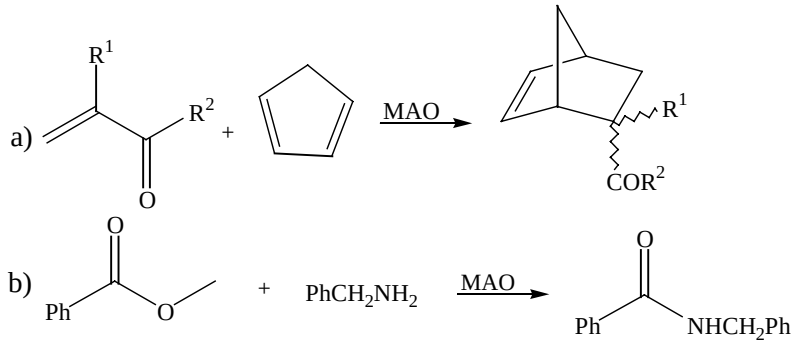

Figure 17. MAO activated a) Diels-Alder reaction and b) amidation (R^1= Me, R^2= H; R^1= H, R^2= Me or R^1= Me, R^2= OMe).[131]

Since the cage aluminoxanes resemble MAO to some extent,[90,94] the interaction of the former with polar compounds is briefly illustrated with a couple of examples herein. In the reaction of **30** (Fig. 11) and *n*-butyl amine, compound **52** was produced, its structure being determined by X-ray crystallography.[132]

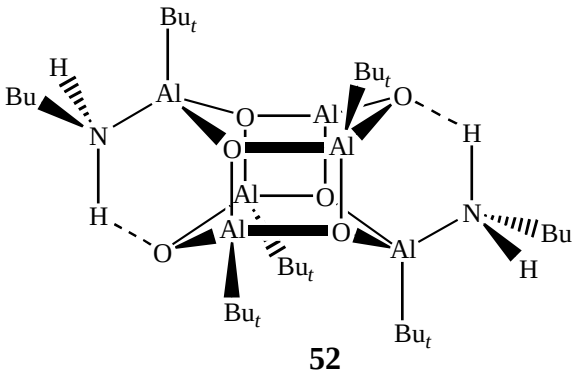

52

Analogous reactions occurred with the other *prim* amines RNH_2 studied (R= Et, Pr, *i*-Pr, *t*-Bu).[132] *Sec* amines R_2NH (R= Et, *i*-Pr, Bu, Ph) did not react, presumably due to the increased steric hindrance present in R_2NH.[132] The reaction of **30** with benzoic acid[133] or with Cl_3CCO_2H[134] produced cage compounds having five-coordinated Al atoms.

4 SOME SYNTHETIC METHODS FOR THE PREPARATION OF STERICALLY HINDERED ALIPHATIC ACYCLOALCOHOLS AND AMINES

4.1 Alcohols

The Grignard and Barbier reactions have been widely applied for the preparation of *tert* alcohols from alkyl halides and ketones or esters.[135,136] The former involves the preparation of an organo-magnesium species RMgX prior to the addition of the substrate. The latter is a one step procedure in which an alkyl halide is introduced into a suspension of Mg turnings and the substrate in ether in order to produce a *tert* alcohol. This method was employed in the **53a** → **54a** conversion (Fig. 18, route A). Instead of Mg, Li and Ca have been employed as metals.[136,137] Thus, **54b** was produced from **53b** without preliminary formation of RLi (Fig. 18, route B).[137] Furthermore, the SmI_2/NiI_2 mediated Barbier reaction of a ketone **53c** or an ester **53d** and *n*-butyl iodide proceeded in high yields to a *tert* alcohol **54c** or **54d** (Fig.18, route C).[138] The reaction times were short, being in the range of 5-30 min. In the absence of NiI_2, the yield of **54c** decreased to 20%. Similarly, the reaction of **53c** and *s*-butyl-, *i*-butyl- or *t*-butyl bromide without the added NiI_2 afforded poor yields of *tert* alcohols even after prolonged reaction times of 1.5-4 days.[139] The concomitant formation of various side products was also noted.[139]

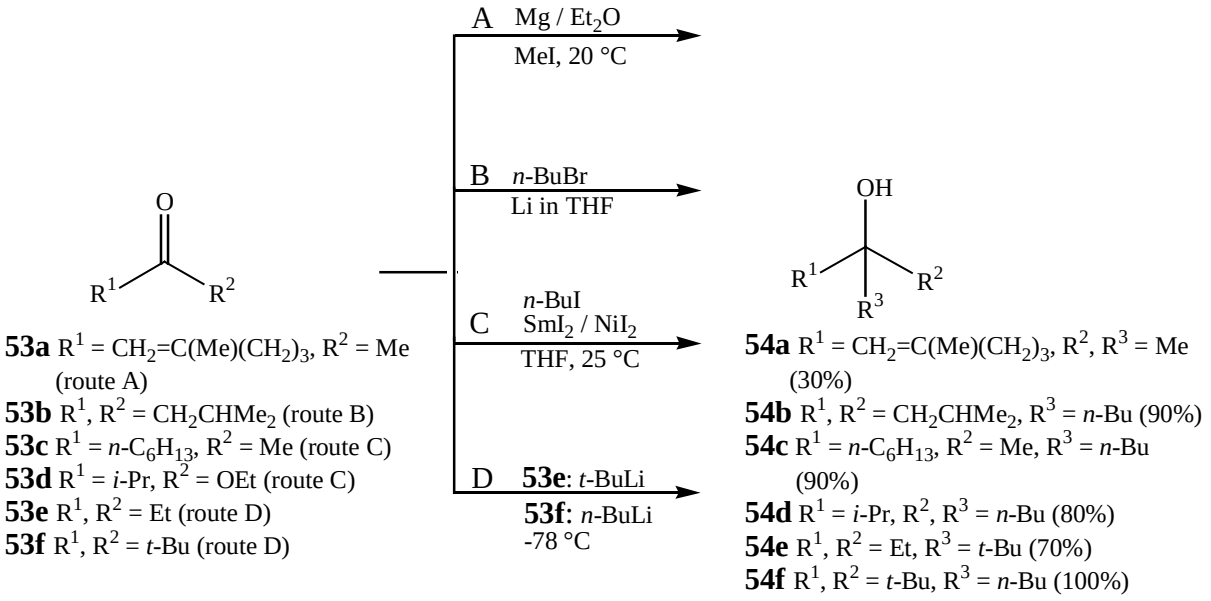

Figure 18. The Barbier reaction of an alkyl halide and a ketone or an ester in the absence of additives (routes A and B) or in the presence of SmI_2/NiI_2 (route C).[136-138] The addition of a ketone into a solution of preformed RLi (route D).[140]

A complication often encountered in synthesis of sterically hindered *tert* alcohols by RMgX is the reduction of a starting carbonyl compound to a *sec* alcohol.[135] Grignard reagents with β-hydrogens are known to favour the reduction. Alternatively, enolisation can occur at the expense of normal 1,2-addition.[135] The latter is typical for **53a-f** (Fig. 18) having an α-hydrogen and bulky R^1 or R^2 substituents.[135] In the synthesis of **54e** and **54f** (Fig. 18, route D), the enolisation and reduction were largely suppressed due to the low reaction temperature (–78 °C).[140] Moreover, the fact that **53e** or **53f** was added into RLi in solution and not *vice versa* was suggested to promote the 1,2-addition. In accordance with this information,[140] (*t*-Bu)$_3$C-OH **55** was synthesised (81%) by adding **53f** into *t*-BuLi solution at –60 - –70 °C.[141]

A number of additives which have been shown to diminish these competing side reactions exists in the literature.[135] Enhanced yields of hindered *tert* alcohols have been obtained by utilising RMgX with anhydrous $CeCl_3$.[142] Thus (*i*-Pr)$_3$-COH was produced from (*i*-Pr)$_2$C=O and *i*-PrMgCl/$CeCl_3$ with the yield of 52%, whereas in the absence of $CeCl_3$ only 3% of the alcohol was formed. In the presence of *t*-BuOLi or the *n*-Bu_4NBr salt, an increased yield of (*i*-Pr)$_3$-COH was obtained (97 and 84%, respectively).[143]

Moreover, organomanganese iodides effected the -COCl → -C=O conversion (Fig. 19).[144] Treatment of the ketone-MnClI complex formed with an alkyllithium or Grignard reagent produced the corresponding *tert* alcohol. Unbranched alkyllithium or organomagnesium reagents and unhindered acyl halides afforded higher yields of the products (50-90%). Reduction of the ketone by $LiAlH_4$ or $NaBH_4$ generated *sec* alcohols.[144]

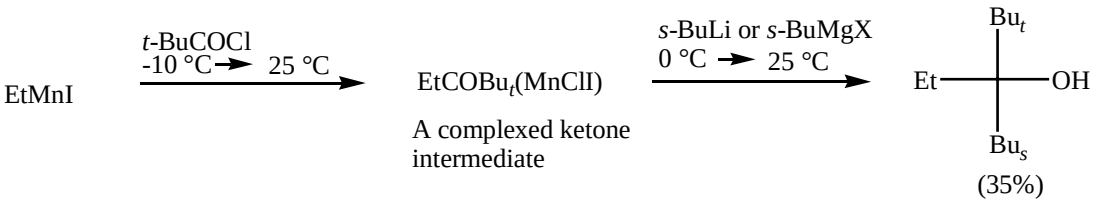

Figure 19. The formation of a *tert* alcohol using an EtMnI reagent.[144]

Trialkylboranes were found to produce *tert* alcohols in their reaction with $CHCl_2OCH_3$ at 25 °C (Fig. 20).[145] Sterically hindered *tert* alcohols were formed with high yields when the $R^1R^2R^3CB(Cl)OMe$ intermediate was converted into a dioxolane derivative prior to the addition of hydrogen peroxide. Moreover, acetal fragmentation to a *tert* alcohol by *n*-BuLi-TMEDA has been reported (TMEDA= *N*,*N*,*N´N´*-tetramethylethylenediamine).[146] The yields were in the range of 84-90%.

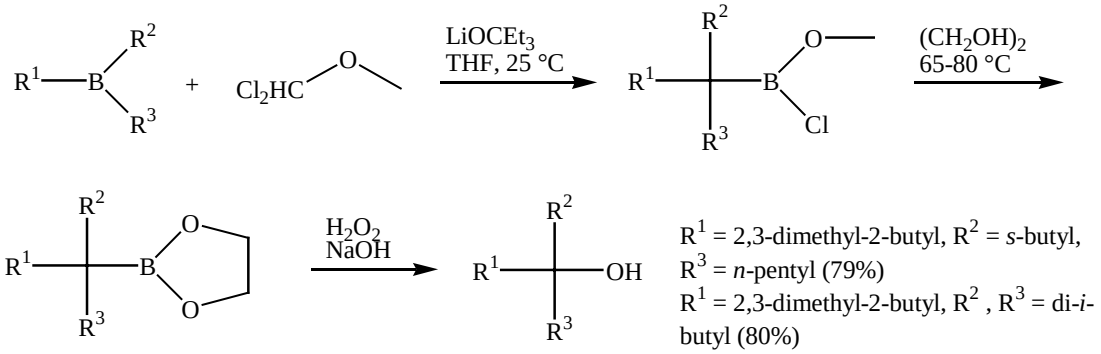

Figure 20. Formation of *tert* alcohols from organoboranes.[145]

In addition, lithiation of sulfide **56** and the subsequent reaction of the formed **57** with isobutyraldehyde afforded *sec* alcohols (Fig. 21).[147] The α-disubstituted **58** was produced at –78 °C whereas **59** formed via a rearrangement of **57** in the presence of TMEDA at –30 °C.

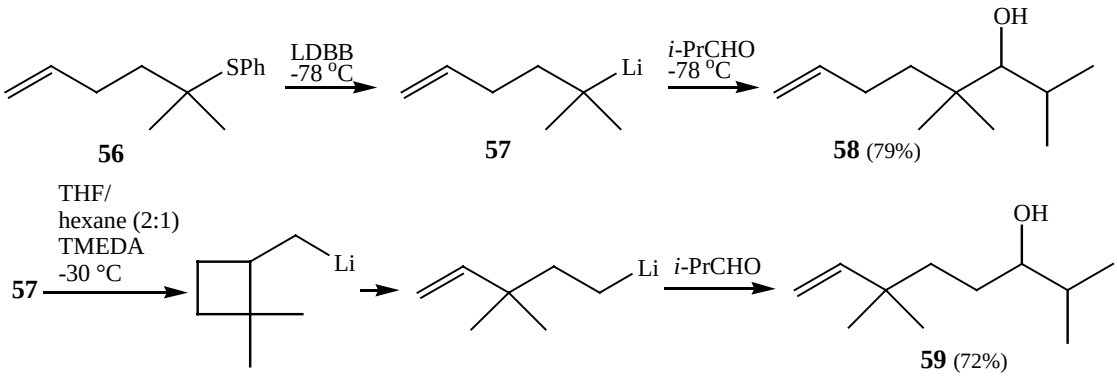

Figure 21. Temperature dependent formation of *sec* alcohols **58** and **59** (LDBB= lithium 4,4´-di-*t*-butylbiphenylide).[147]

4.2 Amines

Tert amines have been synthesised from non-enolisable aldehydes R^1CHO and a titanium reagent R^2-Ti$(NR^3_2)_3$.[148] The yield of 55% for $R^1CH(R^2)(NR^3)_2$ (R^1= *t*-Bu, R^2= Me, R^3= Et) was obtained. An example of *tert* amine formation from a ketone and a *sec* amine using $NaBH(OAc)_3$ as a reducing agent is depicted in Fig. 22.[149] However, a disadvantage of this method is the long reaction time required (8 days). In additon, $(i\text{-Pr})_2NH$ did not react under the experimental conditions employed.

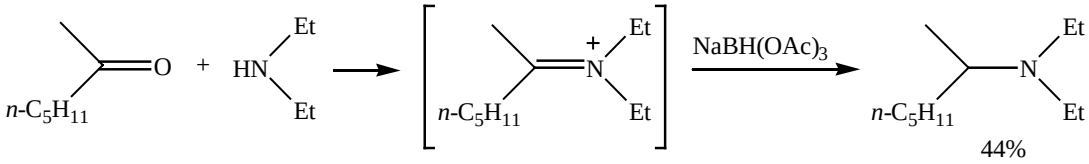

Figure 22. Synthesis of a *tert* amine from a ketone and a *sec* amine.[149]

A more general method for the synthesis of sterically hindered aliphatic *tert* amines has also been presented (Fig. 23).[150] The reaction scheme involves the conversion of an amide derivative into the corresponding iminium salt **60a** or **60b** as a first step. The addition of an organomagnesium or a lithium compound into the reaction mixture produced the amines **61-63**.

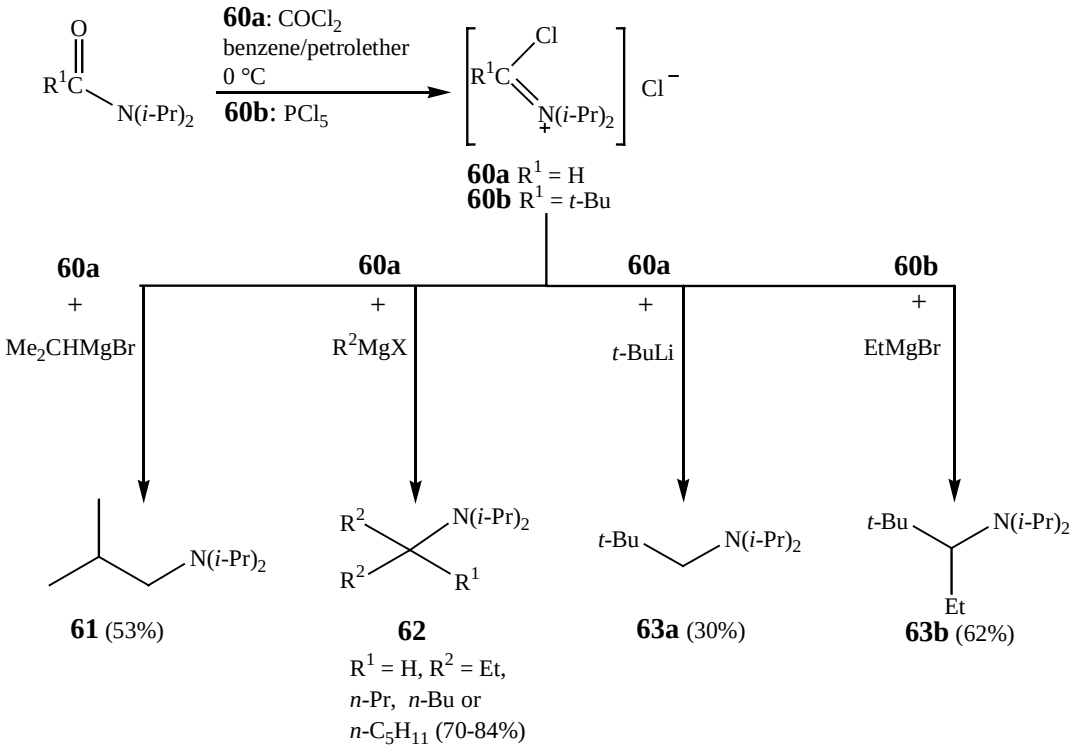

Figure 23. The reaction scheme for the formation of *tert* amines **61**-**63** via iminium salts **60a**-**b**.[150]

Moreover, **64a** (Fig. 24) has been synthesised by direct methylation of di-*t*-butylamine with $MeOSO_2F$ in K_2CO_3/CH_2Cl_2[151] or by the $LiAlH_4$ reduction of di-*t*-butylformamide.[152] The *tert* amines **64b-d** (Fig. 24) were produced in the reaction of di-*i*-propylformamide with the corresponding RMgBr, or in the case of **64d** with MeMgCl.[153,154] Alternatively, **64d** was formed in the reaction of **60a** (Fig. 23) and MeLi.[150] However, the synthesis of tri-*t*-butyl amine **64e**, albeit such a simple molecule has not been accomplished to date,[155,156] in contrast to the oxygen analogue **55** which has been known since the 1940´s.[157] *N*,*N*-dimethyl alkyl amines have been prepared from a *prim* or *sec* alkyl halide in the presence of Me_2NNH_2[158] or $MeCH{=}NNMe_2$.[159] The yields varied in the range of 60-75%.

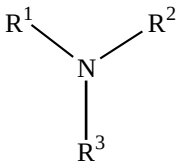

64a R^1, R^2, = *t*-Bu; R^3 = Me
64b R^1, R^2, = *i*-Pr; R^3 = *n*-Et
64c R^1, R^2, = *i*-Pr; R^3 = *n*-Bu
64d R^1, R^2, R^3 = *i*-Pr
64e R^1, R^2, R^3 = *t*-Bu

Figure 24. Structures for *tert* amines.[151-154]

Benzotriazole (BtH in Fig. 25) has been employed as a synthetic auxiliary in the preparation of *tert* amines.[160] The condensation of formaldehyde and BtH produces $BtCH_2OH$ which reacts further

with an alkyl amine to form $R^1N(CH_2Bt)_2$. The addition of a Grignard reagent generates the trialkyl amine. The same methodology has been used in the *sec* amine synthesis of the type $(R^1CH_2)_2NH$. Thus *t*-BuCHO or *i*-PrCHO formed the intermediate $(BtCR^1)_2NH$ in its reaction with BtH and ammonia.[161] This was reduced to the *sec* amine by $LiAlH_4$, the yields being 93 or 90%, respectively. The method was found to be suitable for aliphatic aldehydes not containing α-CH_2 groups. In the case of 1-butanal or ethanal, solely polymeric material was formed.

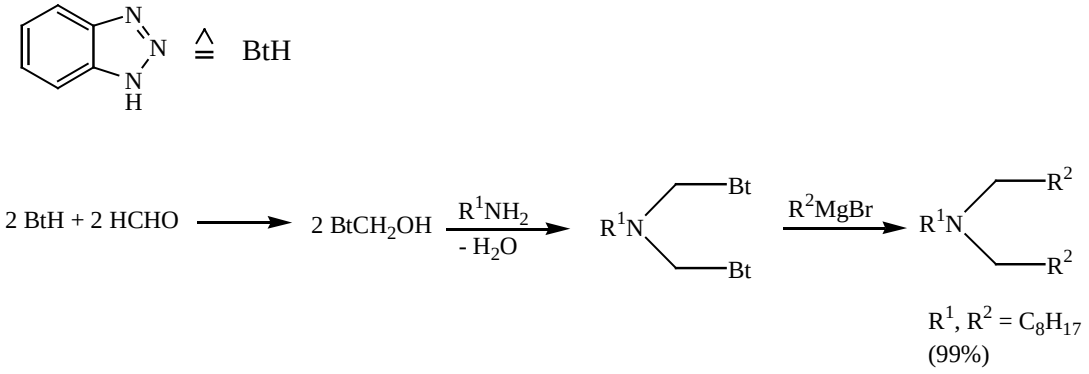

Figure 25. Synthesis of *tert* amines via benzotriazole.[160]

In the presence of $TiCl_4$, a sterically hindered *sec* amine of the type R^1R^2NH was produced from a ketone and a *prim* amine via *in situ* hydrogenation of a ketimine intermediate.[162] The yield for (*t*-Bu)(*i*-Pr)NH or (*t*-$BuCH_2$-CMe_2)(*i*-Pr)NH was 50 and 65%, respectively. Additional procedures for the preparation of hindered *sec* amines have been proposed.[151,163] For example,[151] an alkylamine was oxidised to the nitroso compound **65** (Fig. 26a). The radical reaction of **65** and *t*-$BuNHNH_2$ generated a mixture of **66a** and **66b**, which could be reduced directly to the corresponding amines. These could be separated by distillation. A second method[163] involves the reaction of the nitrone **67** and the Grignard reagent to afford **68** (Fig. 26b).

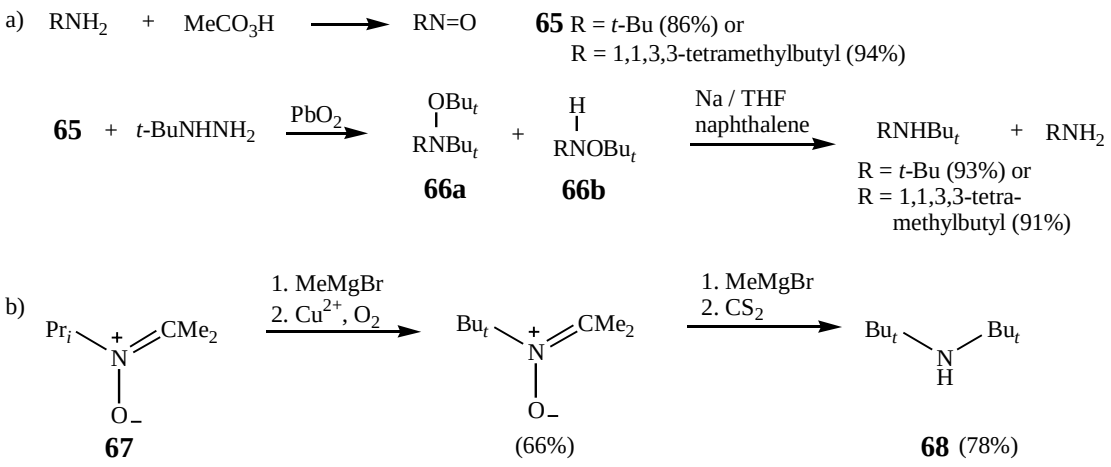

Figure 26. Formation of a *sec* amine from a) nitroso compound **65**[151] and b) nitrone **67**.[163]

Organocerium reagents, prepared from *prim* or *sec* alkyllithium compounds, were found to react with nitriles to afford *prim* amines with the NH_2 group attached to a quaternary carbon atom (Fig. 27).[164] However, *t*-$BuCeCl_2$ did not form the assumed intermediate $R^1R^2C{=}NCeCl_2$ in its reaction with a nitrile.

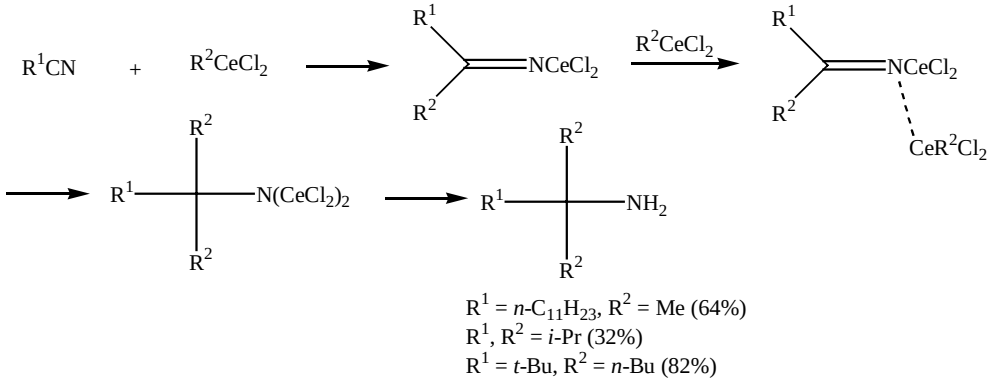

Figure 27. The proposed mechanism for the R^2CeCl_2 addition to a nitrile R^1CN.[164]

INTRODUCTION AND AIMS OF THE PRESENT STUDY

The study ***Synthesis of Functionalised Alkenes and their Reactions with a Zirconocene-Methylaluminoxane Catalyst System*** is part of the research project entitled *New Generation Tailor-made Plastics* generated in the Laboratory of Polymer Technology at the Helsinki University of Technology. The overall goal of the research is to synthesise functionalised PE and PP with MAO activated zirconocene catalysts in one step. Hence, the functional groups embedded in the PE or PP hydrocarbon chain are introduced by direct polymerisation of ethene or propene in the presence of a polar compound referred to as a comonomer. For this purpose, several alkenes bearing OH, NR_1R_2, OR, C=O, CO_2R or $CONR_1R_2$ groups, separated by a spacer chain of $(CH_2)_n$ units (n= 7-10) from their C=C bond, were synthesised (Chapter 5).

Since the catalyst components are Lewis acids, they are prone to react with the comonomer´s free electron pair on its heteroatom.[3] Thus, the reaction with the C=C bond is hindered, and deactivation commonly occurs during polymerisation. Our target was to diminish this catalyst deactivating interaction by employing comonomers with sterically shielded heteroatom moieties. A related goal was to investigate the impact of diverse functionalities on the catalyst activity. In the course of developing synthetic routes to alkenes containing alkyl substituents of various sizes in the vicinity of the functional group, two unexpected reactions were discovered. These are discussed separately in chapters 6 and 7.

Moreover, in the search for functionalised alkenes with superior comonomer properties, a qualitative approach of inspecting interactions between some alkene derivatives and the catalyst components by NMR spectroscopy was undertaken (Chapter 8). Hence, a group of alkene derivatives was allowed to react with the MAO-zirconocene catalyst mixture in an NMR tube. The reaction mixtures of an alkene and MAO (bi component mixture) or an alkene, MAO and Cp_2ZrCl_2 (tri component mixture) were monitored by ^1H and ^{13}C NMR spectroscopy. The structures of the products formed or structural subunits were determined by observing intramolecular connectivities with 2D gradient-selected heteronuclear single quantum coherence (gs-HSQC) and heteronuclear multiple bond correlation (gs-HMBC) NMR techniques. Other 2D NMR methods utilised include the gs-HSQC combined with total correlation spectroscopy (TOCSY) and ^1H-^1H rotating frame Overhauser (ROESY) and/or nuclear Overhauser (NOESY) enhancement spectroscopy.

The copolymerisation results are briefly presented in the last part of this study. This includes the copolymer´s yield, catalyst activity, molar mass distributions and the amounts of functional alkene derivatives in the copolymers produced.

5 SYNTHESIS OF ALKENE DERIVATIVES

The synthesis, NMR and MS data of the compounds not included in the publications I-VI are described herein. The yields reported in Schemes 1-5 are those of the pure compounds. The ^{1}H and ^{13}C NMR spectra were recorded with a Varian Inova 300 MHz spectrometer using toluene-d_8 as a solvent unless otherwise stated. The spectra were referenced to tetramethylsilane (δ 0.00 ppm) added into NMR samples. Mass spectra, as well as high-resolution mass spectra, were recorded on a JEOL JMS-SX102 with an EI potential of 70 eV.

5.1 Alkenols

Five alkenols (Scheme 1) were synthesised for the NMR and/or copolymerisation studies. The synthesis, NMR and MS spectral data for compounds **69a**, **69c**-**e** have been described in publication I. Compound **69b** was prepared from acetaldehyde (depolymerised[165]) and 11-bromoundecene via a Grignard reaction.[166] The NMR and MS data for **69b** are listed in publication III.

Scheme 1

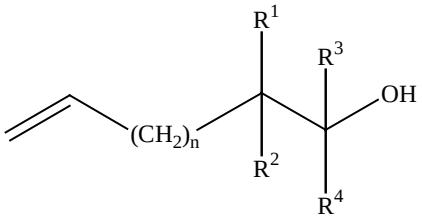

69a n = 9; R^1, R^2, = Me; R^3, R^4 = H (55%)
69b n = 8; R^1, R^2, R^3 = H; R^4 = Me (76%)
69c n = 9; R^1, R^2, = Me; R^3 = H; R^4 = *t*-Bu (25%)
69d n = 6; R^1, R^2, = H; R^3, R^4 = *t*-Bu (21%)
69e n = 9; R^1, R^2, R^3, R^4 = Me (41%)

The problem that arose in the synthesis of sterically hindered compounds **69c**-**e** was the low yields obtained after adequate raw product purification. The raw product mixtures were purified by neutral Al_2O_3 column or by preparative layer chromatography, which only allowed a small-scale operation. Neither the flash chromatography on a silica gel column nor vacuum distillation could be utilised for their purification. The column method effected a partial decomposition of a *tert* alkenol established for **69d**. The distillation method did not afford sufficiently pure compounds. In the case

of **69d**, the distillate contained a small amount of the ketone **74d** (Scheme 5) originating from the side reaction (see section 6.1), whereas unidentified impurities were encountered for **69c**. The preferred scale for a series of copolymerisations is 5.0 g of an alkene derivative. Thus, the use of synthesised alkenols in ethene or propene copolymerisations was quite limited owing to the aforementioned difficulties. The alkenols were more illustrative as models for the interaction with the MAO-Cp_2ZrCl_2 catalyst components monitored by NMR.

5.2 Amides and aminoalkenes

Our aim was to synthesise aliphatic amines similar to **64** (Fig. 24), except with an unsaturated alkyl chain. Amides **70a-f** with alkyl substituents of various sizes (Scheme 2) were prepared in the reaction of 10-undecenoyl chloride and an appropriate nitrogen source by adding the former dropwise into the latter at 0 °C.[167]

Scheme 2

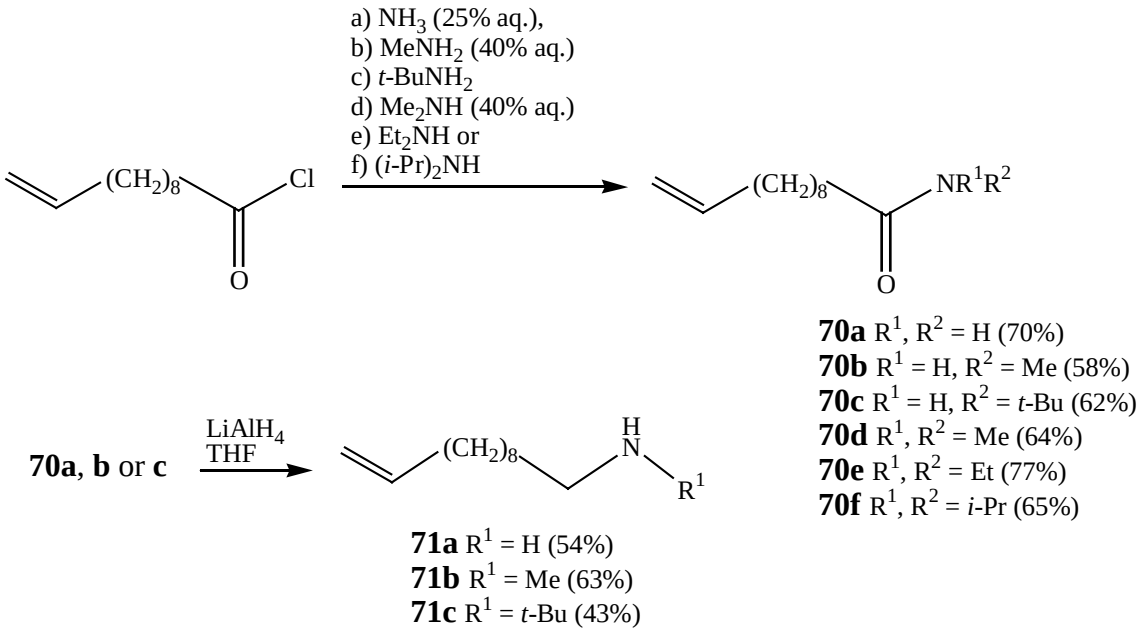

The compounds **70a-c** were subsequently reduced to the aminoalkenes **71a-c** by $LiAlH_4$ in refluxing THF.[167] Spectral data for **70a-f** and **71a-c** are presented in Table 2.

Table 2. Spectral data for compounds **70a-f**, **71a-c**, **72** and **73**. Multiplicity of the observed ^{1}H signal is given in parenthesis: broad (br), singlet (s), triplet (t), quartet (q) or multiplet (m).

Compound	^{1}H NMR (δ in ppm)	^{13}C NMR (δ in ppm)	HRMS
70a[a]	5.80 (m, 1 H), 5.50 (br, NH), 5.00 (m, 2 H), 2.25 (t, 2 H), 2.06 (m, 2 H), 1.66 (m, 2 H), 1.50–1.20 (5∗CH_2)	176.1, 139.4, 114.4, 36.2, 34.0, 29.6, 29.5, 29.4, 29.1, 25.8	calc. for $C_{11}H_{21}NO$ 183.1623, found 183.1619
70b	5.80 (m, 2 H),[b] 5.00 (m, 2 H), 2.60 (d, 3 H), 2.00 (m, 4 H), 1.62 (m, 2 H), 1.40–1.20 (5∗CH_2)	173.0, 139.2, 114.5, 36.5, 34.2, 29.9, 29.8, 29.6, 29.4, 26.2, 26.0	calc. for $C_{12}H_{23}NO$ 197.1780, found 197.1789
70c	5.80 (m, 1 H), 5.00 (m, 2 H), 4.85 (br, NH), 2.00 (m, 2 H), 1.80 (t, 2 H), 1.60 (m, 2 H), 1.40–1.20 (*t*-Bu, 5∗CH_2)	171.4, 139.2, 114.4, 50.6, 37.5, 34.3, 29.9, 29.7, 29.6, 29.4, 28.9, 26.1	calc. for $C_{15}H_{29}NO$ 239.2249, found 239.2245
70d	5.80 (m, 1 H), 5.00 (m, 2 H), 2.70 (s, 3 H), 2.35 (s, 3 H), 2.04 –1.90 (4 H)[c] 1.65 (m, 2 H), 1.40–1.20 (5∗CH_2)	171.5, 139.2, 114.4, 36.2, 34.8, 34.3, 33.2, 30.1, 30.0, 29.9, 29.6, 29.4, 25.5	calc. for $C_{13}H_{25}NO$ 211.1936, found 211.1943
70e	5.80 (m, 1 H), 5.00 (m, 2 H), 3.20 (q, 2 H), 2.80 (q, 2 H), 2.04 (t, 2 H), 1.98 (m, 2 H), 1.70 (m, 2 H), 1.40–1.20 (5∗CH_2), 1.00 (t, 3 H), 0.80 (t, 3 H)	172.1, 139.1, 114.0, 41.9, 40.0, 33.8, 33.1, 29.5, 29.4, 29.3, 29.1, 28.9, 25.5, 14.4, 13.1	calc. for $C_{15}H_{29}NO$ 239.2242, found 239.2249
70f	5.80 (m, 1 H), 5.00 (m, 2 H), 3.60 (br, 1 H), 3.10 (br, 1 H), 2.08 (t, 2 H), 2.00 (m, 2 H), 1.70 (m, 2 H), 1.50–0.80 (4∗CH_3, 5∗CH_2)	170.5, 139.3, 114.4, 48.0, 45.6, 35.3, 34.3, 30.1, 30.0, 29.9, 29.6, 29.4, 25.8, 21.7, 21.4	calc. for $C_{17}H_{33}NO$ 267.2562, found 267.2556
71a	5.80 (m, 1 H), 5.00 (m, 2 H), 2.50 (t, 2 H), 2.00 (m, 2 H), 1.40–1.20 (7∗CH_2), 0.70 (s, NH_2)	139.2, 114.4, 42.7, 34.5, 34.3, 30.2, 30.1, 30.0, 29.6, 29.4, 27.4	EI (m/z) 169 (M^+)[d]
71b	5.80 (m, 1 H), 5.00 (m, 2 H), 2.42 (t, 2 H), 2.30 (s, 3 H), 2.00 (m, 2 H), 1.50–1.20 (7∗CH_2), 0.50 (s, NH)	139.2, 114.4, 52.6, 36.8, 34.3, 30.6, 30.2, 30.0, 29.6, 29.4, 27.8	calc. for $C_{12}H_{25}N$ 183.1981, found 183.1987
71c	5.80 (m, 1 H), 5.00 (m, 2 H), 2.50 (t, 2 H), 2.00 (m, 2 H), 1.50–1.20 (7∗CH_2), 1.04 (s, 9 H), 0.60 (br, NH)	139.2, 114.4, 50.0, 42.8, 34.3, 31.9, 30.2, 30.1, 30.0, 29.6, 29.4, 29.3, 28.0	EI (m/z) 225 (M^+), 210 (M-CH_3), 168 (M-Bu_t)[d]
72	5.80 (m, 1 H), 5.00 (m, 2 H), 2.30 (s, 2 H), 2.00 (m, 2 H), 1.40–1.10 (7∗CH_2), 0.80 (s, 6 H), 0.53 (s, NH_2)	139.2, 114.5, 53.0, 39.9, 34.6, 34.3, 31.2, 30.2, 30.1, 29.7, 29.4, 24.9, 24.4	calc. for $C_{14}H_{29}N$ 211.2302, found 211.2300
73	5.80 (m, 1 H), 5.00 (m, 2 H), 2.17 (t, 2 H), 2.13 (s, 6 H),[e] 2.00 (m, 2 H), 1.50–1.20 (7∗CH_2)	139.2, 114.4, 60.1, 45.6, 34.3, 30.2, 30.1, 30.0, 29.6, 29.4, 28.4, 27.9	calc. for $C_{13}H_{27}N$ 197.2139, found 197.2144

a) Measured with a 200 MHz spectrometer using $CDCl_3$ as a solvent, b) C*H*=C overlapped with the N*H* resonance, c) CH_2C=O (t) overlapped with C=C-CH_2 (m), d) only EI spectrum available and e) overlapped with the residual C*H*D_2 of the solvent.

The main advantage of this method is the facile formation route and purification of the products by distillation. Obviously, the reduction of the parent amide to amine produces an α-CH_2 unit attached to the nitrogen, and hence restricts the degree of steric hindrance achievable by this method. However, it provides a potential large-scale synthetic method required for the copolymerisation investigations in progress.[168] The synthesis of **70g** (R^1, R^2 = *t*-Bu) from the acid chloride and **68** (Fig. 26) was not attempted. In fact, **68** has been found to be unreactive towards benzoyl chloride,[169] whereas its reaction with MeCOCl produced exclusively the amine hydrochloride.[169]

Additionally, two other amines were prepared (spectral data reported in Table 2). The β-dimethylated amine **72** (Scheme 3) was synthesised by first converting 10-undecen-1-ol into a nitrile.[170] The α-anion of the nitrile reacted with methyl iodide to afford the α-disubstituted derivative, which was reduced to **72** by $LiAlH_4$.[171,172]

Scheme 3

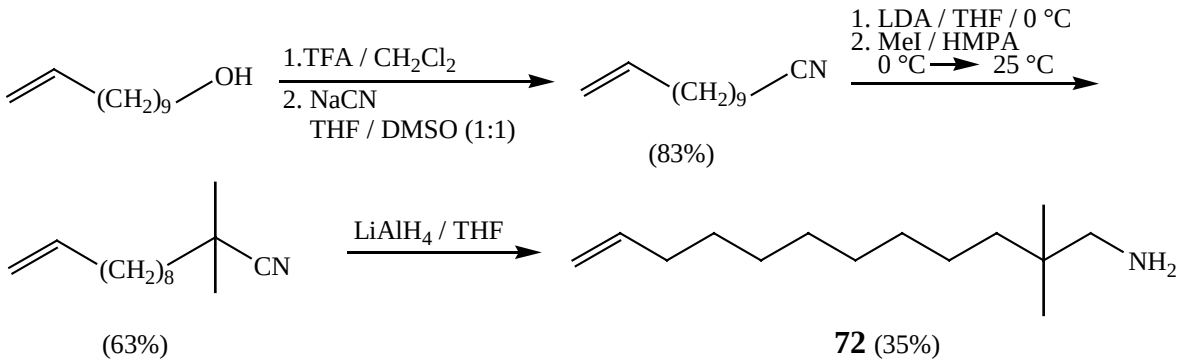

Compound **73** (Scheme 4) was prepared from 11-bromoundecene and Me_2NH (40% aqueous solution) in a one step procedure as described in reference 173.

Scheme 4

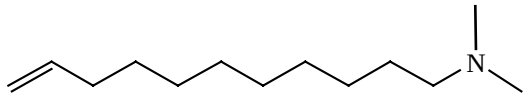

73 (83%)

5.3 Ether, ester and keto groups containing alkenes

Structures for the synthesised ether- and carbonyl functionalised alkenes **74a**-**e** are presented in Scheme 5. Compound **74a** was produced by alkylating 10-undecen-1-ol with MeI in KOH/DMSO at room temperature as previously described.[174] TMS-derivatives **74b**-**c** were synthesised by treating 10-undecen-1-ol or the alcohol **69b** with Me_3SiCl in a pyridine- hexamethyl disilazane mixture at room temperature.[175] The reaction of 10-undecenoic acid with *N*,*N*-carbonyldiimidazole at 40 °C and the subsequent addition of *t*-BuOH/DBU afforded **74d** (DBU= 1,8-diazabicyclo[5.4.0]undec-7-ene).[176] The ketone **74e** was isolated from the reaction of methyl 9-decenoate and *t*-BuLi, the other

product being the alkenol **69d** (publication I). The NMR and MS data for compounds **74a-e** are given in publication III.

Scheme 5

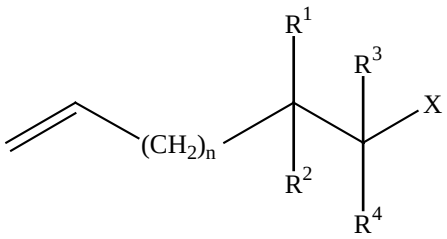

74a n = 7, $R^1 = R^2 = R^3 = R^4$ = H , X = OMe (75%)
74b n = 7, $R^1 = R^2 = R^3 = R^4$ = H, X = $OSiMe_3$ (55%)
74c n = 8, $R^1 = R^2 = R^3$ = H, R^4 = Me, X = $OSiMe_3$ (45%)
74d n = 6, $R^1 = R^2 = R^3 = R^4$ = H, X = $COOBu_t$ (45%)
74e n = 5, $R^1 = R^2 = R^3 = R^4$ = H, X = $COBu_t$ (45%)

6 ABNORMAL GRIGNARD REACTIONS ENCOUNTERED IN ALCOHOL SYNTHESIS

6.1 Enolisation

The alcohol **69d** and ketone **74e** were produced with a ratio approximately 1:1 in the reaction of methyl 9-decenoate and *t*-BuLi at –20 or 0 °C. This is in a drastic contrast to the results obtained with a Barbier type reaction of Li metal, di-*n*-butyl ketone and *n*-butyl bromide at –20 °C.[177] The product $(n\text{-Bu})_3$C-OH was formed with a yield of 91%, when excess starting halide was used. The authors[177] also stated that the reaction is applicable for *sec* and *tert* alkyl halides as well. In the present case, the amount of *t*-BuLi seemed to have a negligible influence on the product distribution. The 1:1 ratio for **69d** and **74e** was confirmed whether 2, 3 or 6 equiv. of *t*-BuLi was added into the THF solution of the ester. Evidently, a ketone intermediate appears in the $-CO_2R^1 \rightarrow -C(OH)R^2R^2$ conversion, and hence the enolisation of the ketone (Scheme 6) competes with the normal 1,2-addition.[135] To avoid this well-known Grignard side reaction,[135] the fully α-substituted methyl ester **75** was synthesised and utilised as a starting material for the alkenol synthesis (*vide infra*).

Scheme 6

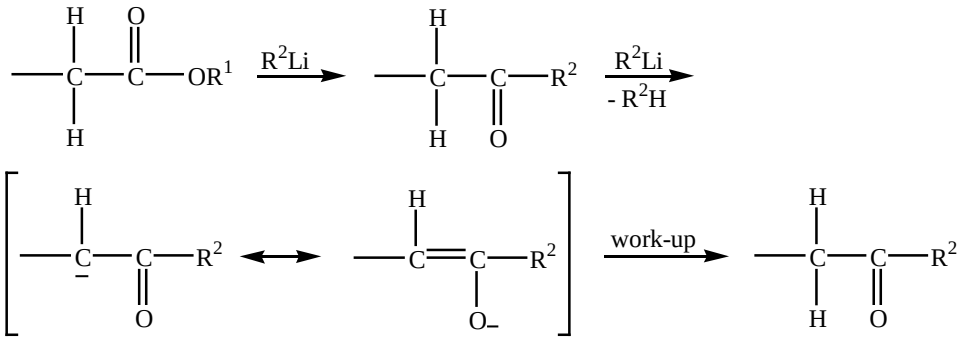

6.2 Alkylation-reduction of an ester to a *sec* alcohol by *t*-BuLi

Originally we were interested in synthesising the *tert* alkenol **76** (Scheme 7) instead of the *sec* alkenol **69c** from the α-dimethyl ester **75** (publication I). However, **76** was not formed despite the various experimental procedures utilised. These included *t*-BuLi addition at –70 or 0 °C and the use of $CeCl_3$ as an additive to promote the *tert* alkenol formation.[178]

Scheme 7

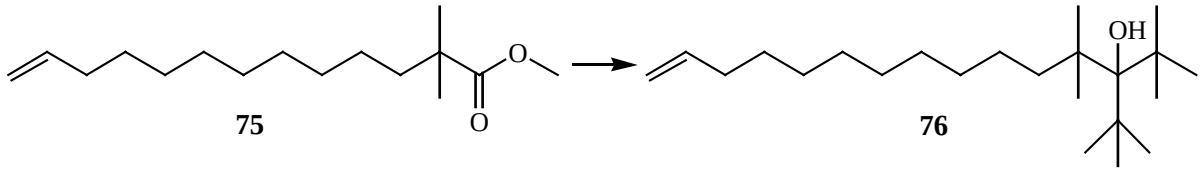

75 **76**

Previously, the short-chain α-disubstituted ester **77** and ketone **53f** (Scheme 8) were found to produce the *sec* and *tert* alcohols **78** and **55** in their reactions with *t*-BuCl and Na metal.[157] The reduction was, however, favoured over the 1,2-addition to a notable extent in both cases. The compound **55** was formed as a sole product when **53f** was treated with *t*-BuLi at –60 - –70 °C.[141] Moreover, **78** appeared as a by-product at temperatures higher than –40 °C.[141] When we performed the reaction of **77** with *t*-BuLi at –70 °C or at 0 °C, **78** and **55** were formed in a ratio 1:3 and 3:2, respectively.

Scheme 8

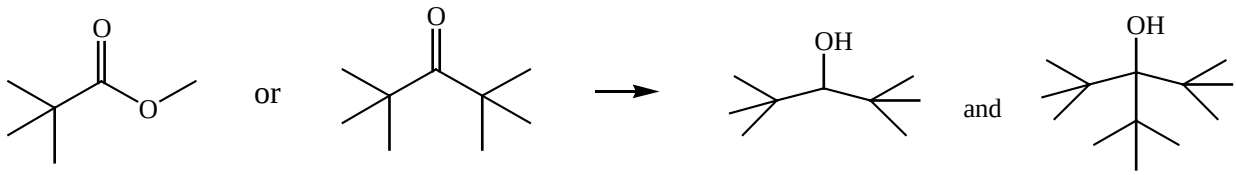

77 **53f** **78** **55**

This prompted us to investigate whether the ketone **79**, prepared from the ester **75** and *t*-BuLi (1 equiv.) at –70 °C reacted similarly to **53f** (publication I). Hence, **79** was treated with *t*-BuLi at –70 °C in the presence[178] or absence of added $CeCl_3$. However, neither 1,2-addition to **76** nor reduction to **69c** occurred, and the unreacted **79** was recovered in both cases. Furthermore, the inverse addition[140] *i.e.* the addition of **79** into the *t*-BuLi solution did not afford the dialkylated **76** or the reduction product **69c**.

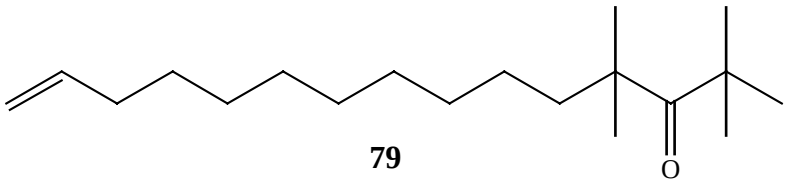

79

6.3 Mechanisms for the ketone reduction to a *sec* alcohol

The mechanism for the reduction by Grignard reagents has been studied mainly using aromatic ketones and various organomagnesium species as model systems.[135,179-184] Reduction has been suggested to occur via a one step concerted mechanism involving a six-membered ring transition state (Fig. 28a).[135,179,180] A related mechanism involving alkyl and organomagnesium radical intermediates has also been proposed (Fig. 28b).[180,181] A variation of the latter is depicted in Fig. 28c where magnesium ketyl abstracts a β-hydrogen atom from the Grignard reagent instead of the alkyl radical.[182]

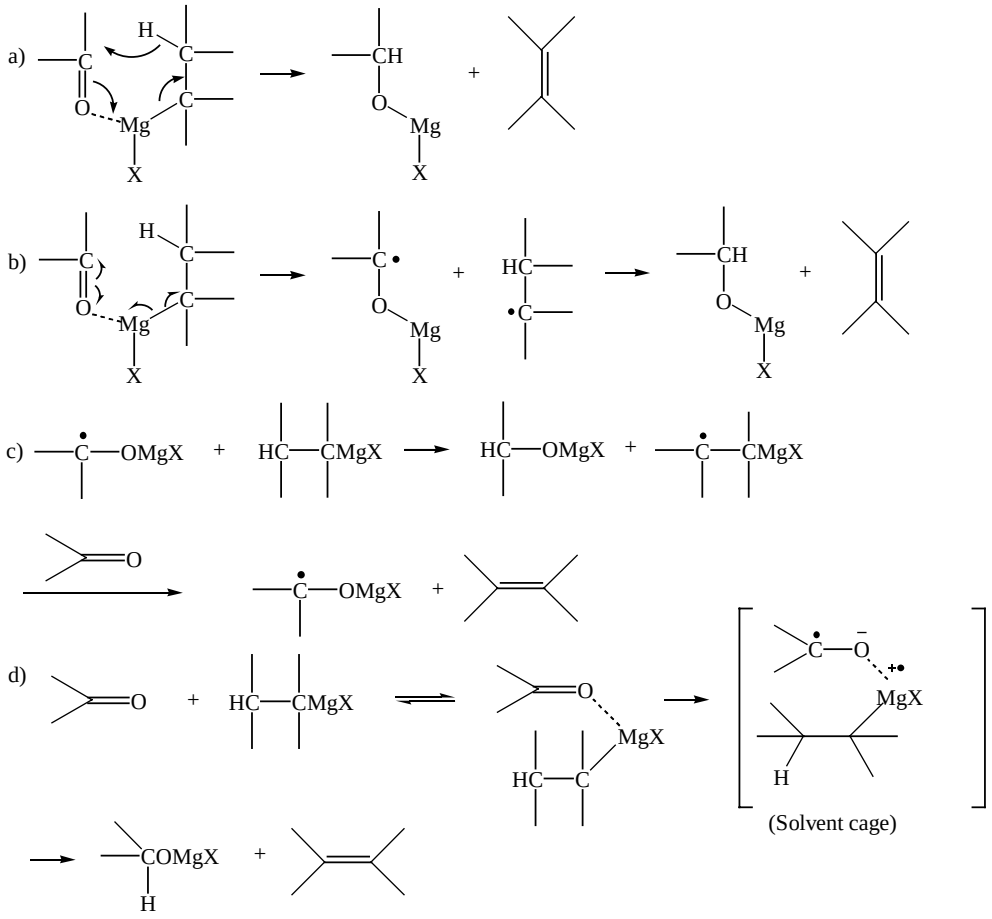

Figure 28. a) A concerted polar mechanism,[135,179,180] b) a two-step radical process,[180,181] c) a radical chain mechanism[182] and d) a radical pair mechanism.[183]

Moreover, the reduction of aromatic ketones by *prim*, *sec* or *tert* Grignard reagents has been proposed to occur via a single electron transfer (SET) mechanism (Fig. 28d).[183] No radical species were, however, observed when the ketone **53f** was treated with *t*-butylmagnesium chloride. The authors[183] concluded that reduction proceeds by the SET mechanism if the reactant is an aromatic ketone or, in a special cases, if an aliphatic ketone has a low enough reduction potential (< –2.0 eV). Some criticism towards the mechanistic pathway in Fig. 28d has also been presented.[184] A freely diffusing ketyl and alkyl radical was considered a more plausible intermediate than a radical ion pair in a solvent cage.

6.4 Mechanisms for the ester reduction to a *sec* alcohol

There are only a few examples of an ester reduction to a *sec* alcohol by organomagnesium reagents in the literature, and with little mechanistic detail.[185-187] The $-CO_2R' \rightarrow -CH(OH)R$ conversion was

accomplished by an RMgX-$LiBH_4$ reagent.[185] Presumably, the reaction proceeds via a ketone intermediate formed in the initial addition of RMgX to the ester. $LiBH_4$ then reduces the ketone to the *sec* alcohol. However, replacing RMgX by RLi produced *tert* alcohols as the main products.[185] According to a related method, the reaction of an ester with RMgX having β-hydrogens and Cp_2TiCl_2 afforded a *sec* alcohol.[186] Another procedure for the monoalkylation-reduction of an ester involved the use of RMgX and diisobutylaluminium hydride. [187]

For the reduction of the aliphatic ester **75** by *t*-BuLi, we suggest the following two mechanisms (publication I). These reaction pathways take into account the fact that the ketone **79** is not reduced under the experimental conditions employed, and thus can not be the intermediate in the **75** → **69c** conversion. The reduction product **69c** is formed when the β-hydrogen atom is abstracted from *t*-BuLi with simultaneous formation of lithium methoxide and isobutene (Fig. 29a). Alternatively, the β-hydrogen atom abstraction could occur prior to alkylation, involving a reduction to an aldehyde in the first step (Fig. 29a). The normal 1,2-addition pathway[179] (Fig. 29b) is prevented by the long hydrocarbon chain and the methyl groups at the α-position to C=O of **75**.

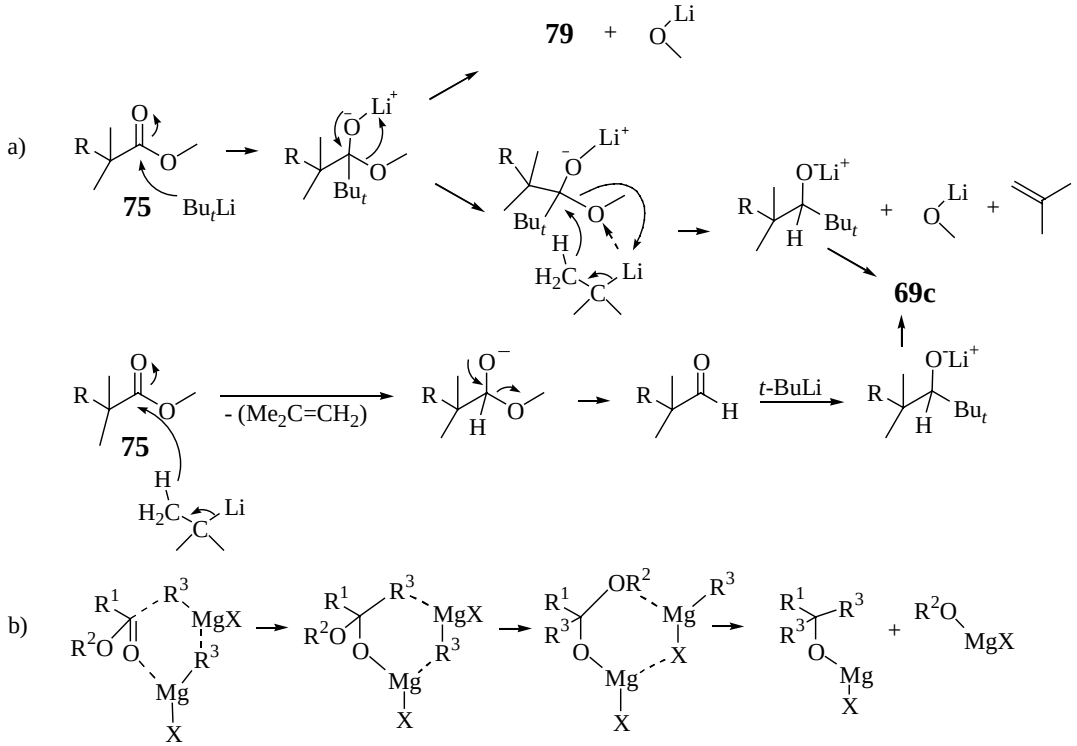

Figure 29. The mechanism proposals for a) the reduction of the ester **75** by *t*-BuLi and b) the normal 1,2-addition by an organomagnesium reagent.[179]

It thus appears that **55** is the only known aliphatic acycloalcohol with three quaternary carbon substituents attached to the C-OH carbon atom. There are, however, examples of mono-, di- and trisubstituted adamantyl derivatives of **55** in the literature.[188]

7 THE USE OF ACETALDEHYDE GENERATED FROM TETRAHYDROFURAN (THF) RING CLEAVAGE BY ORGANOLITHIUM COMPOUNDS IN ORGANIC SYNTHESIS

7.1 Formation of acetaldehyde enolate and its trapping with miscellaneous compounds

The acetaldehyde enolate **80** is formed via THF ring cleavage by an alkyllithium (Fig. 30a).[189] In practice, the generation of **80** is accomplished by adding *n*-BuLi into THF at 25 °C, and stirring the mixture for 16 h at a constant 25 °C.[190-195] The formed **80** is subsequently trapped by introducing it into a THF solution of an organic substrate at 16-25 °C.[191-195] In this way, formamides **81a** together with variable amounts of amines **81b** have been synthesised from aryl azides and **80** (Fig. 30b).[191] In the case of aryl azides with no electron withdrawing substituents heterocyclic compounds such as **81c** in figure 30b were produced.[192]

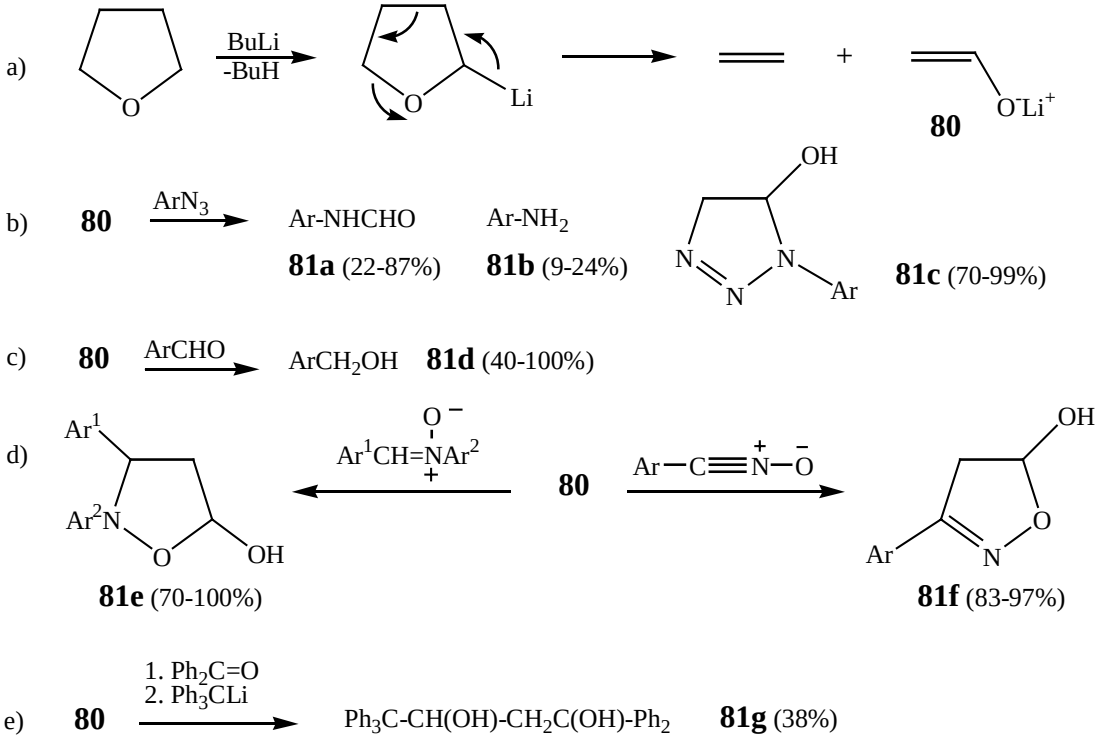

Figure 30. a) The base induced fragmentation of THF to **80**[189] and b-e) its reaction with various aromatic compounds.[191-196]

Non-enolisable aromatic or heteroaromatic aldehydes afforded *prim* alcohols **81d** in their reactions with **80** (Fig. 30c).[193] The compounds of the types **81e** and **81f** were produced in the reaction of **80** with *N*-phenyl nitrones[194] or benzonitrile oxides,[195] respectively (Fig. 30d). Moreover, the condensation of **80** and benzophenone in the presence of Ph_3CLi produced the diol **81g** (Fig. 30e).[196]

7.2 The *C*-alkylation

One previously reported attempt of the direct *C*-alkylation of **80** derived from THF exists in the literature.[190] Solely polymeric material, however, was produced under experimental conditions not accurately specified. The authors[190] stated that the use of the tributyltin enolate of acetaldehyde and its *C*-stannylated isomer effected the *C*-alkylation in the presence of aliphatic or aromatic alkyl halides (Scheme 9, X= Me, Et, CH_2=$CHCH_2$ or $PhCH_2$).

Scheme 9

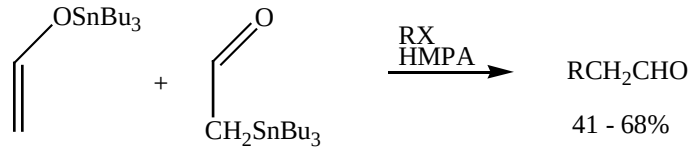

When we treated the *N*,*N*-dialkylamide **70e** or **70f** with *t*-BuLi, the α-*C* of the starting amide was unexpectedly alkylated by acetaldehyde, itself formed by the base-induced fragmentation of THF (publication II). The compounds **82a** and **82b** were produced according to Scheme 10.

Scheme 10

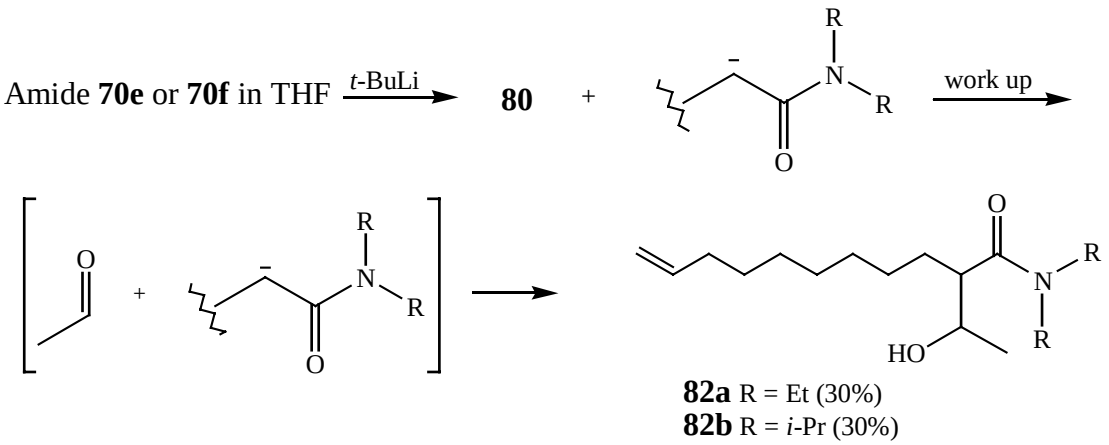

The raw product yield for **82a** or **82b** was ca. 30% when the reaction was conducted at 0 °C. It appears that the yield is not affected by the reaction time. In fact, stirring the reaction mixture for 2.5 h, 5 h or its immediate quenching upon complete addition of *t*-BuLi (12.5 equiv.) afforded the aforementioned raw product yield. However, the alkyllithium/amide mole ratio, reaction temperature and the structure of alkyllithium more noticeably influenced the raw product yield (Table 3).

Table 3. The raw product yields (%) for **82a** and **82b** in various experimental conditions formed from **70e** or **70f**, respectively. The alkyllithium utilised /**70e** or **70f** mole ratio was 3.5:1.

Reaction temperature and time	The yield (%) obtained in the presence of *t*-BuLi		The yield (%) obtained in the presence of *n*-BuLi	
	82a	**82b**	**82a**	**82b**
−70 °C/7 h	0	0	n.p[a]	n.p[a]
0 °C/4 h or 8 h	13	13	4.5	4.5
0 °C/30 min → 25 °C/ overnight	9.0	9.0	n.p[a]	n.p[a]
25 °C/overnight	9.0	9.0	9.0	9.0

a) Not performed.

When **80** was generated,[190] prior to the amide addition, from *n*-BuLi at 25 °C or from *t*-BuLi at 0 °C, only the starting material **70e** or **70f** was recovered. This indicates that the two carbanions (Scheme 10) are present simultaneously in the solution. The quenching medium, aqueous NH_4Cl, then acts as a proton source for the carbanions of which the amide enolate appears to be more long-living. Hence, the aldol reaction does not proceed via an interchange of protons between **80** and the amide enolate.

We found the reaction to be general for *N*,*N*-dialkyl amides except for the *N*,*N*-dimethyl derivatives. In fact, the short-chain $CH_3(CH_2)_2CONRR$ butylamides (R= Et or *i*-Pr) reacted similarly to the compounds **70e-f**. However, a product mixture was obtained with *N*,*N*-dimethyl amide **70d**. The expected $CH_2=CH(CH_2)_8COBu_t$ **83** was identified as the main product (spectral data in Table 4). $CH_3(CH_2)_2CON(CH_3)_2$ reacted analogously to **70d**. Compound **83** was also formed along with a trace amount of $CH_2=CH(CH_2)_8C(Bu_t)_2OH$, when the reaction of **70e** and *t*-BuLi (12.5 equiv.) was conducted in THF-hexane (0.2:9 or 1:9) at 0 °C. The amount of **82a** was negligible in both cases (0% or < 0.5%, respectively).

7.3 The *O*-silylation and acylation

There are a few examples of *O*-silylation[190] and acylation[190,197] of the enolate **80** in the literature. The former was conducted as previously described (*vide supra*), except that a silyl derivative was added into the solution of **80** (Scheme 11).[190] In the acylation procedure, excess acid chloride dissolved in THF-HMPA (1:1) was treated with the preformed **80**.[190] A related method involved the preparation of **80** at 35 °C.[197] The acylation was performed at –40 - –45 °C by introducing **80** into the solution of phenyl thiochloroformate.

Scheme 11

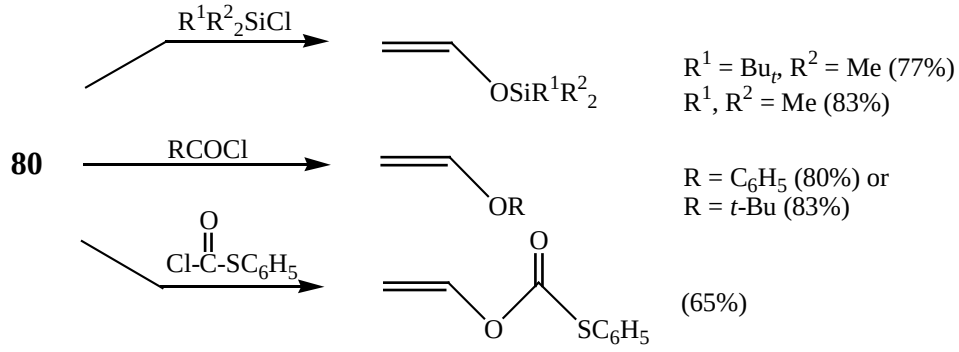

When we treated 10-undecenoyl chloride according to the aforementioned procedure,[190] none of the corresponding *O*-acylated product was formed. Instead, the anhydride $[CH_2{=}CH(CH_2)_8CO]_2O$ **84** was produced, presumably during the aqueous work-up from the unreacted acyl chloride.[198] Moreover, upon treatment of 10-undecenoyl chloride in pure THF with *t*-BuLi at 0 or 25 °C, a complex mixture of products was formed in both cases.[198] The ketone **83** and diketone **85** could be identified, the latter being produced at the higher temperature. Spectral data for **84**-**85** is given in Table 4.

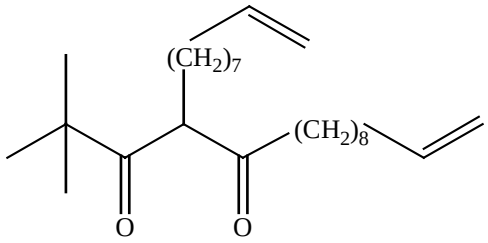

85

Table 4. The spectral data for compounds **83**-**85**. The NMR spectra were measured with a 300 MHz spectrometer using $CDCl_3$ as the solvent. The chemical shifts were referenced to TMS (0.00 ppm).

Compound	^{1}H (δ in ppm)	^{13}C (δ in ppm)	EI or HRMS
83	5.80 (m, 1 H), 5.0 (m, 2 H), 2.46 (t, 2 H), 2.04 (m, 2 H), 1.50–1.20 (bs, H), 1.13 (s, 9 H)	216, 139.2, 114, 46.0, 36.7, 34.0, 29.0, 28.3, 28.0, 27.9, 27.8, 26.0, 24.2	EI m/z 224 (M^+), 167 (M^+-*t*-Bu)
84	5.80 (m, 2 H), 5.0 (m, 4 H), 2.50 (t, 4H), 2.05 (m, 4H), 1.70 (m, 4 H), 1.50-1.20 (bs, 20 H)	169.6, 139.4, 114.1, 35.3, 34.0, 29.3, 29.2, 29.1, 29.0, 28.9, 24.7	Molecular ion not observed; EI m/z 167 (RCO^+)[a]
85	5.80 (m, 2 H), 5.0 (m, 4 H), 4.00 (t, 1 H), 2.45 (t, 2 H), 2.04 (m, 4 H), 1.80 (m, 2 H), 1.50 (m, 4 H), 1.40–1.16 (19 H), 1.2 (s, 9 H)	211.7, 207.2, 139.9, 114.9, 114.8, 63.0, 46.0, 40.3, 34.5, 34.4, 31.3, 30.4, 30.1, 30.0, 29.9, 29.8, 29.7, 29.6, 29.57, 29.52, 28.8, 26.7, 24.1	HRMS calc. for $C_{26}H_{46}O_2$ 390.3498, found 390.3486

a) R is a CH_2=$CH(CH_2)_8$ chain.

8 NMR STUDIES ON FUNCTIONALISED ALKENE-MAO/ZIRCONOCENE CATALYST MIXTURES

Several alkenols, aminoalkenes, ether and carbonyl functionalised alkenes were employed in the NMR investigation of the bi (alkene and MAO) and tri (alkene, MAO and Cp_2ZrCl_2) component reaction mixtures. In addition, the reactions of commercially available 10-undecen-1-ol, 1-undecene and methyl 9-decenoate with the catalyst system were monitored. ^{1}H and ^{13}C spectroscopy were employed in assigning the spectra with HSQC, HSQC-TOCSY, HMBC, ROESY and/or NOESY 2D NMR techniques. ^{1}H-^{1}H ROESY and/or NOESY measurements were further performed to reveal the possible catalyst interaction with the vinyl and/or heteroatom moiety of an alkene. The description of the NMR sample and MAO preparations in toluene-d_8 along with the spectral parameters used in the NMR measurements have been presented in publications III and IV. The spectra were measured at 27 °C unless otherwise stated.

8.1 Interaction with MAO

8.1.1 Alkenols

All the alkenols studied **69a**-**e** and 10-undecen-1-ol formed aluminium alkoxides in their reactions with MAO (publication III except for **69d**[198]). The oxygen containing fragments and their chemical shifts are listed in Table 5. 10-Undecen-1-ol produced one main aluminium alkoxide and some minor species appearing at δ 3.50-4.40 ppm in the presence of MAO. The two moderately substituted **69a** and **69b** formed several oxygen containing -C(Me_2)CH_2-O- or -CH(Me)-O-

fragments which exhibited partially overlapping ^{1}H and ^{13}C resonances, and thus could not be unequivocally assigned. Substantial steric hindrance around the OH group, as in **69c** and **69d**, restricted their interaction with MAO. The prevalence of one or two separate -C-O- fragments could be confirmed, respectively. However, the tetramethyl derivative **69e** generated four different C-O-species (**A**-**D**) in its reaction with MAO. Obviously, the four Me groups in **69e** are not sizeable enough to suppress the formation of various -C-O-Al- ensembles.

Table 5. ^{1}H and ^{13}C chemical shift values for the characteristic molecular fragments formed in the reactions of alkenols and MAO.

Compound	Characteristic fragment	^{1}H δ (ppm)	^{13}C δ (ppm)
10-undecen-1-ol	-*CH*$_2$-O-	4.00	64.6
69a	C(Me$_2$)*CH*$_2$-O	3.44	73.2
		3.70; 3.74; 3.78;	not determined
		3.80; 3.92; 4.06;	not determined
		3.58*	84.7*
69b	-*CH*(Me)-O-	3.81	71.1
		3.96; 4.12; 4.28	not resolved
		3.88*	80.5*
69c	-*CH*(Bu$_t$)-O-	3.66,^{A} 3.40^{B}*	92.5^{A}, 100.1^{B}*
69d	-*C*(Bu$_t$)$_2$-O-		99. 8,^{A} 83.4^{B}
69e	-*C*(Me$_2$)-O-		86.1,^{A} 85.6,^{B}
			78.6,^{C} 76.6^{D}
			88.0^{E}*

The superscripts **A**-**E** refer to the separate species formed in each component mixture. The asterisk (*) refers to the resonances detected solely in the presence of added Cp_2ZrCl_2 (see section 8.2). The -*C*(Bu$_t$)$_2$-O- of **69d** appeared at δ 79.0 ppm in pure toluene-d_8.

Additional evidence for the aluminium alkoxide formation was obtained from the HMBC and ROESY spectra of the bi component mixtures. 10-Undecen-1-ol showed HMBC correlations from its -*C*H$_2$-O- and -*C*H$_2$-CH$_2$-O- resonances at δ 64.6 and 33.3 ppm to the Al-C*H*$_3$ resonance at δ –0.30 ppm. In addition, several ROE correlations, emerging from the different -C*H*$_2$-O signals at δ 3.50-4.40 ppm, to the group of Al-C*H*$_3$ resonances at δ –0.26 - –0.46 ppm were observed. Previously, the chemical shift values of –0.35 ppm,[80] –0.38 ppm[82] and –0.40 ppm[83] have been attributed to TMA present as a free dimer (TMA)$_2$, or mainly bound to MAO. Alternatively, the ^{1}H resonance situated at δ –0.38 ppm has been assigned to the O-AlMe$_2$ chain-end methyl protons of MAO oligomers.[82] According to our interpretation, the main aluminium alkoxide could have formed in the reaction of 10-undecen-1-ol with residual TMA. The reaction of the former with MAO oligomers would account for the presence of the minor -CH$_2$-O-Al- fragments.

HMBC correlations between MAO and compounds **69a-e** were absent from the recorded 2D spectra. Several ^{1}H-^{1}H ROE correlations between MAO and the characteristic fragments (Table 5) appeared instead. The lack of HMBC correlations may arise from the fact that interaction weaker than bonding occurs between MAO and the alkenols. Alternatively, the products formed exhibit conformations in which the evolution of detectable ^{1}H-^{13}C coupling over four bonds is unfavourable. In few cases, were significant differences found for the measured -*C*-O chemical shifts between the separate species formed from a given alkenol and MAO (**69d-e** in Table 5). Presumably, a more electron withdrawing MAO fragment attached to or at a ROESY distance to the -C-O- oxygen atom could effect the deshielding, and hence the observed lower field shifts for the -*C*-O resonances.

The general mechanism for the reaction of an alcohol and aluminoxane has been discussed by Pasynkiewicz (Scheme 12).[24] Evidently, the reaction begins with a complex formation between the oxygen atom of the alcohol and terminal aluminium atom of the aluminoxane. The alkoxyaluminoxane formed may have various structures depending on the size of R^2 group in the alcohol. The structure **86** was suggested to predominate for small R^2 groups (Me, Et) and structure **87** for bulky groups (*i*-Pr, *t*-Bu). The structures **88** and **89** would prevail at elevated temperatures.

Scheme 12

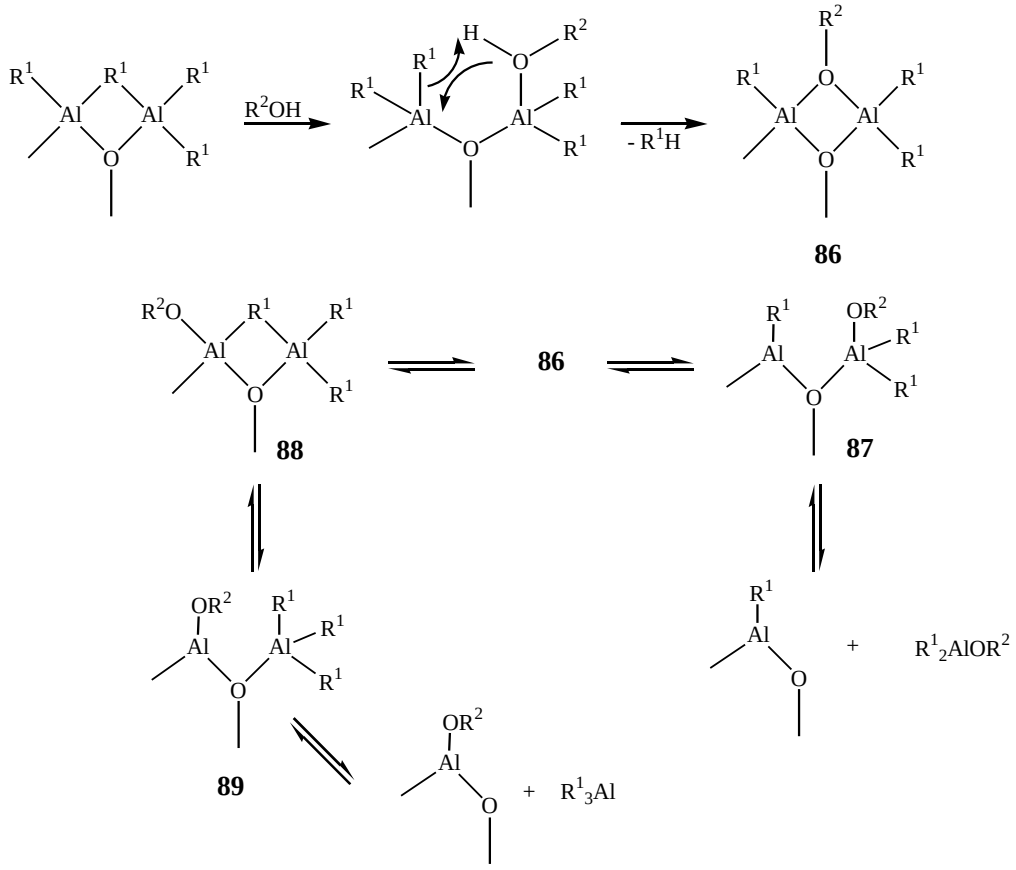

The preference of sterically hindered R^2OH molecules for the structure **87** is in agreement with our results concerning the reaction of **55** and MAO (publication IV). The coalescence temperatures (T_c) for **55** were determined experimentally in the absence and presence of MAO by dynamic ^{13}C NMR spectroscopy. Thus, the rotational energy barries ($\Delta G^{\ddagger}$) obtained for the pure **55** were 8.9 kcal/mol ($\Delta G_1^{\ddagger}$) and 10.1 kcal/mol ($\Delta G_2^{\ddagger}$). The addition of MAO lowered the first barrier to 8.3 kcal/mol whereas the second barrier was increased to 10.8 kcal/mol. This data was compared with the energy barriers calculated for five different MAO models (Scheme 13, **90a-c** and **91a-b**) and for pure TMA by molecular modelling. An open-chain MAO fragment such as **91a** appeared to be consistent with the NMR results. The calculation with 4-, 6- and 8-membered cyclic MAO models afforded energy values distinctly deviating from the experimentally ones. Only one barrier having the energy of 15 kcal/mol was obtained for **90a** and **90b**. In the case of **90c** and **91b**, two barriers with approximately equal energy value (7 kcal/mol) occurred.

Scheme 13

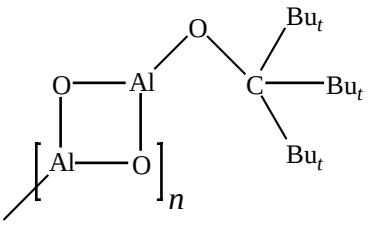

90a *n* = 1
90b *n* = 2
90c *n* = 3

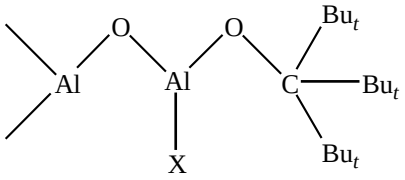

91a X = Me
91b X = OMe_2

Moreover, the molecular modelling results suggest that the formation of aluminium alkoxides cannot be solely due to the free TMA present in the MAO solution. In fact, the calculation with (*t*-Bu)$_3$C-O-$AlMe_2$ produced a significantly higher second energy barrier (18 kcal/mol) than the experimentally obtained value (10.8 kcal/mol). The open chain structure deduced **91a** differs from the complex structures suggested for MAO (*vide supra*). However, the bulky OH surrounding of **55** might effect the MAO moieties in contact with the alcohol.

8.1.2 Aminoalkenes

The C*H* resonances in the vicinity of the nitrogen atom (Scheme 14) were generally shifted to a higher field in the spectra recorded from freshly prepared amine-MAO mixtures in comparison with the pure amines (Table 6).[199] In a few cases, a shift of the N*H* to a lower field occurred in concert with the shift of the aforementioned C*H* signals into a higher field, as established for **71b**, or while ageing the reaction mixture, as exemplified with **72**. Neither phenomenon was noticed for the alkenols studied *i.e.* the -C*H*-O resonances appeared at a lower field in the bi component mixtures than in pure toluene-d_8, whereas the OH protons were undetectable in both cases. The interaction between the NH/NH_2 protons of the amine and the oxygen of MAO could effect the slightly displaced δ-values of *CH* and N*H*/NH_2 signals. However, the existence of a hydrogen bond, N*H* ··· O, cannot be unambiguously deduced, even though the hydrogen bond appears to cause a deshielding for the heteroatom bound protons,[200] and hence a shielding for the C*H* resonances.

Scheme 14

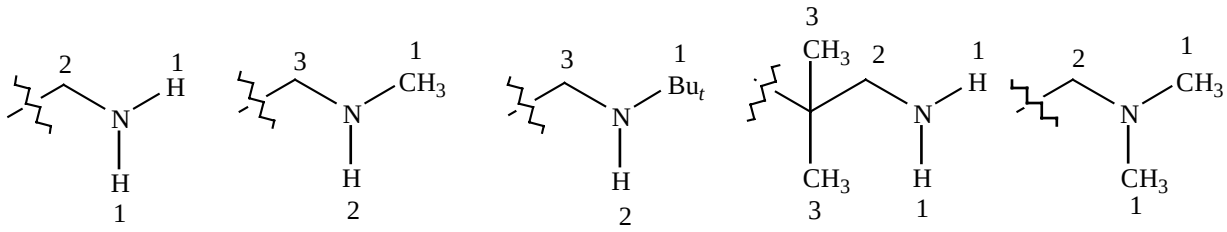

71a **71b** **71c** **72** **73**

Table 6. The characteristic ^{1}H and ^{13}C resonances (δ ppm) monitored by NMR from the amine-MAO mixtures in toluene-d_8. The atomic numbers refer to Scheme 14. The relative strength of ROE correlations detected is described as weak (w), medium (m) or strong (s).

Compound	Atomic number	Amine in the presence of MAO δ_H	Amine in the presence of MAO δ_C	$\Delta\delta_H=(\delta_H{}^1-\delta_H)$[a]	$\Delta\delta_C=(\delta_C{}^1-\delta_C)$[a]	ROE to Al-CH_3
71a	1	not detected	-	-	-	-
	2	2.30	41.9	0.20	0.80	no
71a/aged/**A**	1	0.54	-	0.16	-	no
	2	2.48	42.6	0.02	0.10	–0.40 - –0.60 (m)
71a/aged/**B**	1	0.66	-	0.04	-	no
	2	2.53	43.6	(–)0.03	(–)0.90	–0.40 - –0.60 (m)
71b	1	2.10	35.4	0.20	1.40	no
	2	0.77	-	(–)0.27	-	no
	3	2.35	51.6	0.10	1.00	–0.60 (w)
71c[b]	1	0.80-1.10	28.1	n.d[c]	n.d[c]	no
	2	0.30	-	0.30	-	no
	3	2.16-2.90	44.2-44.4	n.d.[c]	n.d.[c]	no
72/**A**[d]	1	0.98[e]	-	(–)0.45	-	-
	2	2.28	52.3	0.02	0.70	–0.50 (w)
	3	0.57	24.3	0.23	0.60	no
72/aged/**B**	1	0.60	-	(–)0.07	-	
	2	2.60	53.7	(–)0.30	(–)0.67	–0.40 (m)
	3	0.78	25.1	0.02	(–)0.20	no
73	1	2.00[f]	44.4	0.12	1.20	–0.55 (s)
	2	2.24	59.5	(–)0.07	0.60	–0.55 (s)

a) $\delta_H{}^1$ and $\delta_C{}^1$ refer to the ^{1}H and ^{13}C chemical shifts in the absence of MAO, b) see discussion in section 8.2, c) not determined, d) also present in the aged mixture, e) observed solely in the spectrum of the aged sample and f) overlapped with the C=C-CH_2 resonance.

In the case of **71a**, the NH_2 originally at δ 0.70 ppm disappeared upon addition of MAO. By ageing the NMR sample for a few weeks, two different N*H* signals, being part of separate species **A** and **B**, emerged (Table 6). However, the number of protons attached to the N atom could not be unequivocally determined. Furthermore, the 2-CH_2 at δ 2.30 ppm (Table 6) no longer existed in the

spectrum of aged **71a** and MAO. The new species **A** and **B** were formed in the approximate ratio 1:2. The ROE correlations observed (Table 6) could not be determined with accurate δ_H-values due to the partial overlapping of the 2-CH_2 signals of **A** and **B**.

The β-branched *prim* amine **72** reacted with MAO in a manner similar to **71a**. Another nitrogen species **B** was evolved with time, in addition to the originally formed **A** (Table 6). The ROE correlations observed (Table 6) support the presence of two separate species. As for **71a**, the number of nitrogen bound protons could not be unambiguously deduced. On the other hand, the multiplicity of the observed 1-CH_2 of **A** (t) and **B** (d) indicates that the former has an NH_2 group whereas the latter would have an NH group attached into its molecular framework.

The slightly altered chemical shift values and ROE correlations obtained for the *sec* amine **71b** and *tert* amine **73** (Table 6) indicate a prominent coordination between N and Al atoms. The relative strength of the observed ROE correlations (Table 6) increase in the order **71a**<**71b**<**73**, when the measurements from the freshly prepared samples are compared. Hence, the coordination ability of the amines studied towards the Lewis acid MAO appears to be opposite to the base strength determined for a series of amines towards the reference acid $B(CMe_3)_3$.[135] Moreover, as discussed for alkenols, ^{1}H-^{13}C HMBC correlations between MAO and the amines studied were absent from the spectra.

8.1.3 Ether and carbonyl derivatives

The methyl ether **74a** was not found to interact significantly with MAO. Apart from the occurrence of a short-lived complexation as previously encountered with ethers,[74] the ^{1}H and ^{13}C chemical shifts of **74a** remained approximately at the same δ-values as in the absence of MAO. The **74a**-MAO complex was inferred by the presence of a transient HMBC correlation between a ^{13}C resonance at δ 50.7 ppm and a ^{1}H singlet at δ –0.62 ppm. Corresponding HMBC or ROE correlations indicative for complexation were undetectable in the spectrum of TMS-ether **74b** or **74c** and MAO.

The *t*-butyl ester **74d** was partly decomposed to 10-undecenoic acid and to **92** (Fig. 31) in its reaction with MAO. A weak NOE correlation implies the presence of an AlXMe moiety in **92**. In

contrast, the other ester investigated, methyl 9-decenoate, did not form any distinct species with MAO.

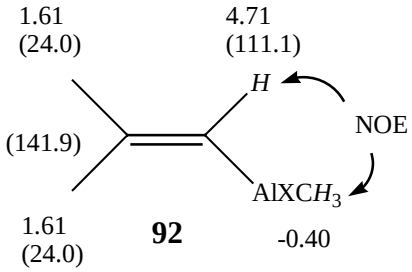

Figure 31. Chemical shift values in ppm (^{13}C in parentheses) for **92**, formed in the reaction of **74d** and MAO (AlXMe= an aluminium species).

The reaction of ketone **74e** and MAO produced two unsaturated species **93A** and **93B** having slightly deviating chemical shift values (Fig. 32). Evidently, this is caused by the dissimilarities in the attached MAO moiety (AlXMe). The observed ROE correlations (Fig. 32), and their absence between the *t*-butyl and methylene protons, support the *Z* configuration for **93A-B**.

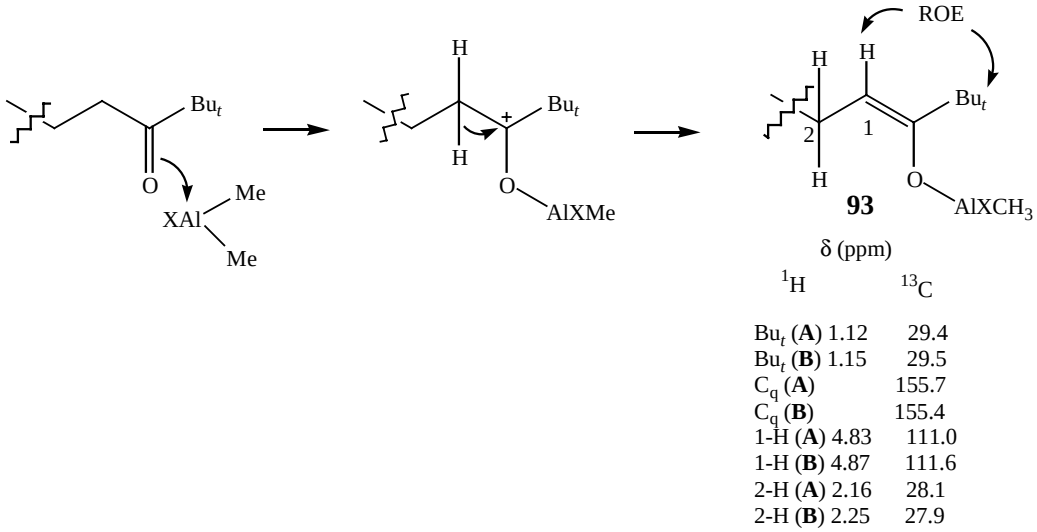

Figure 32. The suggested formation path of **93A** and **93B** from **74e** and MAO (marked as AlXMe).

Overall, the NOESY produced similar positive correlations to the ROESY between the alkenes and MAO, indicating that the molecular clusters formed were relatively small.

8.2 The effect of Cp_2ZrCl_2 on the alkene-MAO interaction

Various zirconocenes appearing in the tri component mixtures studied are presented in Table 7 along with their $\delta_{H,C}$ for Cp rings. The assignation is based on the chemical shifts reported for like zirconocenes in the literature.[103,107,201] A more detailed inspection of the $\delta_{C,H}$-values for diverse [Zr-CH_3]$^+$ cations frequently discussed in the literature[110-112] is, however, ignored in the present approach. The $(CH_2)_n$ chain resonances of the alkenes at the spectral range δ 45-22 ppm severely interfere with the possible Zr-CH_3 signals. Therefore, the low intensity Zr-CH_3 signals cannot be deduced with sufficient reliability.

Table 7. The ^{1}H and ^{13}C resonances for different zirconocene species formed in the reactions of alkene derivatives with MAO/Cp_2ZrCl_2. The symbol → denotes coordination or the presence of a heteroatom at a ROESY distance from the Cp protons. The literature references are given in the brackets.

Entry	^{1}H δ (ppm)	^{13}C δ (ppm)	Assignment (tentative)	Compound number
1	5.78-5.74[a]	112.6	$Cp_2ZrMeCl$ [107]	undecen-1-ol**, 69a-b, 69e, 71a**,[b] **71b-c**, **72**,[b] **73**–**74e**, methyl 9-decenoate
2	5.83	111.7	$Cp_2Zr(Me)$-O-Al- [201]	**69a**, **71a**, **72**, **74e**
3	5.88	115.7	Cp_2ZrCl_2 [this work, 103]	undecen-1-ol, **69b-c**, **69e**, **71a-c**, **72**–**74e**, methyl 9-decenoate
4	5.92	115.1	Cp_2ZrCl_2 → Al or $Cp_2ZrMeCl$ → Al[c]	methyl 9-decenoate
5	5.95	113.5	As in entry 4[c]	undecen-1-ol, **69a-b**
6	6.03	114.3	Cp_2ZrCl_2 → O [103]	**69c**, **74e**
7	6.29,[d] 6.47[d]	133.5,[d] 133.0[d]	substituted Cp ring[c]	undecen-1-ol

a) The δ-value has been found to depend on the Zr/MAO mole ratio.[107] b) The ^{1}H and ^{13}C resonances were barely visible in the spectra measured from the freshly prepared samples. The signals could be clearly observed when measured from the aged samples. c) No literature references available. d) The ^{1}H and ^{13}C resonances were observable solely in the spectra of aged samples.

The Cp_2ZrCl_2 generally enhanced alkoxide formation in the reaction mixtures of the alkenols studied with MAO. Hence, additional oxygen containing fragments were produced (listed in Table 5). In the case of 10-undecen-1-ol, the minor ^{1}H multiplets at δ 3.50-4.40 ppm became more pronounced by the added Cp_2ZrCl_2. However, the aluminium alkoxides originally formed seemed to be unstable in the presence of Cp_2ZrCl_2-MAO. In fact, ^{1}H and ^{13}C resonances characteristic for free 10-undecen-1-ol were observed while ageing the NMR sample for a few weeks. The concomitant disappearance of the zirconocene species present in the freshly prepared sample was also noted

(Table 7, entries 1, 3 and 5). Evidently, a substituted Cp ring can account for the two new signals observed (Table 7, entry 7). The presence of cationic zirconocenes can be excluded since their $^{13}C_{Cp}$ resonances appear generally at a higher field.[110,111]

The decomposition of a formed alkoxide did not occur in the other studied alkenol-Cp_2ZrCl_2/MAO mixtures. In the case of **69c**, the original -CH(Bu_t)-O-Al- species **A** was almost entirely superseded by the new species **B** (Table 5). Its formation seemed to be induced by a zirconocene having an alkenol oxygen in the vicinity of the Zr atom (Table 7, entry 6). This conclusion is supported by the ROE correlation observed between the *t*-butyl and Cp protons. Furthermore, the $\delta_{H,C}$-values of the zirconocene measured are in accordance with the chemical shifts reported for (Cp_2ZrCl_2)O (δ_H 5.98 and δ_C 114.1 ppm).[103]

The amines **71b** and **73** did not seem to be influenced by the addition of Cp_2ZrCl_2. Their characteristic ^1H and ^{13}C resonances appeared at the same δ-values as in the absence of the catalyst (Table 6). The latter and its monomethylated derivative (Table 7, entries 3 and 1) were, however, observed in the recorded spectra. The *prim* amines **71a** and **72** each produced the two nitrogen containing species as previously described (section 8.1.2). Additional species evolved in the presence of Cp_2ZrCl_2. They displayed their 2-CH_2 signals at δ 3.40 ppm (δ_C 56.0 ppm) for **71a** and at δ 3.20 ppm (δ_C 67.0 ppm) for **72**. They were both observable in the spectra of freshly measured samples, indicating that their formation might be due to the zirconocene appearing at δ 5.83 ppm (Table 7, entry 2). Thus $Cp_2Zr(Me)(Cl)$ would account for the formation of nitrogen species detected in the spectra of aged samples.

Moreover, an HSQC-TOCSY correlation between the 2-CH_2 at δ 67.0 ppm and N*H* proton at δ 6.04 ppm was observed in the spectrum of the **72**-MAO/Cp_2ZrCl_2 mixture. This noticeable low field shift (ca. $\Delta\delta_{NH}$ = 5.25 ppm) compared with the δ_{NH}-values of the aged species (Table 6) suggests that an electron withdrawing substituent is attached to the nitrogen. The formation of $Cp_2ZrMeCl$ from Cp_2ZrCl_2 has been suggested to occur via a formal Cl^- transfer to MAO.[103] The formed $[MAOCl]^-$ can react further with the amine **72** producing R-C(Me_2)-CH_2-NHCl. This could account for the downfield N*H* and 2-CH_2 resonances. Furthermore, the 2-CH_2 did not express a ROE correlation to Al-CH_3. Thus, interaction with a MAO moiety having no adjacent methyls, such as -Al-[O-AlMe]$_2$-,

can be inferred. This is in agreement with the NMR data reported for the dimeric $[Cp_2Zr(Me)OAlMe_2]_2$.[201] It displayed its $\delta_{Cp\text{-}H}$ and $\delta_{Cp\text{-}C}$ at 5.86 ppm and 112.4 ppm, respectively.

The tri component mixture of **71a** contained an analogous R-CH_2-NHCl species. Its N*H* signal (ca. δ 5.90 ppm) was discovered by a decoupling experiment due to the methine proton (m) overlapping at δ 5.80 ppm. The R-CH_2-NHCl formed did not display any ROE correlations to Al-C*H*$_3$. However, it experienced mutual chemical exchange with **A** and **B** (δ-values in Table 6) present in the **71a**-catalyst mixture. The exchange process (Fig. 33) was evidenced by the concerted use of ROESY and proton decoupled spectra as described for **71c** (*vide infra*).[199] The fact that chemical exchange remained undetectable by NMR for R-$C_\beta(Me_2)$-CH_2-NHCl might be due to the presence of β-substituents. The methyls could stabilise the aforementioned species by the electron withdrawal effect, and hence prevent the exchange process or render it undetectable in the NMR time-scale.

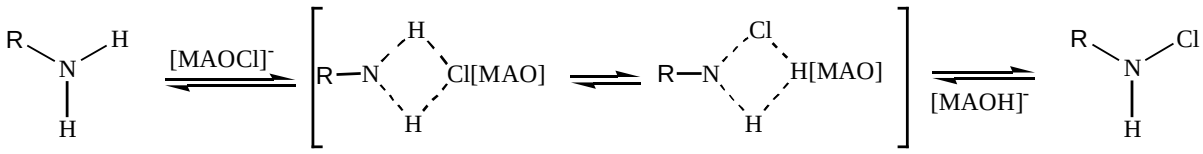

Figure 33. The mechanism suggested for the chemical exchange prevailing in the mixture of *prim* amine **71a** and catalyst components. $[MAOCl]^-$ is derived from the reaction of Cp_2ZrCl_2 and MAO.

In the case of **71c**, a chemical or a conformational exchange process occurred *i.e.* the protons changed their chemical environment in the NMR time scale. Figure 34 displays three diverse 3-C*H*$_2$-N signals for the species **A**-**C** appearing at a ratio of 1:1:3 at –63 °C. Each signal shows ROE correlations to Al-C*H*$_3$. Moreover, positive correlations (in the same phase with the diagonal) were detected between the 3-C*H*$_2$-N resonances. Proton decoupling experiments confirmed that these were not TOCSY but chemical exchange originated correlations experienced by the 3-C*H*$_2$ resonances during the pulse sequence. The 3-C*H*$_2$-N (q) of **A** was simplified into a triplet, when the N*H* resonance at δ 0.40 ppm was saturated in the decoupling experiment. The 3-C*H*$_2$ signals of **B** and **C** (Fig. 34) showed exclusively ^{1}H-^{1}H couplings to the hydrocarbon chain, and hence they appear not to contain an NH proton. By raising the temperature up to +57 °C, the *tert* butyl and the 3-C*H*$_2$-N protons of **A**-**C** reemerged at δ 0.90 and 2.45 ppm, respectively.

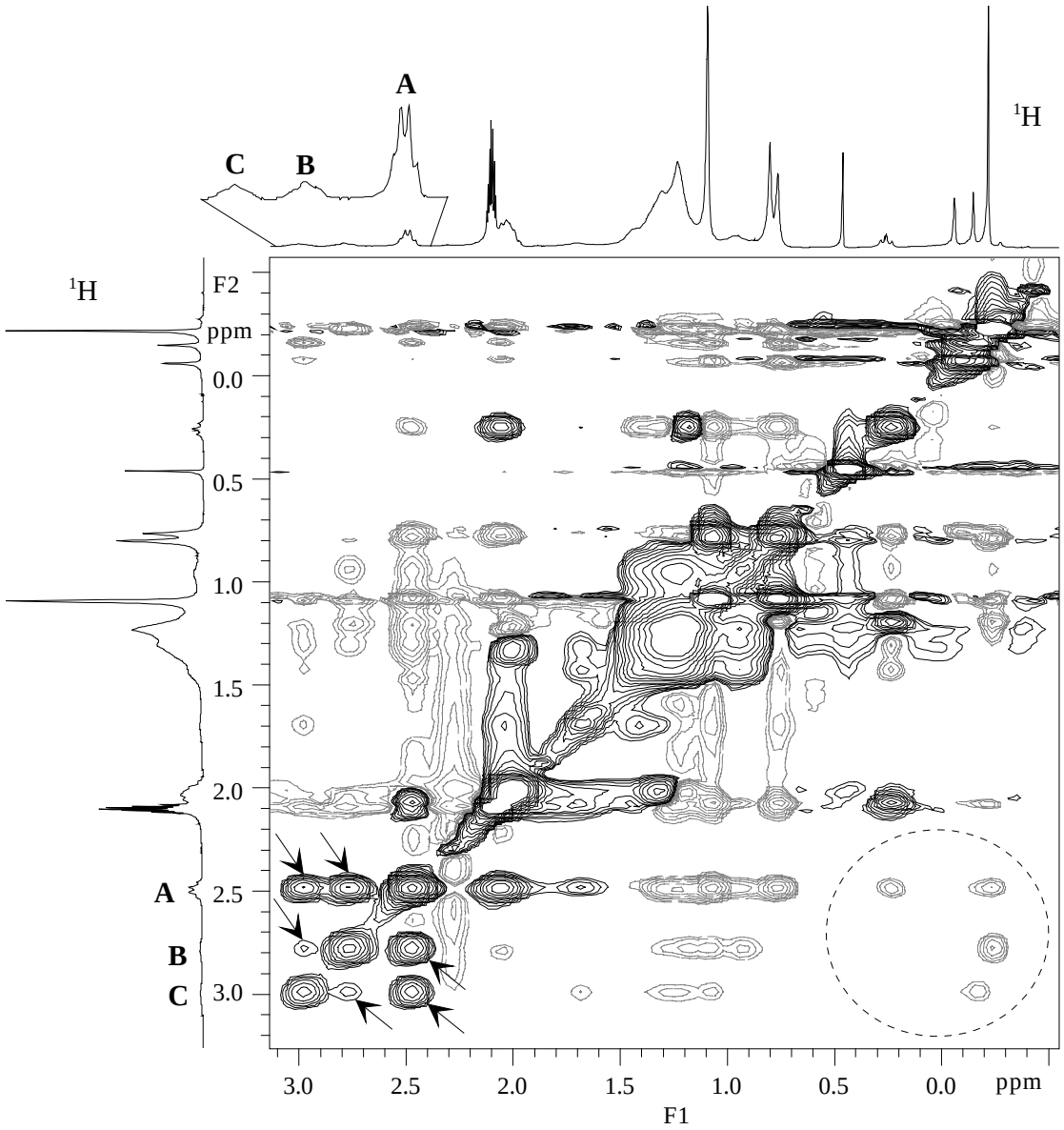

Figure 34. The expanded ROESY spectrum (300 MHz) of **71c**, MAO and Cp_2ZrCl_2 measured at –63 °C. The correlations arising from the chemical exchange between species **A**-**C** are marked with an arrow. The unbroken line contours are TOCSY and broken line ROE correlations. The ROE correlations between C*H*$_2$ of **A**-**C** and N*H* or Al-C*H*$_3$ exist inside the broken line circle.

Presumably, MAO coordinates to **71c** forming a species of the type **A** (Fig. 35). **A** undergoes chemical exchange with **B** and **C,** which contain diverse MAO moieties *i.e.* X and Y are dissimilar oxygen containing Al-fragments. Thus, the experimentally observed interconversion of **B** and **C** can proceed via **A.**

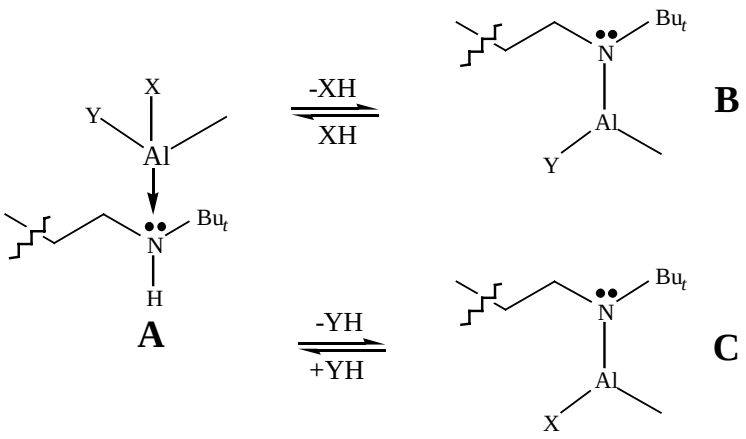

Figure 35. Suggested interconversion pathway for species **A**-**C** formed in the **71c**-MAO/Cp_2ZrCl_2 mixture. X and Y are dissimilar oxygen containing MAO fragments. Stereochemistry has been omitted for clarity.

TMS-derivatives **74b** and **74c** produced four different species **94**-**97** (Scheme 15) in their reaction with the MAO-Cp_2ZrCl_2 catalyst, the dimeric **94** being the most abundant one. In the case of **74c**, the formation of **94**-**97** occurred immediately, whereas **74b** required a reaction time of some weeks in the NMR tube. 1-Undecene reacted similarly to **74c**. The dimer formation has been noticed previously for some silylprotected alcohols in the presence of a zirconocene and a boron based activator.[13] Furthermore, the authors[13] reported that *N*,*N*-dialkyl amines had reacted analogously. However, the characteristic ^1H and ^{13}C signals of **94** were absent in the spectra recorded from the mixtures of amines **71a-c**, **72** or **73** and MAO-Cp_2ZrCl_2.

Scheme 15

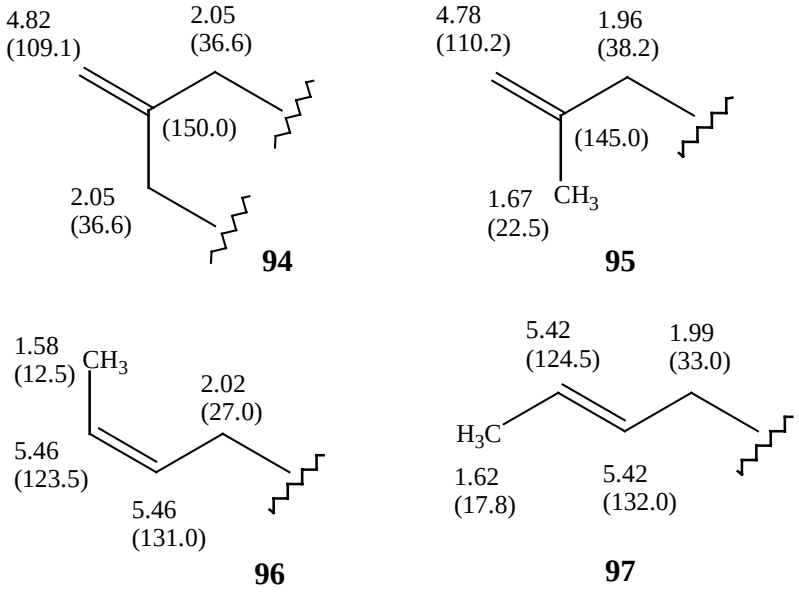

Methyl 9-decenoate and *t*-butyl ester **74d** were not noticeably affected by the presence of Cp_2ZrCl_2. The latter was partly decomposed, as observed in the bi component mixture. In addition to **93A**-**B** (Fig. 32), two other like fragments were generated in the mixture of ketone **74e**, MAO and Cp_2ZrCl_2 while ageing the NMR sample. Their 1-C*H* resonances emerged at δ 4.29 and 4.43 ppm each showing a ROE correlation to a new *t*-Bu proton signal at δ 1.14 or 1.18 ppm, respectively. Presumably, these new unsaturated fragments were formed via a zirconocene, having its Cp at δ_H 6.03 ppm. This is substantiated by the fact that other zirconocenes originally present (Table 7, entries 1 and 2) were no longer observed, except for the residual Cp_2ZrCl_2.

A common feature for all the tri component mixtures studied was the lack of any detectable interaction between the C=C bond of the alkenes and zirconocenes formed. The $^{a}CH_2=^{b}CH$ signals were displayed at approximately δ 5.00 (^{a}H), 114 (^{a}C), 5.80 (^{b}H) and 140 ppm (^{b}C), as with in the absence of the catalyst. The vinyl protons did not exhibit ROE or NOE correlations to Cp protons. Moreover, these ^{1}H-^{1}H correlations were not found in the spectra of **74b**-**c** or 1-undecene and MAO-Cp_2ZrCl_2. Thus, the interaction between Zr and the vinyl moiety of the alkene appears to be undetectable under the experimental conditions despite that the unsaturated fragments **94**-**97** (Scheme 15) were evidently formed by a zirconocene species in the aforementioned tri component mixtures.

9 COPOLYMERISATION STUDIES

Ethene or propene copolymerisation in the presence of functionalised alkenes were performed with the $Et(Ind)_2ZrCl_2$-MAO catalyst system. The apparatus and method for polymerisation, as well as the copolymer characterisation, are described in publications V and VI. The copolymerisations of alkene derivatives containing nitrogen are still in progress,[168] and therefore the results presented herein are preliminary.

The various oxygen-functionalised alkenes copolymerised with propene (publication V) are presented in Table 8. One can notice that all the comonomers employed decreased the catalyst activity significantly compared with the homopolymerisation of propene. However, by investigating the effect of a functional group (OH, CO_2R, C=O or CO_2H) on the catalyst activity, we learned that the most significant deactivation occurred in the copolymerisation of the ketone **74e**. In fact, only a trace amount of the copolymer was produced. In contrast, the *tert* alkenols appeared to be the least

detrimental to the activity. The use of **69d** as a comonomer was, however, quite limited owing to the problems that arose in its synthesis (*vide supra*). When the concentration of 2-methyl-3-buten-2-ol was increased to 10 mmol/l, the catalyst activity of 2600 kg/mol$_{Zr}$•h could still be obtained. The corresponding activities for 10-undecen-1-ol, 5-hexen-1-ol and **69b** were 800, 1100 or 510 kg/mol$_{Zr}$•h, respectively.

Table 8. The effect of a functional group on the catalyst activity (A) in propene copolymerisation. Polymerisation conditions: $Et(Ind)_2ZrCl_2$ $4.8•10^{-6}$ mol, polymerisation temperature (T_p) 30 °C, propene pressure (p) 3.0 bar, Al/Zr= 4000 mol/mol, and polymerisation time (t_p) 1 h. The concentration of the comonomer was 3.3 mmol/l, except for **69d** (6.7 mmol/l) and methyl 9-decenoate (1.7 mmol/l).

Comonomer	A [kg/mol$_{Zr}$•h][a]	Yield of the copolymer [g]
-	16 600	79.3
10-undecenol	2600	12.4
5-hexenol	3900	18.7
2-methyl-3-buten-2-ol	8600	41.0
s-alkenol **69b**	2600	12.6
t-alkenol **69d**	3200	15.1
ester **74d**	2400	11.3
methyl 9-decenoate	1600	7.7
ketone **74e**	<100	traces
10-undecenoic acid	3500	16.5

a) The unit of A is expressed as yield of the copolymer in kg *per* the mole amount of $Et(Ind)_2ZrCl_2$ *per* t_p in hours.

Similarly, the *t*-butyl group of an ester hindered the catalyst deactivation more effectively than the methyl group (Table 8). Moreover, the activity did not vary noticeably in propene copolymerisations with the ester **74d** or 10-undecenoic acid. An increase in the concentration from 3.3 to 6.7 or 10 mmol/l decreased the activity to 1100 and 340 kg/mol$_{Zr}$•h for the former whereas for the latter case the activity values of 1100 and 580 kg/mol$_{Zr}$•h were determined.

The highest amount of alkene derivative in the copolymer produced was achieved with 10-undecen-1-ol (0.7 mol-%), calculated from the ^{1}H NMR spectrum. In the case of 5-hexen-1-ol or **69b**, the copolymer contained 0.3 mol-% of the alkenol used. The finding that 2-methyl-3-buten-2-ol was not incorporated into the copolymer produced presumably originates from its two adjacent methyl groups in respect to the C=C bond, as previously described.[22] A common feature for all the copolymers produced was the narrow molar mass distributions (M_w/M_n 1.7-1.9) obtained, indicating compositionally uniform products.

When ethene was copolymerised with 10-undecen-1-ol, methyl ether **74a**, TMS-ether **74b** (publication VI) or amine **71b**,[168] the catalyst deactivation occurred approximately to the same extent in each case when compared with the ethene homopolymerisation (Table 9). Consequently, the magnitude of deactivation seemed not to depend significantly on the functional group, when the dissimilarities at the surrounding heteroatom are merely diminutive *i.e*. OH, OMe, OTMS and NHMe as in the inspected series. However, a slightly increased activity in the order NH_2<NHMe/$NHBu_t$<NMe_2 could be established for the amine series investigated (compounds **71a-c** and **73**).[168] Hence, replacing a heteroatom bound hydrogen by an alkyl group diminishes the catalyst deactivation, as evidenced in the alkenol-propene copolymerisations.

Table 9. The activities and yields obtained in some ethene copolymerisations. Polymerisation conditions: $Et(Ind)_2ZrCl_2$ $5.0 \bullet 10^{-6}$ mol, concentration of comonomer 16.7 mmol/l, T_p 60 °C, p_{ethene} 1.5 bar, Al/Zr= 4000 mol/mol, Al/comonomer= 4.0 mol/mol, and t_p 20 min.

Comonomer	A [kg/mol_{Zr}•h]	Yield of the copolymer [g]
-	10100[a]	3.2[b]
10-undecen-1-ol	1200	2.0
methyl ether **74a**	1700	2.8
TMS-ether **74b**	2500	4.2
amine **71b**	1800	3.0

a) $Et(Ind)_2ZrCl_2$ $1.0 \bullet 10^{-6}$ mol in ethene homopolymerisation and b) yield for ethene homopolymer.

Furthermore, the comonomer content in the various ethene copolymerisation products appeared not to vary noticeably. As can be seen from Fig. 36, nearly equal amounts of methyl ether **74a**, *prim* amine **71a**, *sec* amine **71b** and *tert* amine **73** were determined in the products. The highest comonomer incorporation was achieved with 10-undecen-1-ol and its TMS-protected derivative **74b**. However, **74b** is present as a free alcohol in the product due to the hydrolysis upon the acidic work-up procedure. The compounds **74b** and **73** expressed reactivities comparable to 1-undecene at the low comonomer concentration level (Fig. 36). In addition, the molar mass distributions remained narrow, being in the range of 1.7-2.2.

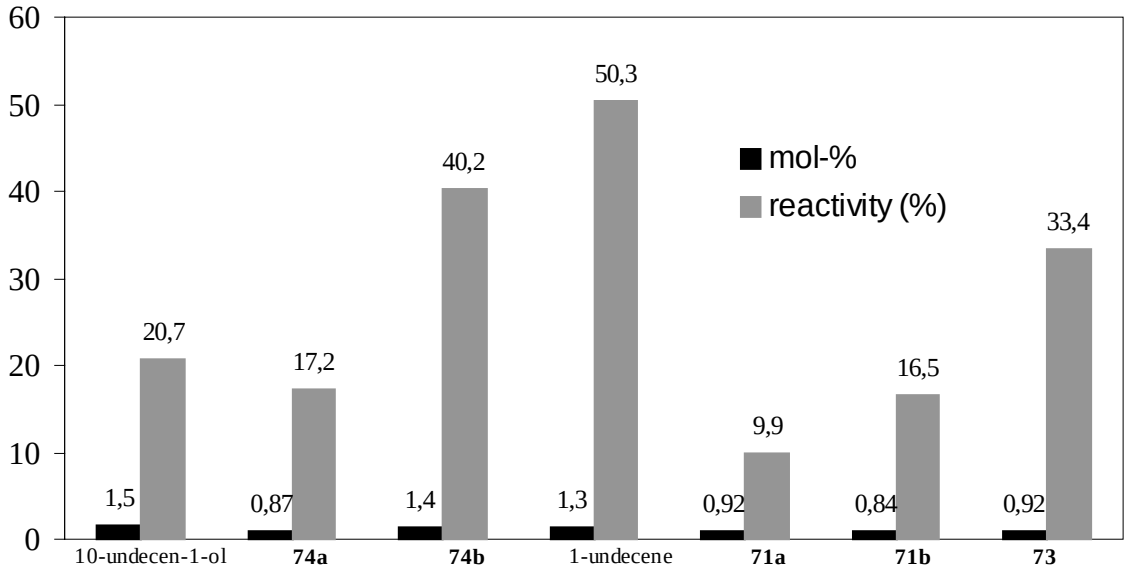

Figure 36. The comonomer content (mol-%) in the ethene copolymerisation products and reactivity (%). The former is calculated from the ^{1}H NMR spectra. The latter refers to the comonomer conversion *i.e.* the amount of reacted comonomer *per* the amount of comonomer in the feed. Polymerisation conditions: $Et(Ind)_2ZrCl_2$ $5.0 \bullet 10^{-6}$ mol ($1.0 \bullet 10^{-6}$ mol for 1-undecene copolymerisation), T_p 60 °C, p_{ethene} 1.5 bar, Al/Zr= 4000 mol/mol, Al/comonomer= 4.0 mol/mol (for 1-undecene 0.8), and t_p 20 min (for **73** 30 min). The comonomer concentration was 16.7 mmol/l.

Overall, the comparison of 10-undecen-1-ol, methyl ether **74a**, silyl ether **74b** and amine **71b** in respect to their copolymerisability with ethene indicates that an Al-X bond formation is not a prerequisite for the polymerisation to occur (X=O, N). This conclusion is consistent with our NMR results concerning the interaction of the alkene derivatives and catalyst components. In fact, only the alcohol of the aforementioned compounds formed one main RO-Al- fragment in its reaction with the catalyst system (*vide supra*). The compounds **71b**, **74a** and **74b** merely experienced coordination with MAO. The formation of the unsaturated species **94**-**97** (Scheme 15) in the case of **74b** is apparently of minor importance due to the prolonged reaction time required. Moreover, the effect of the functional group on the copolymerisability and catalyst deactivation becomes more pronounced in the case of carbonyl functionalised comonomers. Our copolymerisation results imply that a keto or amido group is the most detrimental to the catalyst system utilised. In fact, small amounts of amidoalkenes can be copolymerised with ethene.[168] Increasing the steric hindrance from -CONHMe to -CON(*i*-Pr)$_2$ did not noticeably diminish the catalyst deactivation. This indicates that the steric hindrance in the vicinity of the heteroatom in an alkene is not solely responsible for its copolymerisability.

10 SUMMARY

A variety of structural proposals for MAO exists. Different linear and/or cyclic, as well as cage-like, MAO models have been suggested. Methods for investigating the MAO structure involve mainly NMR spectroscopy. It is also the most commonly utilised method for studying the interaction of MAO with a zirconocene catalyst. In the course of the present study, 1D and 2D NMR techniques (^{1}H, ^{13}C, HSQC, HMBC, HSQC-TOCSY, ROESY, NOESY) were employed as tools for monitoring the interaction(s) between functionalised alkenes and MAO-Cp_2ZrCl_2 catalyst components. Thus several alkenols, aminoalkenes and carbonyl functionalised alkenes were synthesised and subsequently screened by NMR to find suitable candidates for copolymerisations with ethene or propene.

In developing synthetic routes to functionalised alkenes, an unusual reaction *i.e.* the reduction of an α-disubstituted methyl ester to a *sec* alkenol was discovered. Moreover, two mechanisms for the -CO_2R → -CH(OH)- conversion not involving a ketone intermediate were suggested. The original target molecule, CH_2=CH(CH_2)$_9$C(Me_2)C(Bu_t)$_2$OH, proved to be, however, unavailable by the synthetic methods utilised. Moreover, a new twist on the use of THF as a source of acetaldehyde enolate was discovered. The treatment of an *N*,*N*-dialkyl substituted amide dissolved in THF with *t*-BuLi effected the R-CH_2-CONR$^1_2$ → R-[CH_3CH(OH)]-CHCONR$^1_2$ conversion. This α-*C*-alkylation appeared to be a general reaction for *N*,*N*-dialkyl amides (N ≠ Me), albeit a precaution rather than a synthetic method.

The alkenols studied produced aluminium alkoxides in their reactions with MAO or the MAO-Cp_2ZrCl_2 mixture, even in the case of sterically hindered substrates. The (Bu_t)$_3$C-O-Al- fragment with an open-chain MAO moiety was deduced for tri-*t*-butyl carbinol, a subunit for the sterically hindered long-chain alkenols. The amines exhibited diverse interaction towards the catalyst system. The RNAl- species, produced in the reaction of a *prim* or *sec* amine, still contained at least one nitrogen bound proton. Moreover, chemical exchange between the separate species could be established for the mixture of CH_2=CH(CH_2)$_9$NH(R) (R=H or *t*-Bu) and the catalyst components. Despite the different mode of reactivity, both alkenols and amines appeared to follow a common trend when copolymerised with ethene or propene *i.e.* catalyst activities improved in the order *prim*<*sec*<*tert* derivative.

Moreover, the bond formation between the heteroatom of the comonomer and Al of MAO appears not to be decisive for the diminished catalyst spoiling in copolymerisations. In fact, equal catalyst activity was confirmed in copolymerisations of 10-undecen-1-ol, its methyl or TMS ether derivative or the amine CH_2=CH(CH_2)$_9$NHMe. However, the formation of a CH_2O-Al bond could be established exclusively for 10-undecen-1-ol. The carbonyl functionalised alkenes deactivated the catalyst system to a larger extent compared with the other alkenes investigated. This finding suggests that the functional group itself is more crucial for the catalyst deactivation than the steric hindrance in the heteroatom vicinity of an alkene.

Overall, the modification of the heteroatom surroundings by introducing alkyl groups does not cause only one type of effect on the MAO-alkene interaction. The fact that alkyl groups can exert inductive or field effect, and therefore alter the heteroatom electronic properties, should also be noted. Furthermore, since the experimental conditions differ in these two procedures, the NMR results are indicative rather than imperative in respect to the copolymerisation. So far, the NMR studies applied provide an insight into the molecular structures formed in the catalyst system.

REFERENCES

1. B. A. Krentsel, V. I. Kleiner and L. L. Stotskaya, *Polymers and Copolymers of Higher α-Olefins*, VCH Publishers, Munich, 1997.
2. J. Huang and G. L.Rempel, *Prog. Polym. Sci.*, 1995, **20**, 459.
3. H. H. Brintzinger, D. Fischer, R. Mülhaupt, B. Rieger and R. M. Waymouth, *Angew. Chem., Int. Ed. Engl.*, 1995, **34**, 1143.
4. W. Kaminsky, *Macromol. Chem. Phys.*, 1996, **197**, 3907.
5. W. Kaminsky and M. Arndt, *Adv. Polym. Sci.*, 1997, **127**, 143.
6. H. Sinn and W. Kaminsky, *Adv. Organomet. Chem.*, 1980, **18**, 99.
7. H. Sinn, J. Bliemeister, D. Clausnitzer, L. Tikwe, H. Winter and O. Zarnke, in *Some New Results on Methylaluminoxane in Transition Metals and Organometallics as Catalysts for Olefin Polymerization*, eds. W. Kaminsky, H. Sinn, Springer, Berlin, 1988, p. 257.
8. G. W. Coates and R. M. Waymouth, in *Transition Metals in Polymer Synthesis: Ziegler-Natta Reaction in Comprehensive Organometallic Chemistry II: a Review of the Literature 1982-1994*, ed. L. S. Hegedus, Pergamon, London, 1995, vol. 12, p.1193.
9. W. Kaminsky, *Catal. Today*, 1994, **20**, 257.
10. M. Bochmann, *J. Chem. Soc., Dalton Trans.*, 1996, 255.
11. C. O´Driscoll, *Chem. Br.*, 1998, **34**, 43.
12. M. R. Kesti, G. W. Coates and R. M. Waymouth, *J. Am. Chem. Soc.*, 1992, **114**, 9679.
13. U. M. Stehling, K. M. Stein, D. Fischer and R. M. Waymouth, *Macromolecules*, 1999, **32**, 14.
14. U. Anttila, K. Hakala, T. Helaja, B. Löfgren and J. Seppälä, *J. Polym. Sci., Part A: Polym. Chem.*, 1999, **37**, 3099.
15. J. J. Eisch, in *Aluminum in Comprehensive Organometallic Chemistry II: a Review of the Literature 1982-1994*, ed. A. McKillop, Pergamon, London, 1995, vol. 11, p. 277.
16. T. C. Chung, *Macromol. Symp.*, 1995 **89**, 151.
17. T. C. Chung, H. L. Lu and C. L. Li, *Polym. Int.*, 1995, **37**, 197.
18. T. C. Chung, H. L. Lu and C. L. Li, *Macromolecules*, 1994, **27**, 7533.
19. T. C. Chung and H. L. Lu, *J. Mol. Catal.*, 1997, **115**, 115.
20. P. Aaltonen and B. Löfgren, *Macromolecules*, 1995, **28**, 5353.
21. P. Aaltonen, G. Fink, B. Löfgren and J. Seppälä, *Macromolecules*, 1996, **29**, 5255.

22. P. Aaltonen and B. Löfgren, *Eur. Polym. J.*, 1997, **33**, 1187.

23. J. H. Rogers, A. W. Apblett, W. M. Cleaver, A. N. Tyler and A. R. Barron, *J. Chem. Soc. Dalton Trans.*, 1992, 3179.

24. S. Pasynkiewicz, *Macromol. Symp.*, 1995, **13**, 1.

25. K. Radhakrishnan and S. Sivaram, *Macromol. Rapid Commun.*, 1998, **19**, 581.

26. M. M. Marques, S. G. Correia, J. R. Ascenso, A. F. G. Ribeiro, P. T. Gomes, A. R. Dias, P. Foster, M. D. Rausch and J. C. W. Chien, *J. Polym. Sci., Part A: Polym. Chem.*, 1999, **37**, 2457.

27. C.-E. Wilen and J. H. Näsman, *Macromolecules*, 1994, **27**, 4051.

28. M. J. Schneider, R. Schäfer and R. Mülhaupt, *Polymer*, 1997, **38**, 2455.

29. R. Goretzki and G. Fink, *Macromol. Rapid Commun.*, 1998, **19**, 511.

30. A. Tsuchida, C. Bolln, F. G. Sernetz, H. Frey and R. Mülhaupt, *Macromolecules*, 1997 **30**, 2818.

31. S. Bruzaud, H. Cramail, L. Duvignac and A. Deffieux, *Macromol. Chem. Phys.*, 1997, **198**, 291.

32. R. Kravchenko and R. M. Waymouth, *Macromolecules*, 1998, **31**, 1.

33. J. Suhm, M. J. Schneider and R. Mülhaupt, *J. Mol. Catal*., 1998, **128**, 215.

34. M. Arndt, W. Kaminsky, A.-M. Schauwienold and U. Weingarten, *Macromol. Chem. Phys*., 1998, **199**, 1135.

35. H. Drögemüller, K. Heiland and W. Kaminsky, in *Copolymerization of Ethene and α-Olefins with a Chiral Zirconocene/Aluminoxane Catalyst in Transition Metals and Organometallics as Catalysts for Olefin Polymerization*, eds. W. Kaminsky and H. Sinn, Springer, Berlin, 1988, p. 303.

36. J. C. W. Chien and D. He, *J. Polym. Sci., Part A: Polym. Chem.*, 1991, **29**, 1585.

37. M. Galimberti, F. Piemontesi, O. Fusco, I. Camurati and M. Destro, *Macromolecules*, 1998, **31**, 3409.

38. M. Galimberti, M. Destro, O. Fusco, F. Piemontesi and I. Camurati, *Macromolecules*, 1999, **32**, 258.

39. V. Busico, R. Cipullo, G. Talarico, A. L. Segre and L. Caporaso, *Macromolecules*, 1998, **31**, 8720.

40. J. Jin, T. Uozumi, T. Sano, T. Teranishi, K. Soga and T. Shiono, *Macromol. Rapid Commun*., 1998, **19**, 337.

41. N. Naga, Y. Ohbayashi and K. Mizunuma, *Macromol. Rapid Commun*., 1997, **18**, 837.

42. C. Lehtinen, P. Starck and B. Löfgren, *J. Polym. Sci., Part A: Polym. Chem*., 1997, **35**, 307.

43. A. Rossi, J. Zhang and G. Odian, *Macromolecules*, 1996, **29**, 2331.

44. W. Kaminsky, A. Bark, N. Spiehl, N. Möller-Lindenhof and S. Niedoba, in *Isotactic Polymerization of Olefins with Homogeneous Zirconium Catalysts in Transition Metals and Organometallics as Catalysts for Olefin Polymerization*, eds. W. Kaminsky and H. Sinn, Springer, Berlin, 1988, p. 291.

45. R. Quijada, J. Dupont, M. S. L. Miranda, R. B. Scipioni and G. B. Galland, *Macromol. Chem. Phys*., 1995, **196**, 3991.

46. P. Lehmus, O. Härkki, R. Leino, H. J. G. Luttikhedde, J. H. Näsman and J. V. Seppälä, *Macromol. Chem. Phys*., 1998, **199**, 1965.

47. W. Kaminsky and R. Spiehl, *Makromol. Chem*., 1989, **190**, 515.

48. W. Kaminsky, A. Bark and M. Arndt, *Makromol. Chem., Macromol. Symp*., 1991, **47**, 83.

49. C. H. Bergström and J. V. Seppälä, *J. Appl. Polym. Sci*., 1997, **63**, 1063.

50. C. H. Bergström, T. L. J. Väänänen and J. V. Seppälä, *J. Appl.Polym. Sci*., 1997, **63**, 1071.

51. D. Ruchatz and G. Fink, *Macromolecules*, 1998, **31**, 4669.

52. D. Ruchatz and G. Fink, *Macromolecules*, 1998, **31**, 4684.

53. D. Ruchatz and G. Fink, *Macromolecules*, 1998, **31**, 4674.

54. D. Ruchatz and G. Fink, *Macromolecules*, 1998, **31**, 4681.

55. I. Kim and Y. J. Kim, *Polym. Bull*., 1998, **40**, 415.

56. I. Kim, *Macromol. Rapid Commun*., 1998, **19**, 299.

57. M. J. Schneider and R. Mülhaupt, *Macromol. Chem. Phys*., 1997, **198**, 1121.

58. M. Arnold, O. Henschke and F. Köller, *Macromol. Reports A33 (Suppls. 3&4)*, 1996, 219.

59. O. Henschke, F. Köller and M. Arnold, *Macromol. Rapid Commun*., 1997, **18**, 617.

60. L. Jia, X. Yang, A. M. Seyam, I. D. L. Albert, P.-F. Fu, S. Yang and T. J. Marks, *J. Am. Chem. Soc*., 1996, **118**, 7900.

61. L. Oliva, L. Izzo and P. Longo, *Macromol. Rapid Commun*., 1996, **17**, 745.

62. L. Oliva, P. Longo, L. Izzo and M. di Serio, *Macromolecules*, 1997, **30**, 5616.

63. L. Oliva, L. Caporaso, C. Pellecchia and A. Zambelli, *Macromolecules*, 1995, **28**, 4665.

64. J. Ren and G. R. Hatfield, *Macromolecules*, 1995, **28**, 2588.

65. T. C. Chung, H. L. Lu and R. D. Ding, *Macromolecules*, 1997, **30**, 1272.

66. W. Kaminsky and A. Noll, in *Polymerization of Phenyl Substituted Cyclic Olefins with Metallocene/Aluminoxane Catalysts in Ziegler Catalysts, Recent Scientific Innovations and Technological Improvements*, eds. G. Fink, R. Mülhaupt and H. H. Brintzinger, Springer, Berlin, 1995, p. 149.

67. C. H. Bergström, P. G. Starck and J. V. Seppälä, *J. Appl. Polym. Sci*., 1998, **67**, 385.

68. N. Naga, T. Shiono and T. Ikeda, *Macromolecules*, 1999, **32**, 1348.

69. D.-H. Lee, K.-B. Yoon, J.-R. Park and B.-H. Lee, *Eur. Polym. J*., 1997, **33**, 447.

70. M. Hackmann, T. Repo, G. Jany and B. Rieger, *Macromol. Chem. Phys*., 1998, **199**, 1511.

71. S. Marathe and S. Sivaram, *Macromolecules*, 1994, **27**, 1083.

72. W. Kaminsky, D. Arrowsmith and H. Winkelbach, R. *Polym. Bulletin*, 1996, **36**, 577.

73. J. J. Eisch, in *Aluminum in Comprehensive Organometallic Chemisry II: a Review of the Literature 1982-1994*, ed. C. E. Housecroft, Pergamon, London, 1995, vol. 1, p. 431.

74. S. Pasynkiewicz, *Polyhedron*, 1990, **9**, 429.

75. Courtesy of Dr. J. Enqvist.

76. E. Giannetti, G. M. Nicoletti and R. Mazzocchi, *J. Polym. Sci., Part A: Polym. Chem*., 1985, **23**, 2117.

77. D. W. Imhoff, L. S. Simeral, S. A. Sangokoya and J. H. Peel, *Organometallics*, 1998, **17**, 1941.

78. A. R. Barron, *Organometallics*, 1995, **14**, 3581.

79. I. Tritto, C. Mealares, M. C. Sacchi and Locatelli, P. *Macromol. Chem. Phys*., 1997, **198**, 3963.

80. L. Resconi, S. Bossi and L. Abis, *Macromolecules*, 1990, **23**, 4489.

81. I. Tritto, M. C. Sacchi, P. Locatelli and S. X. Li, *Macromol. Symp*., 1995, **97**, 101.

82. I. Tritto, M. C. Sacchi, P. Locatelli and S. X. Li, *Macromol. Chem. Phys*., 1996, **197**, 1537.

83. D. E. Babushkin, N. V. Semikolenova, V. N. Panchenko, A. P. Sobolev, V. A. Zakharov and E. P. Talsi, *Macromol. Chem. Phys*., 1997, **198**, 3845.

84. M. S. Howie, presented at the Metallocene Conference, Houston TX, 1993.

85. T. Sugano, K. Matsubara, T. Fujita and T. Takahashi, *J. Mol. Catal*., 1993, **82**, 93.

86. A. R. Siedle, W. M. Lamanna, J. M. Olofson, B. A. Nerad and R. A. Newmark, *ACS Symp. Ser*., 1993, **517**, 156.

87. A. R. Siedle, W. M. Lamanna, R. A. Newmark, J. Stevens, D. E. Richardson and M. Ryan, *Makromol. Chem., Macromol. Symp*., 1993, **66**, 215.

88. A. R. Siedle, W. M. Lamanna, R. A. Newmark and J. N. Schroepfer, *J. Mol. Catal*., 1998, **128**, 257.

89. A. R. Barron, *Polyhedron*, 1995, **14**, 3197.

90. M. R. Mason, J. M. Smith, S. G. Bott and A. R. Barron, *J. Am. Chem. Soc*., 1993, **115**, 4971.

91. S. Lasserre and J. Derouault, *Nouv. J. Chem*., 1983, **7**, 659.

92. J. L. Atwood, D. C. Hrneir, R. D. Priester and R. D. Rogers, *Organometallics*, 1983, **2**, 985.

93. R. Fusco, L. Longo, F. Masi and F. Garbassi, *Macromolecules*, 1997, **30**, 7673.

94. A. R. Barron, *Macromol. Symp*., 1995, **97**, 15.

95. W. Hagendorf, A. Harder and H. Sinn, *Macromol. Symp*., 1995, **97**, 127.

96. H. Sinn, *Macromol. Symp*., 1995, **97**, 27.

97. J. Bliemeister, W. Hagendorf, A. Harder, B. Heitmann, I. Schimmel, E. Schmedt, W. Schnuchel, H. Sinn, L. Tikwe, N. von Thienen, K. Urlass, H. Winter and O. Zarncke, in *The Role of MAO-Activators in Ziegler Catalysts, Recent Scientific Innovations and Technological Improvements*, eds. G. Fink, R. Mülhaupt and H. H. Brintzinger, Springer, Berlin, 1995, p. 57.

98. D. Cam, E. Albizzati and P. Cinquina, *Makromol. Chem*., 1990, **191**, 1641.

99. W. Kaminsky, *Macromol. Symp*., 1995, **97**, 79.

100. J. C. W. Chien and B. P. Wang, *J. Polym. Sci., Part A: Polym. Chem*., 1988, **26**, 3089.

101. W.-M. Tsai and J. C. W. Chien, *J. Polym. Sci., Part A: Polym. Chem*., 1994, **32**, 149.

102. J. C. W. Chien and R. Sugimoto, *J. Polym. Sci., Part A: Polym. Chem*., 1991, **29**, 459.

103. W. Kaminsky, A. Bark and R. Steiger, *J. Mol. Catal*., 1992, **74**, 109.

104. W. Kaminsky and R. Steiger, *Polyhedron*, 1988, **7**, 2375.

105. S. Gürtzgen, R. Rieger and W. Uzick, *Macromol. Symp*., 1995, **97**, 217.

106. L. A. Nekhaeva, G. N. Bondarenko, S. V. Rykov, B. A. Nekhaev, B. A. Krentzel, V. P. Marlin, L. I. Vyshinkaya, I. M. Khrapova, A. V. Polonskii and N. N. Korneev, *J. Organomet. Chem*., 1991, **406**, 139.

107. D. Cam and U. Giannini, *Makromol. Chem*., 1992, **193**, 1049.

108. I. Kim and R. F. Jordan, *Polym. Bull*., 1997, **39**, 325.

109. A. R. Siedle, R. A. Newmark, W. M. Lamanna and J. N. Schroepfer, *Polyhedron*, 1990, **9**, 301.

110. I. Tritto, R. Donetti, M. C. Sacchi, P. Locatelli and G. Zannoni, *Macromolecules*, 1997, **30**, 1247.

111. C. Sishta, R. M. Hathorn and T. J. Marks, *J. Am. Chem. Soc*., 1992, **114**, 1112.

112. I. Tritto, R. Donetti, M. C. Sacchi, P. Locatelli and G. Zannoni, *Macromolecules*, 1999, **32**, 264.

113. T. Haselwander, S. Beck and H. H. Brintzinger, in *μ-Cl- and μ-CH_3-Bridges in Metallocene-Based Ziegler-Natta Catalyst Systems, Solution-NMR Studies in Ziegler Catalysts, Recent Scientific Innovations and Technological Improvements*, eds. G. Fink, R. Mülhaupt and H. H. Brintzinger, Springer, Berlin, 1995, p. 182.

114. N. Herfert and G. Fink, *Makromol. Chem., Rapid Commun*., 1993, **14**, 91.

115. D. Coevoet, H. Cramail and A. Deffieux, *Macromol. Chem. Phys*., 1998, **199**, 1451.

116. D. Coevoet, H. Cramail and A. Deffieux, *Macromol. Chem. Phys*., 1998, **199**, 1459.

117. S. Beck, M.-H. Prosenc and H.-H. Brintzinger, *J. Mol. Catal*., 1998, **128**, 41.

118. X. Yang, C. L. Stern and T. J. Marks, *J. Am. Chem. Soc*., 1991, **113**, 3623.

119. X. Yang, C. L. Stern and T. J. Marks, *J. Am. Chem. Soc*., 1994, **116**, 10015.

120. M. Bochmann, S. J. Lancaster, M. B. Hursthouse and K. M. A. Malik, *Organometallics*, 1994, **13**, 2235.

121. J. I. Amor, T. Cuenca, M. Galakhov, P. Gomez-Sal, A. Manzanero and P. Royo, *J. Organomet. Chem*., 1997, **535**, 155.

122. L. Jia, X. Yang, C. L. Stern and T. J. Marks *Organometallics*, 1997, **16**, 842.

123. M. Bochmann and S. J. Lancaster, *Organometallics*, 1993, **12**, 633.

124. M. Bochmann and S. J. Lancaster, *Angew. Chem., Int. Ed. Engl*., 1994, **33**, 1634.

125. A. Cano, T. Cuenca, P. Gomez-Sal, A. Manzanero and P. Royo, *J. Organomet. Chem*., 1996, **526**, 227.

126. M. Bochmann, A. J. Jagger and J. C. Nicholls, *Angew. Chem., Int. Ed. Engl*., 1990, **29**, 780.

127. A. D. Horton and J. H. G. Frijns, *Angew. Chem., Int. Ed. Engl*., 1991, **30**, 1152.

128. C. J. Harlan, S. G. Bott and A. R. Barron, *J. Am. Chem. Soc*., 1995, **117**, 6465.

129. J. Turunen, T. T. Pakkanen and B. Löfgren, *J. Mol. Catal*., 1997, **123**, 35.

130. C. Janiak, B. Rieger, R. Voelkel and H.-G. Braun, *J. Polym. Sci., Part A: Polym. Chem*., 1993, **31**, 2959.

131. M. Akakura and H. Yamamoto, *Synlett*, 1997, 277.

132. Y. Koide, S. G. Bott and A. R. Barron, *Organometallics*, 1996, **15**, 5514.

133. Y. Koide and A. R. Barron, *Organometallics*, 1995, **14**, 4026.

134. Y. Koide, S. G. Bott and A. R. Barron, *Organometallics*, 1996, **15**, 2213.
135. J. March, *Advanced Organic Chemistry*, Wiley, New York, 1992, 4th ed., p. 920.
136. C. Blomberg and F. A. Hartog, *Synthesis*, 1977, 18.
137. P. J. Pierce, D. H. Richards and N. F. Scilly, *J. Chem. Soc., Perkin Trans. 1*, 1972, 1655.
138. F. Machrouhi, B. Hamann, J.-L. Namy and H. B. Kagan, *Synlett*, 1996, 633.
139. P. Girard, J.-L. Namy and H. B. Kagan, *J. Am. Chem. Soc*., 1980, **102**, 2693.
140. J. D. Buhler, *J. Org. Chem*., 1973, **38**, 904.
141. P. Bartlett and E. B. Lefferts, *J. Am. Chem. Soc*., 1955, **77**, 2804.
142. T. Imamoto, N. Takiyama and K. Nakamura, *Tetrahedron Lett*., 1985, **26**, 4763.
143. H. G. Richey and J. P. DeStephano, *J. Org. Chem*., 1990, **55**, 3281.
144. G. Cahiez, J. Rivas-Enterrios and H. Granger-Veyron, *Tetrahedron Lett*., 1986, **27**, 4441.
145. H. C. Brown, J.-J. Katz and B. A. Carlson, *J. Org. Chem*., 1973, **38**, 3968.
146. T.-S. Ho, *Synth. Commun*., 1983, **13**, 769.
147. F. Chen, B. Mudryk and T. Cohen, *Tetrahedron*, 1994, **50**, 12793.
148. D. Seebach and M. Schiess, *Helv. Chim. Acta*, 1982, **65**, 2598.
149. A. F. Abdel-Magid, C. A. Maryanoff and K. G. Carson, *Tetrahedron Lett*., 1990, **31**, 5595.
150. G. Wieland and G. Simchen, *Liebigs Ann. Chem*., 1985, 2178.
151. E. J. Corey and A. W. Gross, *Tetrahedron Lett.*, 1984, **25**, 491.
152. C. A. Audeh, S. E. Fuller, R. J. Hutchinson and J. R. L. Smith, *J. Chem. Res. (S)*, 1979, 270.
153. F. Kuffner and E. Polke, *Monatsh. Chem.*, 1951, **82**, 330.
154. F. Kuffner and W. Koechlin, *Monatsh. Chem.*, 1962, **93**, 476.
155. F. S. Guziec and F. F. Torres, *J. Org. Chem.*, 1993, **58**, 1604.
156. CA-on-line search
157. P. D. Bartlett and A. Schneider, *J. Am. Chem. Soc*., 1945, **67**, 141.
158. R. F. Smith and K. J. Coffman, *Synth. Commun.*, 1982, **12**, 801.
159. R. F. Smith, J. L. Marcucci and P. S. Tingue, *Synth. Commun.*, 1992, **22**, 381.
160. A. R. Katritzky, S. Rachwal and G. J. Hitchings, *Tetrahedron*, 1991, **47**, 2683.
161. A. R. Katritzky, X. Zhao and G. J. Hitchings, *Synthesis*, 1991, 703.
162. J. C. Stowell and J. Padegimas, *Synthesis*, 1974, 127.

163. M. A. Schwartz and X. Hu, *Tetrahedron Lett.*, 1992, **33**, 1689.

164. E. Ciganek, *J. Org. Chem*., 1992, **57**, 4521.

165. L. F. Fieser and M. Fieser, *Reagents for Organic Synthesis*, Wiley, New York, 1967, p. 3.

166. N. L. Drake and G. B. Cooke, in *Methyl Isopropyl Carbinol in Organic Syntheses*, ed. A. H. Blatt, Wiley, New York, 1946, p. 406.

167. A. C. Cope and E. Ciganek, in *N,N-Dimethylcyclohexylmethylamine in Organic Syntheses*, ed. N. Rabjohn, Wiley, New York, 1963, p. 339.

168. K. Hakala, B. Löfgren and T. Helaja, (manuscript in preparation)

169. T. Back and D. H. R. Barton, *J. Chem. Soc., Perkin Trans. 1*, 1977, 924.

170. F. Camps, V. Gasol and Guerrero, A. *Synth. Commun.*, 1988, **18**, 445.

171. J.-A. MacPhee and J.-E. Dubois, *Tetrahedron* , 1980, **36**, 775.

172. L. H. Amundsen and L. S. Nelson, *J. Am. Chem. Soc.*, 1951, **73**, 242.

173. P. Anton and A. Laschewsky, *Makromol. Chem., Rapid Commun.*, 1991, **12**, 189.

174. R. A. W. Johnstone and M. E. Rose, *Tetrahedron*, 1979, **35**, 2169.

175. T. W. Greene and P. G. M. Wuts, *Protective Groups in Organic Synthesis*, Wiley, New York, **1991**, 2nd ed., p. 68.

176. S. Ohta, A. Shimabayashi, M. Aono and M. Okamoto, *Synthesis*, 1982, 833.

177. P. J. Pierce, D. H. Richards and N. F. Scilly, *Org. Synth.*, 1972, **52**, 19.

178. T. Imamoto, N. Takiyama, K. Nakamura, T. Hatajima and Y. Kamiya, *J. Am. Chem. Soc.*, 1989, **111**, 4392.

179. K. Nützel, in *Methoden zur Herstellung und Umwandlung magnesiumorganischer Verbindungen in Houben-Weyl, Methoden der Organischen Chemie, Band XIII/2a*; ed. E. Müller, Georg Thieme Verlag, Stuttgart, 1973, p. 261.

180. T. Holm, *Acta Chem. Scand., Ser. B*, 1983, **B 37**, 567.

181. F. F. Blicke and L. D. Powers, *J. Am. Chem. Soc.*, 1929, **51**, 3378.

182. K. Okuhara, *J. Am. Chem. Soc.*, 1980, **102**, 244.

183. E. C. Ashby and A. B. Goel, *J. Am. Chem. Soc.*, 1981, **103**, 4983.

184. C. Walling, *J. Am. Chem. Soc.*, 1988, **110**, 6846.

185. D. L. Comins and J. J. Herrick, *Tetrahedron Lett.*, 1984, **25**, 1321.

186. F. Sato, T. Jinbo and M. Sato, *Tetrahedron Lett.*, 1980, **21**, 2175.

187. I. Marek, C. Meyer and J.-F. Normant, *Org. Synth.*, 1996, **74**, 194.

188. G. Molle, S. Briand, P. Bauer and J.-E. Dubois, *Tetrahedron*, 1984, **40**, 5113.

189. R. B. Bates, L. M. Kroposki and D. E. Potter, *J. Org. Chem.*, 1972, **37**, 560.

190. M. E. Jung and R. B. Blum, *Tetrahedron Lett.*, 1977, **43**, 3791.

191. F. Baduri, L. Di Nunno, S. Florio and S. Valzano, *Tetrahedron*, 1984, **40**, 1731.

192. L. Di Nunno and A. Scilimati, *Tetrahedron*, 1986, **42**, 3913.

193. L. Di Nunno and A. Scilimati, *Tetrahedron*, 1988, **44**, 3639.

194. L. Di Nunno and A. Scilimati, *Tetrahedron*, 1991, **47**, 4121.

195. L. Di Nunno and A. Scilimati, *Tetrahedron*, 1987, **43**, 2181.

196. P. Tomboulian, D. Amick, S. Beare, K. Dumke, D. Hart, R. Hites, A. Metzger and R. Nowak, *J. Org. Chem.*, 1973, **38**, 322.

197. A. J. Duggan and F. E. Roberts, *Tetrahedron Lett.*, 1979, **7**, 595.

198. T. Helaja (unpublished results)

199. T. Helaja *et al.* (manuscript in preparation)

200. H. Günther, *NMR Spectroscopy*, Wiley, New York, 1994, p. 97.

201. G. Erker, M. Albrecht, S. Werner and C. Krüger, *Z. Naturforsch.*, 1990, **45b**, 1205.

Appendix VII

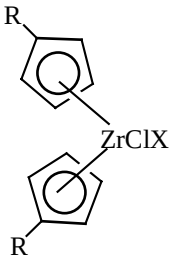

Cp_2ZrCl_2 (R = H, X = Cl)
(n-BuCp)$_2ZrCl_2$ (R= n-Bu, X = Cl)
$Cp_2Zr(Me)Cl$ (R = H, X = M)e
(t-BuCp)$_2ZrCl_2$ (R= t-Bu, X = Cl)
$(Me_3SiCp)_2ZrCl_2$ (R= Me_3Si, X = Cl)

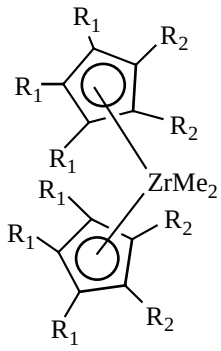

Cp_2ZrMe_2 (R^1, R^2 = H)
$Cp^*_2ZrMe_2$ (R^1, R^2 = Me)
Cp'_2ZrMe_2 (R^1= H, R^2 = Me)

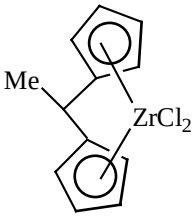

$MeCH(Cp)_2ZrCl_2$

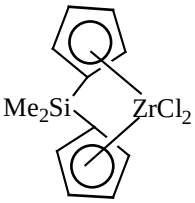

$Me_2Si(Cp)_2ZrCl_2$

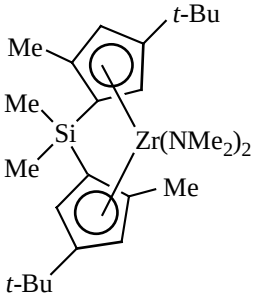

$Me_2Si(2\text{-}Me\text{-}4\text{-}Bu_t\text{-}Cp)_2Zr(NMe_2)_2$

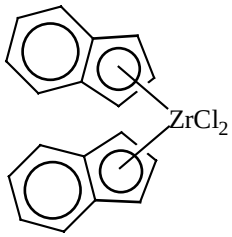

Ind_2ZrCl_2

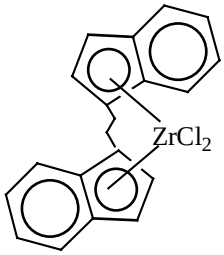

$Et(Ind)_2ZrCl_2$

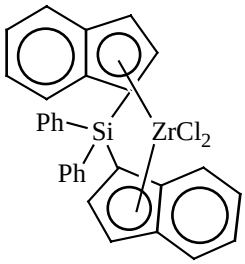

$Ph_2Si(Ind)_2ZrCl_2$

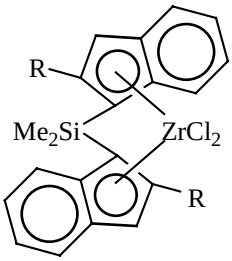

$Me_2Si(Ind)_2ZrCl_2$ (R= H)
$Me_2Si(2\text{-}MeInd)_2ZrCl_2$ (R= Me)

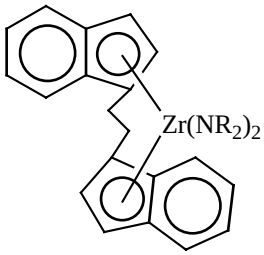

$Et(Ind)_2Zr(NMe_2)_2$ R = Me
$Et(Ind)_2Zr(NBu_2)_2$ R= n-Bu

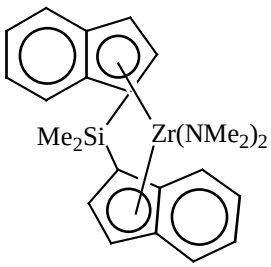

$Me_2Si(Ind)_2Zr(NMe_2)_2$

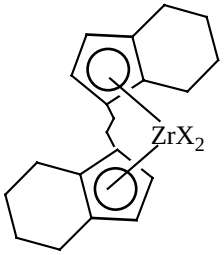

$Et(IndH_4)_2ZrCl_2$ (X= Cl)
$Et(IndH_4)_2ZrCl_2$ (X= Me)

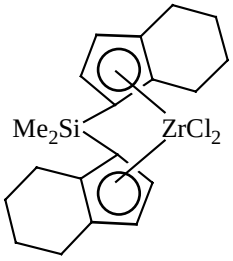

$Me_2Si(IndH_4)_2ZrCl_2$

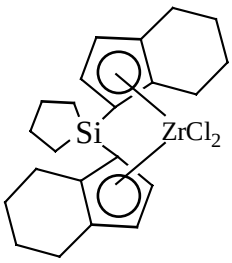

1,4-butanediylSi$(IndH_4)_2ZrCl_2$

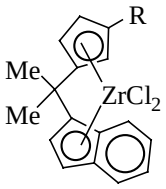

$Me_2C[(Cp)(Ind)]ZrCl_2$ (R= H)
$Me_2C[(3\text{-}MeCp)(Ind)]ZrCl_2$ (R= Me)
$Me_2C[(3\text{-}Bu_tCp)(Ind)]ZrCl_2$ (R= *t*-Bu)

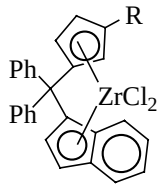

$Ph_2C[(Cp)(Ind)]ZrCl_2$

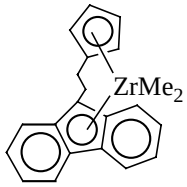

$Et[(Cp)(Flu)]ZrMe_2$

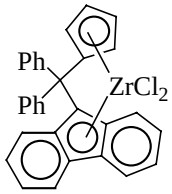

$Ph_2C[(Cp)(Flu)]ZrCl_2$

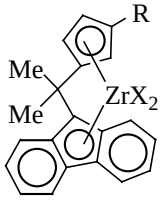

$Me_2C[(Cp)(Flu)]ZrCl_2$ (R= H, X= Cl)
$Me_2C[(3\text{-}MeCp)(Flu)]ZrCl_2$ (R= Me, X= Cl)
$Me_2C[(3\text{-}Pr_iCp)(Flu)]ZrCl_2$ (R= *i*-Pr, X= Cl)
$Me_2C[(3\text{-}Bu_tCp)(Flu)]ZrCl_2$ (R= *t*-Bu, X =Cl)
$Me_2C[(Cp)(Flu)]ZrMe_2$ (R= H, X = Me)

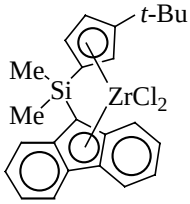

$Me_2Si[(3\text{-}Bu_tCp)(Flu)]ZrCl_2$

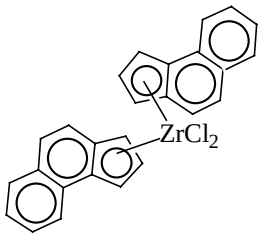

$(Benz[e]Ind)_2ZrCl_2$

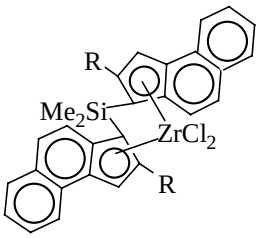

$Me_2Si(2\text{-}MeBenz[e]Ind)_2ZrCl_2$
(R= Me)
$Me_2Si(Benz[e]Ind)_2ZrCl_2$
(R= H)